

Roughex dependent regulation of the *Drosophila* cell cycle

Inaugural-Dissertation
zur Erlangung des Doktorgrades
der Mathematisch-Naturwissenschaftlichen Fakultät
der Universität zu Köln

vorgelegt von

Edan Foley
aus Galway, Irland

Köln 2000

INTRODUCTION.....	5
The Eukaryotic cell cycle.....	5
Cdk regulation.....	6
Cyclin Dependent Kinase Inhibitors (CKIs).....	10
The <i>Drosophila</i> cell cycle.....	12
Roughex (Rux).....	13
Goal of this project.....	16
RESULTS.....	19
Rux protein structure.....	19
Rux protein localization.....	21
Rux interacts with CycA and CycB in <i>Drosophila</i> embryos.....	25
Rux inhibits Cdk1/CycA and Cdk1/CycB complexes.....	31
Rux interacts with CycA via two distinct RXL motifs.....	42
A role for Rux in exit from mitosis.....	49
Mild heat pulses affect the mitotic program in <i>Drosophila</i> embryos.....	56
Rux expression drives cells from metaphase to interphase.....	62
SIC1 functions as a CKI in <i>Drosophila</i> embryos.....	65
Downregulation of Rux activity during cell cycle progression.....	68
DISCUSSION.....	84
Rux is a novel <i>Drosophila</i> CKI.....	84
Rux does not target CycA for degradation.....	88
Rux functions during mitosis.....	89
The heat shock response in <i>Drosophila</i> embryos affects mitosis.....	90
Rux is downregulated prior to S phase.....	92
Similarities between Rux and other CKIs.....	94
A model for Rux function.....	96
MATERIALS AND METHODS.....	99
Materials.....	97
Computers and software.....	99
<i>Drosophila melanogaster</i>	99
Antibodies.....	99
<i>Escherichia coli</i>	99
DNA Molecular weight markers.....	100
Oligonucleotides.....	100
Restriction endonucleases.....	101
DNA constructs.....	101
Protein molecular weight markers.....	101
GST-fusion proteins.....	101
Films.....	101
Media, solutions and buffers.....	101
Agarose gel loading buffer.....	101
Coomassie staining solution.....	102
Destaining solution.....	102
GST-wash buffer.....	102
GST-Suspension buffer.....	102
GST-binding buffer.....	103

GST-elution buffer.....	103
Homogenization buffer.....	103
Immunoprecipitation buffer.....	103
Pre-kinase wash buffer.....	104
Kinase assay buffer.....	104
Laemmli sample buffer (4X).....	104
DNA Mini-prep buffers and solutions.....	104
Resuspension buffer P1.....	104
Lysis buffer P2.....	104
Neutralization buffer P3.....	105
Na-acetate buffer.....	105
2l 10XPBS.....	105
2l 10XPBT.....	105
10XPonceau S.....	105
SDS-Polyacrylamide minigels.....	105
10l 10X running buffer for SDS-PAGE.....	105
1l 4X Resolving gel buffer.....	106
500ml 4X Stacking gel buffer.....	106
Stripping buffer.....	106
Squashing buffer.....	106
1l Transfer buffer for western blots.....	106
TE.....	106
1l 50X TAE.....	106
Terrific broth.....	107
METHODS	108
DNA METHODS	108
Restriction digests of DNA.....	108
Dephosphorylation of DNA ends.....	108
Klenow fill in of DNA ends.....	108
Eluting DNA.....	108
Agarose gel electrophoresis.....	108
DNA ligation.....	108
Preparation of electrocompetent cells.....	109
Transformation.....	109
Isolation of Plasmid DNA.....	109
Precipitation of DNA.....	110
Site directed mutagenesis.....	110
DNA sequencing.....	110
Single fly PCR.....	110
Isolation of mRNA from flies.....	110
RT-PCR.....	111
Database searches.....	111
BIOCHEMICAL METHODS	111
Production of GST fusion proteins.....	111
Determining protein concentration.....	112
Gel electrophoresis of proteins.....	112

Coomassie blue staining	112
Ponceau S staining	113
Western blotting	113
SP6 <i>in vitro</i> transcription	113
Rabbit reticulocyte <i>in vitro</i> translation.....	113
Kinase assays.....	114
Phosphorimaging	114
DROSOPHILA METHODS	115
Maintenance of flies	115
Collecting embryos.....	115
Production of embryo extracts.	115
Precipitation of proteins from <i>Drosophila</i> embryos.....	116
Fixation of embryos.....	116
<i>In situ</i> hybridization	116
Immunohistology	116
RNA injection into <i>Drosophila</i> embryos.....	117
Microscopy	117
ZUSAMMENFASSUNG	125
Abbreviations	128
Single and three letter code for amino acids.....	129
Publications	130
Acknowledgements	131
Lebenslauf.....	132

INTRODUCTION

The Eukaryotic cell cycle.

The classical eukaryotic cell cycle is divided into four phases (Fig. 1a). This is illustrated graphically in Fig. 1a using a typical *Drosophila* imaginal disc cell cycle as an example. To permit cell division to occur the entire chromosomal content of DNA is replicated once during a period of DNA synthesis (S phase). Replicated DNA is segregated into two daughter cells during mitosis (M phase) in such a way that both cells receive an equal complement of DNA. Cytokinesis follows chromosomal segregation during M phase, creating two distinct daughter cells with a pre-S phase complement of DNA. Two

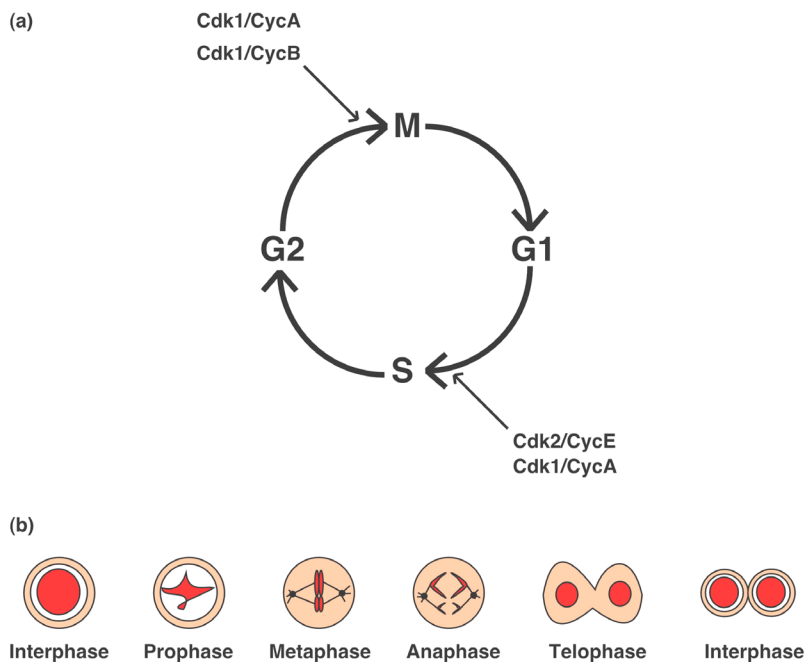


Figure 1.1: A *Drosophila* imaginal disc cell cycle.

A typical cell cycle is divided into four phases; a period of chromosomal DNA segregation (mitosis or M phase), a period of DNA replication (S phase) and two intervening gap phase (G1 and G2) (a). In *Drosophila* mitosis is triggered by the catalytic activity of Cdk1, complexed to its cyclin partners A and B. S phase is induced by Cdk2/CycE and Cdk1/CycA. Mitosis is subdivided into four distinct phases (b). During interphase DNA is in a relaxed decondensed form. In prophase DNA starts to condense. Nuclear envelope integrity is disrupted at the prophase/metaphase transition. Condensed DNA aligns on the metaphase plate in a compact form during metaphase. Cohesive forces between sister chromatids and pushing forces generated by mitotic spindles emanating from the spindle poles align DNA on the metaphase plate. Cohesion is disrupted at the metaphase/anaphase transition by proteolysis of cohesins. Sister chromatids are pulled to opposing poles in anaphase by the mitotic spindle. In telophase DNA decondenses and cytokinesis establishes two sister cells.

Gap phases, G1 and G2 separate mitosis and S phase. S phase and the accompanying gap phases are often collectively referred to as interphase. Mitosis is further divided into four phases, defined by DNA morphology (Fig. 1b). As cells exit interphase DNA condenses in a period known as prophase. During metaphase highly condensed sister chromatids align on the metaphase plate. Metaphase is maintained by pushing forces from the spindle poles and cohesive forces between sister chromatids. The cohesive force is established by a conserved family of proteins, known as cohesins (Guacci et al., 1997; Michaelis et al., 1997). Cohesin activity has been studied in greatest detail for *S. cerevisiae*. In the budding yeast the cohesin complex consists of the four proteins Smc1, Smc3, Scc1 and Scc3, where Smc1 and Smc3 are responsible for DNA contact. Cohesins associate with DNA at many regions along the chromosome arms and at centromeric regions. At the metaphase/anaphase transition cohesion between sister chromatids is disrupted by cohesin proteolysis.

This proteolysis is catalyzed by separins (Nasmyth et al., 2000). Separins have been characterized in a number of organisms and are highly divergent, with the exception of a conserved C-terminal separin domain. The budding yeast separin, Esp1p cleaves Scc1 at two places, disrupting cohesion (Uhlmann et al., 1999). Separins are maintained in an inactive state until the metaphase/anaphase transition by associated proteins known as securins (Ciosk et al., 1998). Securins have been characterized in budding and fission yeast; Pds1p and Cut2p respectively. In budding yeast cohesion Pds1p is destroyed during metaphase, releasing Esp1p and allowing cohesin proteolysis (Uhlmann et al., 1999). In higher eukaryotes cohesion is lost during prophase for most of the chromatid, excluding the kinetochore (Losada et al., 1998). Kinetochore cohesion is disrupted at the metaphase to anaphase transition. In higher eukaryotes it is still not clear which activities function as securins and separins. In *Drosophila* the genes *pimples* (*pim*) and *three rows* (*thr*) are obviously involved in this process as mutations in either gene fail to disrupt kinetochore cohesion at the metaphase to anaphase transition (D'Andrea et al., 1993).

Cdk regulation

The eukaryotic cell cycle is driven by the activities of a conserved family of proline-directed serine/threonine kinases; the Cyclin Dependent Kinases (CDKs) (Nurse, 1990). CDKs are relatively inert kinases that are fully active after association with positive regulatory subunits, the cyclins (Fisher, 1997) and after CDK phosphorylation on a conserved threonine residue (T161) (Fig. 2). T161 is in a structural element, the T-loop,

which blocks substrate access to the active site of CDKs (Morgan, 1995). Phosphorylation of T161 opens the active site allowing access of substrates to CDKs. T161 phosphorylation is catalyzed by a CDK Activating Kinase (CAK) (Solomon et al., 1992). The budding yeast CAK, CIV1 is a monomeric kinase of approx. 40kDa molecular weight (Kaldis et al., 1996; Thuret et al., 1996). The true nature of CAK in higher eukaryotes has not been fully resolved. A heterotrimeric complex of Cdk7/CycH/Mat1p has CAK activity *in vitro* and *cdk7* temperature sensitive mutants in *Drosophila* are lethal with several cell cycle defects (Devault et al., 1995; Fisher and Morgan, 1994; Larochelle et al., 1998). However, this complex also phosphorylates the C-terminal domain of RNA polymerase II and is believed to play a role in transcription (Roy et al., 1994; Serizawa et al., 1995). It is not clear whether the ability of Cdk7 to activate other CDKs is an *in vitro* artifact, or whether it reflects an *in vivo* property of Cdk7. As well as activation by CAK, CDKs are inactivated by inhibitory phosphorylation on conserved threonine 14 and tyrosine 15 residues by *wee* and *myt* kinases (Morgan, 1995). Inactivation of CDK by *wee* or *myt* is reversed by dephosphorylation mediated by the Cdc25 phosphatase (Russell and Nurse, 1986). Two Cdc25 homologues exist in *Drosophila*; *string* (*stg*) and the germline homologue *twine* (*twe*).

Lower eukaryotes such as budding and fission yeast have only one CDK (CDC28 and *cdc2*, respectively), while several CDK homologues exist in higher eukaryotes. CDK homologues adapted cell cycle stage specificity as they evolved. It has been proposed that the committing step to cell cycle initiation in metazoans is catalyzed by complexes of Cdk4 or Cdk6 with Cyclin D (CycD) (Kato et al., 1993). CDK/CycD complexes are proposed to respond to external signals such as mitogen stimulation by initiating cell division. CDK/CycD complexes phosphorylate pocket proteins such as Rb, thereby relieving Rb-mediated inhibition of the transcription factor E2F (Matsushime et al., 1994). Rb inhibits E2F in a simple stoichiometric way as well as by recruiting histone deacetylase activity to E2F-responsive genes (Dyson, 1998). Deacetylation leads to localized DNA condensation, making genes inaccessible to transcription factors. E2F is required for the transcription of numerous genes involved in the transition from G1 to S phase such as ribonucleotide reductase and CycE (Dyson, 1998). Cdk2/CycE also phosphorylates Rb, enhancing E2F activation. *Drosophila* has only one Cdk4/6 homologue, Cdk4 and *cdk4* mutants have been described recently (Meyer et al., 2000). *Drosophila* Cdk4 has Rb-phosphorylating activity and associates with CycD, suggesting that Cdk4 function has been conserved during evolution. Interestingly, Cdk4/CycD

activity is neither specific to G1, nor necessary for the cell cycle in *Drosophila* (Datar et al., 2000; Meyer et al., 2000). Cdk4 null mutants are not lethal and the entire cell cycle, not just G1 is prolonged in mutants. Similarly, overexpression of Cdk4/cycD accelerates the entire cell cycle, not just G1. It appears instead that CycD may play a role in growth regulation in *Drosophila*. In concurrence with these phenotypes, knock-out mice where individual CycD genes have been deleted also have hypotrophic phenotypes (Fantl et al., 1995). Thus, the exact *in vivo* functions of CycD and its associated CDKs remain to be clarified.

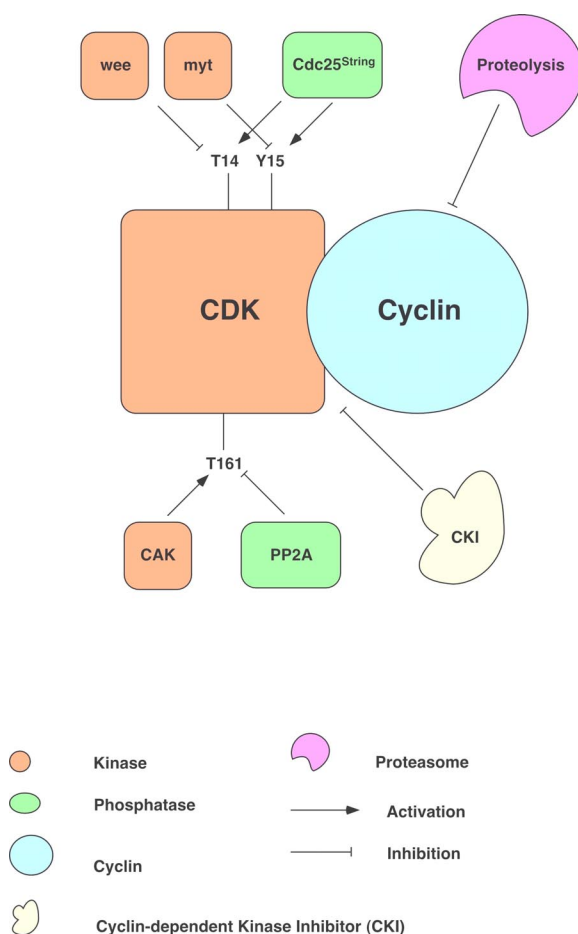


Fig. 1.2: CDK regulation.

Numerous activities regulate CDK in positive and negative manners. CDKs are fully active after association with cyclin partners and phosphorylation of a conserved threonine residue (T161). Association with cyclins puts bound ATP in the correct orientation and phosphorylation of the T loop leads to a CDK conformational rearrangement. The negatively charged phosphate group on T161 is attracted to a basic cluster away from the active site, exposing the active site to CDK substrates. CDKs are downregulated by phosphorylation of conserved threonine (T14) and tyrosine residues (Y15) situated close to the active site. Inhibitory phosphates are removed by the conserved CDC25 phosphatase in a step that is limiting for entry into mitosis. A critical means of CDK inactivation at specific times is ubiquitin-mediated proteolysis of cyclin proteins. A third form of CDK regulation is non-covalent inhibition by CDK Inhibitor (CKI) proteins. Arrows indicate upregulation of CDK/cyclin activity and bars indicate down regulation.

In higher eukaryotes S phase is triggered by Cdk2, while entry into mitosis relies on Cdk1 activity. Cdk1 associates with Cyclin A (CycA) and B-type cyclins, while Cdk2 associates with Cyclin E (CycE). Mammalian Cdk2 also associates with CycA and Cdk2/CycA has S phase functions in mammals (Pagano et al., 1992). The contribution of individual CDKs and cyclins to S phase and M phase in *Drosophila* has been studied in detail. Mitosis relies on Cdk1, which associates with CycA, Cyclin B (CycB) and Cyclin B3 (CycB3), while Cdk2 associates with Cyclin E (Knoblich et al., 1994). CycA is the only essential mitotic cyclin. Homozygous *cycA* mutants die during G of the 16th cycle (Lehner and O'Farrell, 1989). Cdk1/CycA also contributes to S phase, but is not essential for this aspect of the cell cycle (Sprenger et al., 1997). Homozygous *cycB* and *cycB3* mutants are viable (Jacobs et al., 1998), indicating that their functions are essential for cell cycle progression, although *cycB3* mutant females are sterile. The mitotic cyclins have dynamic patterns of subcellular localization. CycA and CycB are cytoplasmic during interphase and accumulate in the nucleus in prophase (Jacobs et al., 1998; Lehner and O'Farrell, 1989). Nuclear envelope breakdown occurs during the prophase/metaphase transition, after which all cyclins are uniformly distributed throughout the cytoplasm. As mitosis progresses the cyclins are destroyed in a stereotypical temporal order. CycA is destroyed at the metaphase to anaphase transition, CycB is destroyed during the anaphase to telophase transition and CycB3 during late telophase (Sigrist et al., 1995).

Sequential cyclin inactivation by proteolysis is a characteristic of all higher eukaryotic mitotic programs. (Hunt et al., 1992). Cyclins are destroyed by the proteasome in a ubiquitin dependent manner (Koepp et al., 1999). In the case of CycB destruction depends on a conserved motif, the destruction box (RXXLXXXXN) at the N-terminus of the protein (Glotzer et al., 1991). Removing the destruction box from CycB confers stability to the protein and attaching the CycB destruction box to heterologous proteins can induce their destruction (Glotzer et al., 1991). Destruction boxes have been observed in other proteins that are turned over during mitosis, suggesting that this signal motif may be a general mediator of protein destruction during mitosis (Cohen-Fix et al., 1996; Leismann et al., 2000). It has not been demonstrated which motif determines CycA destruction. Cdk1 inactivation by cyclin destruction is necessary for progression through mitosis. An N-terminal truncated CycA (CycA Δ 170) is stable in *Drosophila*. *Drosophila* embryos expressing CycA Δ 170 arrest in metaphase (Sigrist et al., 1995).

Indestructible CycB expression leads to an anaphase arrest and indestructible CycB3 expression leads to a telophase arrest.

Multi-ubiquitin chains attached to lysine residues serve as a tag directing cyclins to the proteasome for destruction (Hochstrasser, 1996). Ubiquitins are transferred to substrates in a three-step reaction. A ubiquitin-activating enzyme, E1 hydrolyzes ATP and forms a high-energy thioester between a cysteine of its active site and the C terminus of ubiquitin. Activated ubiquitin is transferred to ubiquitin-conjugating enzymes, E2s, which form thioester-linked complexes with ubiquitin. Finally, ubiquitin is covalently attached to the substrate protein either directly by the E2s, or by ubiquitin-protein ligases, E3s. Recently a novel ubiquitination factor, E4, was identified that drives multiubiquitin chain assembly, yielding long chains (Koepl et al., 1999). The Anaphase Promoting Complex/Cyclosome (APC/C) is an E3 ligase that targets mitotic cyclins for destruction in a large number of organisms (Zachariae and Nasmyth, 1999). The APC/C targets mitotic cyclins for destruction during M phase and G1. In budding yeast the two proteins Cdc20p and Hct1p confer specificity on the APC/C in a poorly understood manner (Fang et al., 1998; Kramer et al., 1998; Schwab et al., 1997; Visintin et al., 1998). Homologues of both proteins have been identified in many organisms. The *Drosophila* homologues Fizzy (Fzy) and Fizzy-related (Fzr) are required for APC/C function during mitosis and G1 respectively (Dawson et al., 1993; Dawson et al., 1995; Sigrist and Lehner, 1997). A second multiprotein E3 complex, the SCF (Skp1-Cullin-F-box protein) triggers the degradation of many cell cycle proteins in G1. (Bai et al., 1996). Substrates are recognized by specific F-box proteins in SCF complexes and then ubiquitinated. Recognition by F-boxes often depends on substrate phosphorylation (Feldman et al., 1997; Skowyra et al., 1997; Skowyra et al., 1999).

Cyclin Dependent Kinase Inhibitors (CKIs).

A further conserved mechanism of down-regulating CDK activity is mediated by CDK Inhibitor (CKI) proteins (Peter and Herskowitz, 1994; Sherr and Roberts, 1999; Sherr and Roberts, 1995). CKIs have been identified in a large number of organisms, and function by associating with CDKs, cyclins or both. CKIs inhibit CDK activity and prevent CDK activation without covalent modification of CDKs. Mammalian CKIs fall into two distinct families. The INK4 family of inhibitors specifically inhibits CycD in complex with Cdk4 and Cdk6 (Guan et al., 1994; Serrano et al., 1993). A second family of CKIs, the KIP/CIP family functions downstream of CycD/CDK complexes (Toyoshima and Hunter,

1994). This family consists of the three proteins p21, p27 and p57. All three function by inhibiting the S phase cyclins, CycA and CycE. The KIP/CIP family of CKIs has an additional, unexpected function. They are required for the formation of active CDK/CycD complexes (Cheng et al., 1999). The sequestration of KIP/CIP inhibitors by CDK/CycD has a secondary consequence of releasing active Cdk2/CycA and Cdk2/CycE complexes, which are free to induce S phase. Interestingly, no CKI has been characterized in mammals that specifically inhibits mitotic cyclins, although both budding and fission yeast have such a CKI; SIC1 and *rum1* respectively (Correa-Bordes and Nurse, 1995; Mendenhall, 1993). A search of the recently completed *Drosophila* genome did not reveal any CKIs of the INK4 family. *Drosophila* has a single gene that belongs to the p21/p27 class of CKIs, *dacapo* (de Nooij et al., 1996; Lane et al., 1996). *Dacapo* is required for the establishment of the first G1 state of embryonic development during cycle 17. It binds CycE/Cdk2 and inhibits kinase activity *in vivo* and *in vitro* (Lane et al., 1996). *Dacapo* is also required at later stages, such as during eye development, for the establishment and maintenance of G1.

CKIs function as inducible cell cycle repressors or as intrinsic elements of the cell cycle. A classical inducible CKI is the budding yeast protein Far1p (Chang and Herskowitz, 1990). FAR1 is induced in response to mating factor or nutrient deprivation and enforces a G1 arrest by down-regulating the activities of the yeast G1 cyclins; Cln1p, Cln2p and (Peter et al., 1993; Valtz et al., 1995). In higher eukaryotes p21 can be induced by the p53 transcription factor in response to DNA damage. This elicits a G1 arrest by inhibiting the activities of CycA and CycE.

The yeast protein Sic1p is one of the best studied CKIs which function as an integral element of the cell cycle apparatus (Mendenhall, 1993). Sic1p is required to maintain a G1 state by inhibiting the B-type cyclins, Clb5p and Clb6p (Schwob et al., 1994). CDC28/CLB5 and CDC28/CLB6 are essential for execution of S phase in yeast. Sic1p inhibits Clb5p and Clb6p in G1, preventing premature S phases. CLN levels rise as cells pass START, the point of commitment to execution of a cell cycle. Single and double CLN mutants are viable, but yeast mutants lacking all three CLNs are lethal (Richardson et al., 1989). Mutants arrest in G1 with high levels of Sic1p. Removing SIC1 from this mutant background restores viability, indicating that the only essential function performed by the CLNs is to downregulate Sic1p (Dirick et al., 1995). CDC28/Cln complexes phosphorylate SIC1 at the end of G1. Phosphorylated Sic1p is recognized by Cdc4p an F-box component of an SCF complex (Feldman et al., 1997). Sic1p is then

ubiquitinated and turned over by the proteasome. Sic1p proteolysis is essential for cell cycle progression, as expression of SIC1 isoforms lacking CDC28 phosphorylation sites leads to a G1 arrest (Nishizawa et al., 1998). Sic1p proteolysis allows Cdc28p/Clb5p and Cdc28p/Clb6p complexes to initiate S phase.

As well as contributing to regulation of the G1-S transition recent data has emerged supporting a role for Sic1p in exit from mitosis (Donovan et al., 1994). In late interphase and early mitosis cellular levels of Sic1p are relatively low due to high Cdc28p kinase activity. Cdc28p phosphorylates the Sic1p transcription factor Swi5p, resulting in a cytoplasmic accumulation of Swi5p (Moll et al., 1991). cdc28p also directly phosphorylates Sic1, thereby targeting it for degradation (Feldman et al., 1997). This depression of Sic1p proteins levels is reversed at the metaphase to anaphase transition due to the release of the Cdc14p phosphatase from the nucleolus. The Cdc14p phosphatase is retained in the nucleolus by Net1p during interphase (Shou et al., 1999; Visintin et al., 1999). At the metaphase to anaphase transition Net1p is inactivated by proteins of the Mitotic Exit Network (MEN) signaling cassette (Jaspersen et al., 1998; Shou et al., 1999). Cdc14p dephosphorylates several key proteins, including Sic1p, Swi5p and Hct1p. Hct1p is the budding yeast homologue of Fzr. In its unphosphorylated form Hct1p is inactive and targets mitotic cyclins for destruction (Zachariae et al., 1998). Swi5p accumulates in the nucleus in its unphosphorylated form and activates the transcription of Sic1p (Toyn et al., 1997). Unphosphorylated Sic1p is no longer a target for the proteasome, allowing the protein to accumulate. The consequence of Hct1p and Sic1p activation is a precipitous drop in Cdc28p activity, forcing an exit from mitosis and entry into G1.

The *Drosophila* cell cycle.

Many deviations from the standard cell cycle described above have been reported in *Drosophila* (Edgar et al., 1994). The first thirteen divisions are extremely rapid. They are nuclear cycles as opposed to cell cycles and occur synchronously in a common syncytium. Each division occurs in approx. 10min and consists entirely of S and M phases with no intervening gap phases (Edgar and Lehner, 1996). The first thirteen divisions occur entirely under the control of maternally provided products. These products are exhausted after the 13th division at the mid-blastula transition (MBT). A prolonged interphase is introduced and all subsequent divisions depend on the correct transcription of zygotic genes. The first G2 is introduced in the 14th cycle by the inhibitory

phosphorylation of Cdk1 on T14 and Y15 . Entry into mitosis depends on transcription of the *cdc25^{stg}* phosphatase, which relieves Cdk1 inhibition (Edgar and O'Farrell, 1990). *cdc25^{stg}* is transcribed in a complex pattern of 25 domains with bilateral symmetry along the anterior/posterior axis and mitosis 14 occurs in an almost identical pattern of domains (Foe, 1989). Cycle 15 and 16 also have extended interphases which are established in G2 (Edgar and O'Farrell, 1990). None of cycles 14, 15 or 16 have a G1. S phase follows the preceding mitosis immediately. After completion of the 16th division a prolonged G1 is introduced to most cycles, with the exception of cells of the nervous system. Several internal cells such as the salivary glands undergo repeated rounds of DNA replication (endocycles) without intervening divisions. Proliferative cycles recommence only after completion of embryogenesis. Most external structures are laid aside as columnar epithelia, known as imaginal discs. Imaginal disc proliferation starts in the first instar stage and proceeds into the third instar stage where patterning occurs.

Roughex (Rux).

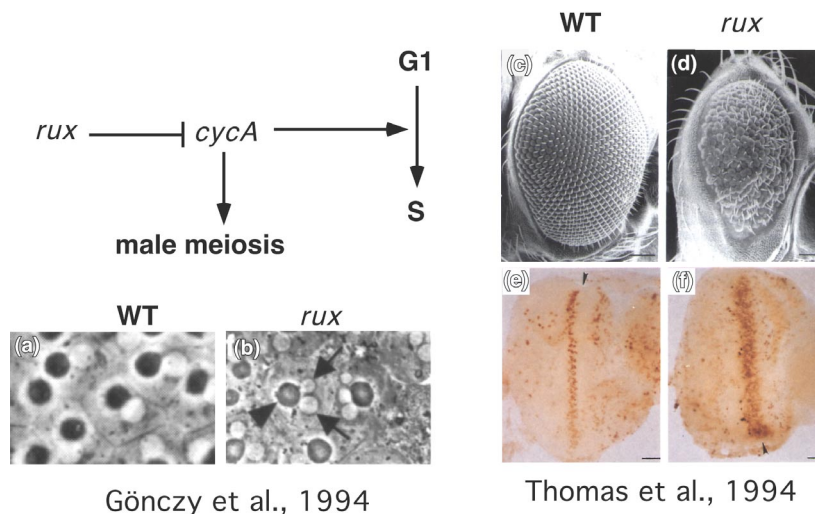


Fig. 1.3: Rux is a negative regulator of Cdk1/CycA in *Drosophila*.

Rux inhibits CycA during male meiosis and eye development. After completion of WT male meiosis haploid nuclei (transparent) are visible paired up with dense mitochondrial nebenkern (dark circles) (a). In *rux* mutant two nuclei (arrows) are visible with every nebenkern (arrowhead). The extra nucleus is the result of an aberrant 3rd meiotic division in *rux* mutants (b). Eye patterning is also disturbed in *rux* mutants. The mature adult eye consists of a regular lattice array of approx. 800 individual ommatidia (c). During eye disc development a G1 is established in the morphogenetic furrow (e, arrowhead). A wave of S phase cells lies posterior to the morphogenetic furrow. In *rux* mutants eye patterning is grossly disturbed (d). This is a result of precocious S phases occurring in the morphogenetic furrow (f). (c) and (d) are scanning electron micrographs and (e) and (f) are antibody staining of third instar larval discs with anterior to the right. S phases are visualized in (e) and (f) by staining with an anti-BrdU antibody. (a) and (b) are taken from (Gonczy et al., 1994) and (c-f) are taken from (Thomas et al., 1994).

Several activities contribute to establishment of G1 at the correct stages of *Drosophila* development. After completion of mitosis Cdk1 is inactivated by inhibitory phosphorylation on T14 and Y15. Cyclin levels are maintained low by APC/C dependent destruction. Dacapo also contributes to establishment of the first G1, as mutants fail to arrest in G1 of cycle 17 and perform an additional division. An additional gene product, Roughex (Rux), contributes to the establishment and maintenance of G1 at different stages of development (Sprenger et al., 1997; Thomas et al., 1994; Thomas et al., 1997). Rux was originally identified in a screen looking for genes involved in eye development (Thomas et al., 1994). Mutants have rough and reduced eyes and the gene was mapped to the X chromosome, giving rise to the name. Mutant males are also sterile. Antibody staining or *in situ* hybridization with RNA probes does not reveal the endogenous pattern of Rux expression, presumably due to low level expression. Several mutant alleles exist and two mutant alleles, *rux*⁸ and *rux*⁴ have been sequenced (Thomas et al., 1994). The wild type gene codes for a 335 amino acid protein with a predicted molecular weight of 38kDa and antibody staining demonstrate that it is a nuclear protein. A database search does not reveal any homologues, indicating that Rux is a novel protein.

One of the most obvious aspects of mutations at the *rux* locus are rough eyes in adult flies. Patterning of the eye imaginal disc commences in the third instar (Ready et al., 1976). Patterning is often viewed as two mitotic waves sweeping from the posterior to the anterior of the disc. The two waves are separated by an indentation along the dorso-ventral axis of the disc, the morphogenetic furrow (MF). Whereas, cells anterior to the MF are asynchronous and all cell cycle stages are distinguishable cells are synchronized within the MF. G2 cells immediately anterior to the MF are driven into mitosis and G1 cells are retained in G1 (Thomas et al., 1994). The consequence is that all cells are synchronized in G1 within the MF. Some of the cells posterior to the MF enter a second synchronous round of division before differentiation, while others differentiate immediately. The resulting adult eye is characterized by a reiterative array of cell shaped ommatidia. In *rux* mutants the regular shape of the adult eye is completely abolished (Thomas et al., 1994). This arises from a disturbance of the stereotyped cell cycle pattern in the eye disc. A G1 is not established in the MF in *rux* mutants. Instead the MF is characterized by a band of precocious S phases. Removing a single copy of *cycA* or *cdc25*^{sig} restores a G1 to the MF and rescues the eye phenotype of *rux* mutants, indicating that CycA activity is elevated in the developing eye of *rux* mutants.

The sterile phenotype of *rux* mutant males is also caused by disturbances in cell cycle progression (Gonczy et al., 1994). During spermatogenesis males normally undergo two separate meiotic divisions, generating haploid sperm. *rux* males perform an additional meiotic division which resembles meiosis II. The result is aneuploid nuclei and male sterility. Fertility is restored to mutant males by removing a single copy of *cycA* or *cdc25^{twe}*, the germline homologue of *cdc25^{stg}*, indicating that the molecular basis of this phenotype is also an increase of CycA activity in *rux* mutants. As both the rough eyes and male fertility of *rux* mutants are rescued by lowering *cycA* levels it is likely that Rux downregulates CycA activity during development. Male flies containing an extra copy of the WT *rux* gene are sterile due to an arrest of the cell cycle in meiosis I, indicating that Rux is a dose-dependent regulator of meiosis. Rux performs additional functions besides downregulating CycA in the eye and during male meiosis, as mutants display a considerably reduced viability (Thomas et al., 1994).

Overexpression of Rux at different stages of development also has several cell cycle consequences. Rux overexpression in embryos arrests cells in G2 (Foley et al., 1999; Thomas et al., 1997). Rux overexpression in various imaginal discs also prevents execution of mitosis. Instead endocycles are often observed (Thomas et al., 1997). An additional consequence of Rux overexpression is an alteration in the subcellular localization of CycA and CycB. CycA and B are normally cytoplasmic in interphase cells. Rux overexpressing cells in the embryo and the eye disc show a large accumulation of both cyclins in the nucleus (Foley et al., 1999; Sprenger et al., 1997; Thomas et al., 1997). Rux overexpression also inhibits S phase functions of CycA. Overexpression of CycA or CycA Δ 170 leads to ectopic S phases in the embryonic epidermis. A co-expression of Rux inhibits these ectopic S phases (Sprenger et al., 1997). As Rux prevents S phases performed by CycA Δ 170 inhibition does not rely solely on cyclin destruction.

Previous attempts to describe *in vitro* interactions between Rux and CycA were not successful (Thomas et al., 1997). Rux interacts with CycE in a two-hybrid assay, however it could not be determined if Rux also interacts with CycA, as full-length CycA is toxic to yeast. A GST-Rux fusion protein does not inhibit the *in vitro* kinase activity of Cdk2/CycE or Cdk1/CycA, however it should be noted that the GST tag is extremely bulky and has almost the same molecular weight as Rux. Rux has four potential CDK phosphorylation sites and Cdk1/CycA and Cdk2/CycE precipitated from embryonic extracts phosphorylate Rux. Overexpression of Rux does not inhibit CycE-dependent S

phases, but CycE does downregulate Rux protein levels. Rux protein levels were detected by anti-lacZ staining of discs expressing a Rux-lacZ fusion under the control of the *rux* promoter. Rux protein is detected in cells anterior to the MF and is downregulated in cells that reenter S phase. Overexpression of CycE from a heat inducible promoter lowers Rux levels, suggesting that *rux* is destroyed in cells that enter S phase.

Goal of this project

The data described above strongly argue for a role for Rux as a regulator of CycA in *Drosophila*. Rux overexpression prevents CycA-dependent S phases and inhibits mitosis. Rux is a nuclear protein and leads to a nuclear accumulation of CycA. Furthermore, removing a single copy of *cycA* suppresses the *rux* mutant phenotype. However, the exact manner in which Rux regulates CycA is not clear. To address this issue this project focuses on the following points.

1. A biochemical characterization of Rux-mediated inhibition of CycA. The effects of Rux on Cdk1/CycA kinase activity were monitored *in vivo* and *in vitro*. Several questions were addressed in this section; Does Rux physically interact with CycA? Is Rux a CKI or is it an adapter protein that recruits an unknown CKI to Cdk1/CycA complexes?
2. Identification of key residues in the Rux protein. Site directed mutagenesis and truncated versions of the Rux protein were analyzed to identify the residues in Rux required for nuclear localization, interaction with CycA and Rux destruction.
3. Cell cycle stages of Rux function. The data described above suggest that Rux is required to prevent a premature G1 to S transition during eye development. However, it is possible that Rux may also function during other stages of the cell cycle, as CycA is necessary for mitosis. Comparisons were performed between *rux* mutants and WT embryos to determine if other stages of the cell cycle are disturbed in *rux* mutants.
4. Analysis of Rux turnover. Examination of eye discs expressing a Rux-lacZ fusion protein suggests that Rux is stable in G1 and turned over prior to S phase. The molecular basis for Rux destruction, the residues required for this turnover and the role of CycE in this process were analyzed *in vivo* and *in vitro*.

RESULTS

Rux protein structure

Rux does not have any obvious homologues in the data bases. However, the primary amino acid sequence of Rux has several distinct motifs. Rux has three RXL sequences in its primary amino acid sequence (Fig. 2.1A and B). The amino acid sequence RXL has been implicated in numerous proteins as necessary for interactions with cyclins (Chen et al., 1996). There are two sites which conform to the minimal (S/TP) consensus for Cdk-mediated phosphorylation and two sites which have the extended (S/TPXR/K) consensus sequence (Fig. 2.1A and B). Rux also has a putative bipartite Nuclear Localization Sequence (NLS) at the C-terminus (Dingwall and Laskey, 1991), and a potential PEST sequence from amino acids 222 to 243. PEST sequences have been implied in several proteins as being required for proteasome-mediated destruction (Rechsteiner and Rogers, 1996). The importance of these sequence elements for Rux function will be discussed below.

Several *rux* mutant alleles were used in this study. *rux*⁸ has been described previously and is considered a null allele (Thomas et al., 1994). It is an 11bp deletion in the coding region that leads to a frameshift after amino acid 78, followed by an additional 7 out-of-frame amino acids. Mutant flies display a greatly reduced viability, have rough and reduced eyes and males are sterile. The *rux*² and *rux*³ alleles were sequenced in this study. *rux*³ carries a frame shift mutation that encodes a protein with 21 out of frame amino acids after amino acid 320 (Fig. 2.1A). This mutation eliminates the second basic cluster in the NLS. *rux*³ and *rux*² mutant males are fertile, meaning that the mutation can be maintained as a homozygous stock. Genomic DNA was isolated from single *rux*² mutant flies and sequenced. The reading frame in these mutants is intact. The 910bp upstream of the genomic DNA have sufficient promoter activity to rescue the *rux* mutant phenotype (Thomas et al., 1997). A series of primers were designed to amplify sections of this promoter region by PCR (Fig. 2.1C). DNA fragments of the expected length were amplified from WT genomic DNA, but not *rux*² DNA (Fig. 2.1C), indicating that this particular mutation affects the *rux* promoter. As *rux*² males are fertile, this is still a certain amount of expression from the promoter, at least during spermatogenesis. However, this level is not sufficient to rescue the eye phenotype.

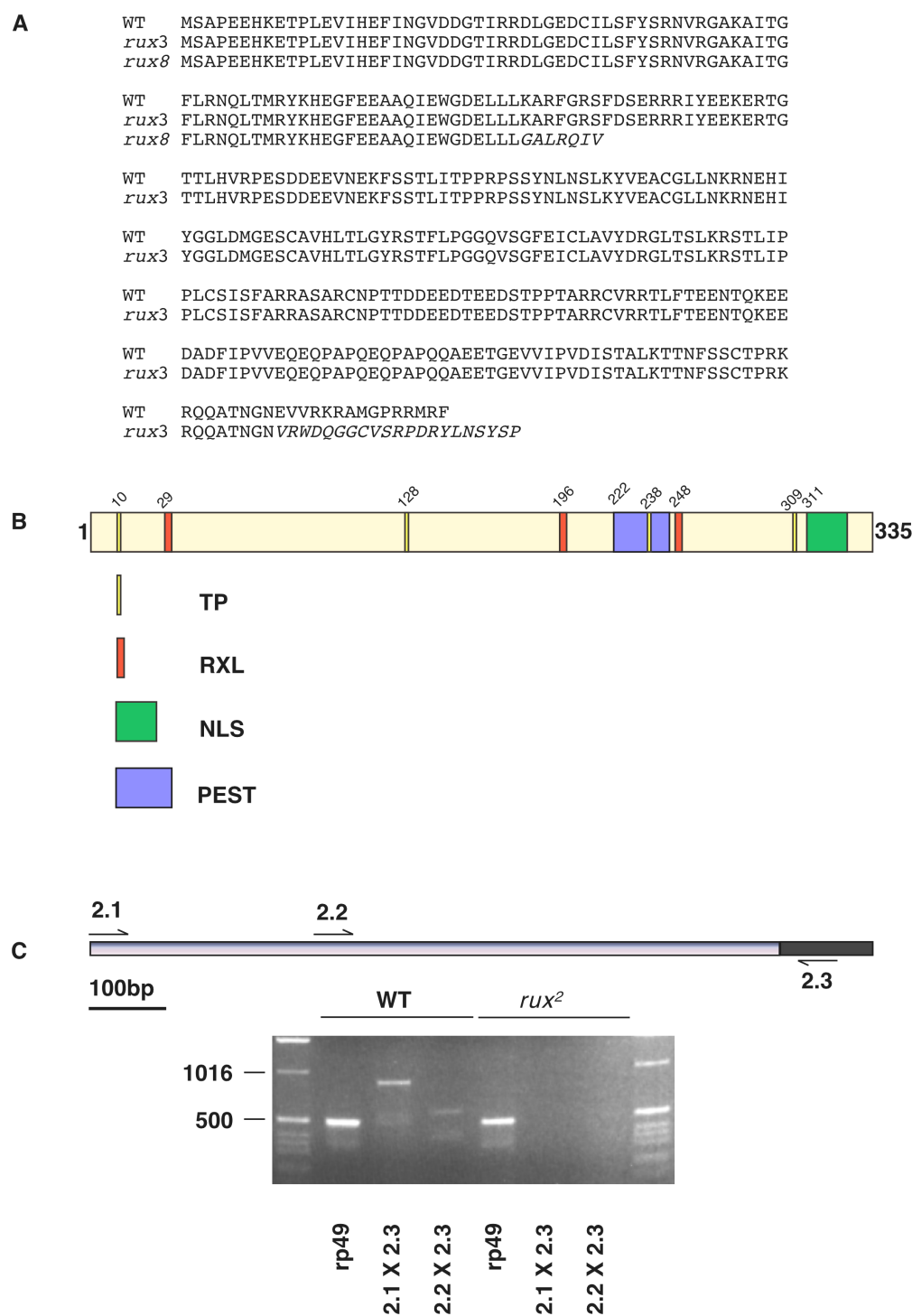


Fig. 2.1: Schematic representation of the Rux protein.

(A) The primary amino acid sequence of WT *rux* and two mutant alleles, *rux*³ and *rux*⁸ used in this study. Italicized residues indicate the out of frame amino acids. **(B)** A schematic representation of the WT Rux protein, indicating potential CDK-phosphorylation sites (TP), cyclin-binding motifs (RXL), a putative bipartite nuclear localization sequence (NLS) and a PEST motif (PEST). **(C)** A schematic representation of the region 900bp upstream of the start site of the *rux* ORF. The ORF is represented as a black box and the promoter as a gray box. The scale bar represents 100bp. The relative positions of the three primers 2.1, 2.2 and 2.3 used to amplify genomic DNA are indicated. Genomic DNA was isolated from single WT or homozygous *rux*² mutant flies. As a control the *rp49* locus was amplified with the primers *rp491* and *rp492* for WT (lane 2) and *rux*² (lane 5). PCR amplification with primers 2.1 and 2.3 and primers 2.2 and 2.3 successfully amplified fragments of the expected length for WT DNA (lanes 3 and 4 respectively), but not *rux*² DNA (lanes 6 and 7 respectively). 1kb ladders are loaded in lanes 1 and 8.

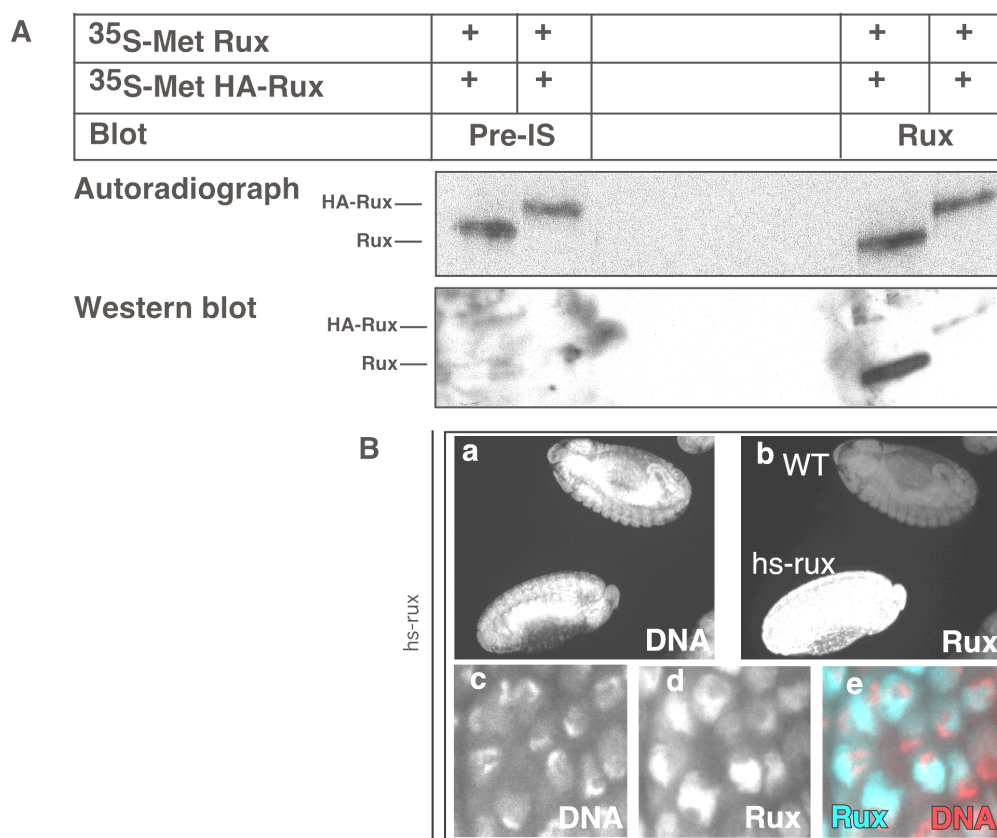


Fig. 2.2: Production of an anti-Rux antiserum.

(A) Rats were immunized with a gel slice containing purified GST-Rux. Purified immune serum recognizes *in vitro* translated WT Rux and HA-tagged Rux on a Western blot, whereas the pre-immune serum does not. To confirm translation of the proteins they were radiolabeled with ³⁵S-Met and visualized by autoradiography. **(B)** Anti-Rux antiserum recognizes a protein in embryos after induction of *rux* expression from a heat-inducible transgene (b, *hs-rux*), whereas WT embryos of the same stage do not stain as intensely (b, WT). The protein recognized by the antiserum is nuclear (d), and is excluded from the nucleolus (c and e).

Rux protein localization.

A polyclonal antiserum was prepared against Rux to analyze Rux protein expression and localization. For immunization a GST-Rux fusion protein was purified using glutathione-agarose beads. This protein was isolated as an SDS polyacrylamide gel slice and used to immunize rats. The antiserum recognizes *in vitro* translated Rux and HA-tagged Rux protein (Fig. 2.2A, blot: Rux), whereas the pre-immune serum did not (Fig. 2.2A, blot: PIS). The antiserum also recognized a protein in embryos upon induction of *rux* expression through a heat-inducible promoter (Fig. 2.2Bb, *hs-rux*) and not in WT embryos of the same stage (Fig. 2.2Bb, WT). Thus, this antiserum is specific for the Rux protein, but it does not detect endogenous Rux expression. The Rux protein expressed upon induction from the heat-inducible promoter is nuclear (Fig. 2.2Bd-e) in agreement with a previous report which looked at the

Fig. 2.3: The nuclear localization of Rux is determined by a bipartite NLS in the C-terminus.

(A) Sequence of the C-terminus of Rux from amino-acids 308 to 319 and the consensus sequence for a bipartite NLS. The basic clusters in Rux are indicated in bold. The amino acid sequence of a deletion construct (Rux Δ NLS), where the second basic cluster is removed is also shown. Z indicates a stop codon.

localization of overexpressed Rux or a Rux-lacZ fusion in the eye disc (Thomas et al., 1997).

To determine if the nuclear localization of Rux is mediated by its C-terminal bipartite NLS a hemagglutinin (HA)-tagged Rux construct was made where the NLS was deleted (Fig. 2.3A, HA-Rux Δ NLS). This was transiently expressed in *Drosophila* embryos by injecting RNA encoding the deletion construct into pre-cellular embryos. After a 2hr recovery period, injected embryos were stained with a monoclonal anti-HA antibody to determine the subcellular localization of HA-Rux Δ NLS. As a control embryos were injected with RNA encoding a HA-tagged full length Rux (HA-Rux). Similar to WT Rux, HA-Rux is a nuclear protein (Fig. 2.3Ba). Therefore, an N-terminally attached tag on the Rux protein does not affect the subcellular localization of Rux. HA-Rux Δ NLS is exclusively cytoplasmic (Fig. 2.3Be), indicating that the putative C-terminal NLS is responsible for nuclear localization. Interestingly, CycA colocalizes in the nucleus with Rux during interphase. This observation is in agreement with previous reports that overexpression of Rux leads to a nuclear translocation of CycA (Sprenger et al., 1997; Thomas et al., 1997).

(B) HA-Rux is a nuclear protein (a) that induces a nuclear accumulation of CycA (b). HA-Rux Δ NLS is a cytoplasmic protein, confirming that nuclear accumulation of Rux is mediated by a bipartite NLS in the C-terminus (e). Rux Δ NLS and CycA colocalize in the cytoplasm (h).

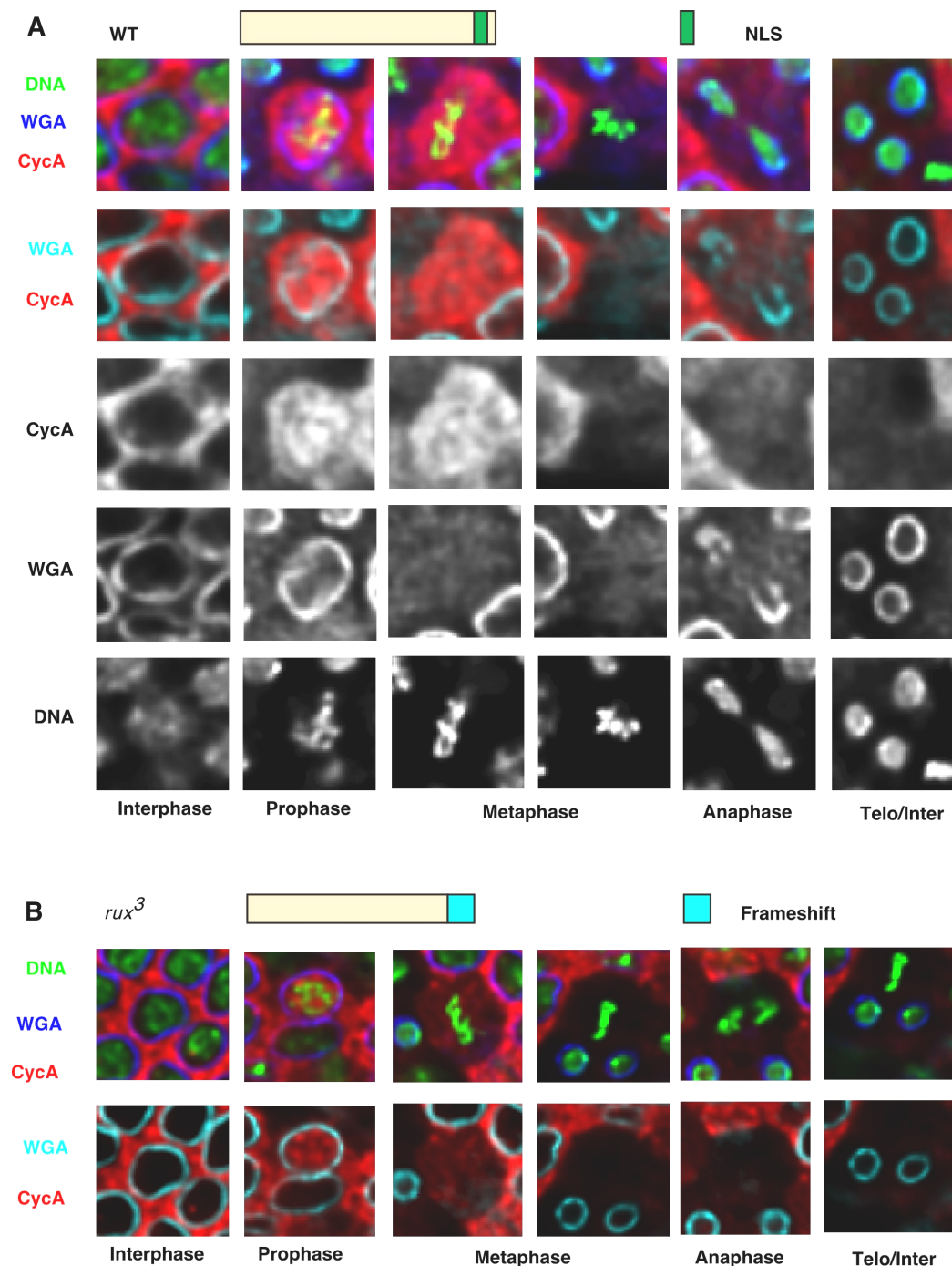


Fig. 2.4: The dynamic subcellular distribution of CycA is not disturbed in *rux³* mutants.

(A) Individual cells from WT embryos in the 14th cell cycle are stained for DNA with bisbenzidine, CycA with anti-CycA antibodies and the nuclear envelope with wheat germ agglutinin (WGA). WGA binds specifically to O-linked glycosylated proteins of the nuclear envelope. DNA morphology is used as a marker for the different cell cycle stages. DNA is decondensed during interphase, condenses during prophase and aligns on the metaphase plate during metaphase. Sister chromatids are pulled to separate poles during anaphase and decondense in telophase. The nuclear envelope is intact during interphase. Nuclear envelope breakdown occurs at the prophase/metaphase transition and persists through anaphase and telophase. CycA is a cytoplasmic protein during interphase, accumulates transiently in the nucleus during prophase, is distributed evenly throughout the cell following nuclear envelope breakdown and is destroyed during metaphase. (B) CycA has the same subcellular distribution in *rux³* mutants as in WT embryos.

CycA displays a dynamic change in subcellular localization during progression through the cell cycle. The protein is cytoplasmic during S phase and G2 and accumulates in the nucleus during prophase. After nuclear envelope breakdown at the prophase/metaphase transition CycA is found throughout the cell. The protein is then destroyed during metaphase (Fig. 2.4A). As WT Rux induces a nuclear accumulation of CycA, it is conceivable that the nuclear accumulation of CycA observed in Wt cells is mediated by Rux. To determine if this is the case CycA localization was analyzed in *rux* mutant embryos. *rux*³ was used for this analysis, as this mutation affects the NLS in Rux. HA-RuxΔNLS has a very similar sequence to *rux*³, strongly arguing that *rux*³ is an endogenous RuxΔNLS. The subcellular localization of CycA during the cell cycle was compared for WT and *rux*³ embryos (Fig. 2.4A and B respectively). In both cases CycA was strictly cytoplasmic during interphase, accumulated in the nucleus during prophase, was homogeneously distributed in the cell following nuclear envelope breakdown and was destroyed upon progression through metaphase. These results suggest that Rux does not govern the nuclear accumulation of CycA during prophase.

Rux interacts with CycA and CycB in *Drosophila* embryos

As CycA segregates into the same subcellular compartments as overexpressed Rux it is possible that both proteins form a physical complex. This was examined in co-precipitation experiments. Rux was overexpressed in 3-5hr embryos from a heat-inducible promoter. Rux was then precipitated from a hs-rux embryonic extract and the precipitate analyzed for CycA by Western Blotting. CycA coprecipitated with Rux (Fig. 2.5A, lane 4). CycA did not precipitate with pre-immune serum (lane 3) and Rux antiserum did not coprecipitate the even-skipped control proteins (lane 6), indicating that the interactions observed between Rux and CycA are specific. The same results

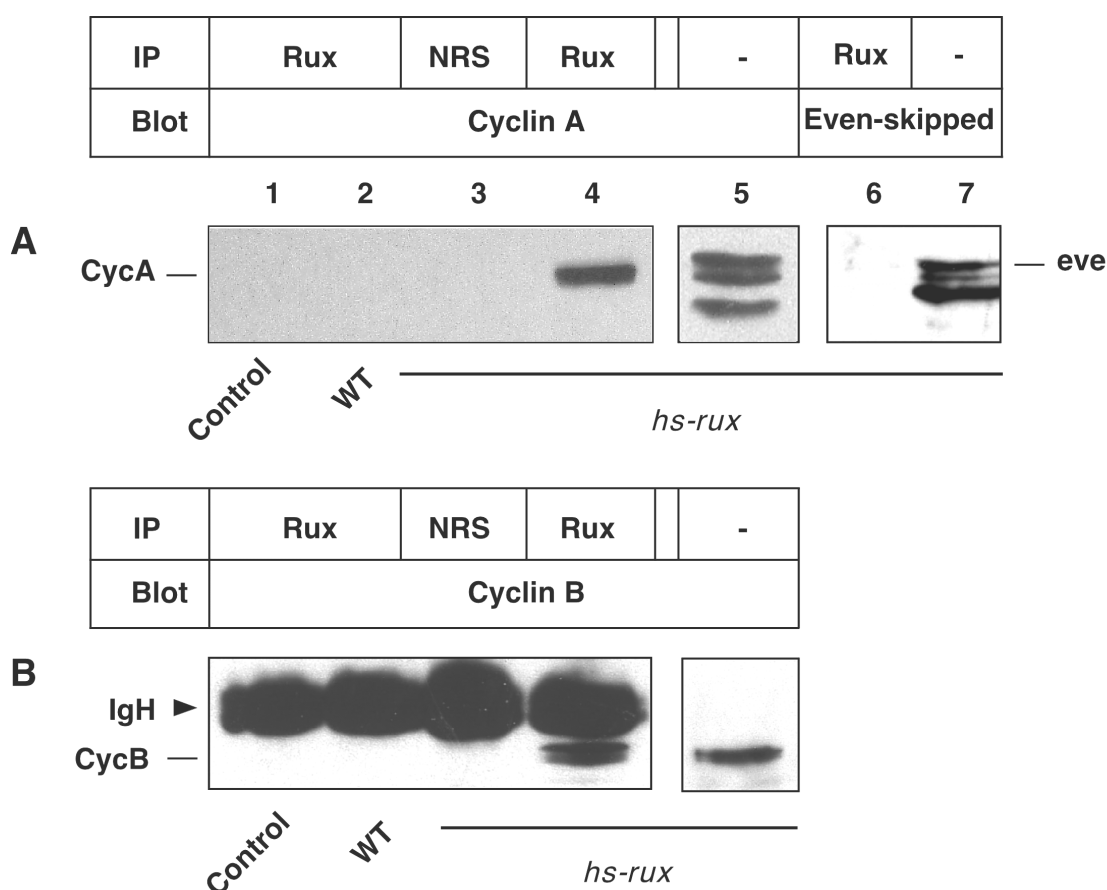


Fig. 2.5: Rux physically associates with CycA and CycB.

Rux was overexpressed in 3-5hr embryos from a heat-inducible transgene (lanes 3-7, hs-rux). An extract prepared from hs-rux embryos was precipitated with normal rat serum (lane 3, NRS) or rat anti-Rux (lane 4) serum. As controls buffer (lane 1) or a WT extract (lane 2) was precipitated with the Rux antiserum. The individual precipitates were probed by Western blotting for the presence of CycA (upper panel) or CycB (lower panel) with anti-CycA and anti-CycB antibodies respectively. As controls unprecipitated extract was probed for CycA or CycB (lane 5). The Rux antiserum specifically precipitates CycA and CycB from hs-rux extracts. The arrowhead in the CycB blot indicates the position of the heavy chain from the IP reaction. As a control extract was precipitated with the anti-Rux antiserum and assayed for the presence of the even-skipped protein (lane 6). Unprecipitated extract was probed with anti-eve antiserum to show the expected position of the protein (lane 7).

were observed when the precipitate fractions were analyzed by Western blotting with an anti-CycB antiserum (Fig. 2.5B). Thus, it appears that Rux physically associates with both mitotic cyclins A and B.

CycA and CycB are required for execution of mitosis. As Rux interacts with both cyclins the effect of Rux on progression through mitosis was examined. Rux was expressed in segmental stripes of the embryonic epidermis by crossing UAS-rux flies to *prd-GAL4* flies. *prd-GAL4* induces gene expression from UAS promoters during cell cycle 15 (data not shown). Expression of Rux using the *prd-GAL4* driver line inhibited progression through mitosis (Fig. 2.6). Nuclear density was approximately twice as high in interstripes as in paired stripes (Fig. 2.6b and c), showing that Rux overexpression induces a pre-mitotic cell cycle arrest.

The kinase activity of Cdk1 in embryos overexpressing Rux was measured to determine whether Rux induces a cell cycle arrest by downregulating Cdk1. A standard assay of Cdk1 activity is to monitor its ability to incorporate radiolabeled phosphate into the *in vitro* substrate histone H1. Cdk1 was precipitated from a number of different 3-5hr extracts and analyzed in a H1 kinase assay (Fig. 2.7). The H1 kinase activity precipitated from wild-type embryos was set to 100% (lane 5). CycA induction led to an almost eight-fold increase in kinase activity (lane 6). This was reduced to WT levels when Rux was co-expressed (lane 7). Kinase activity in embryos overexpressing Rux (lane 8) was approx. 40% of wild-type embryos. Thus, it appears that Rux inhibits Cdk1 activity in embryos.

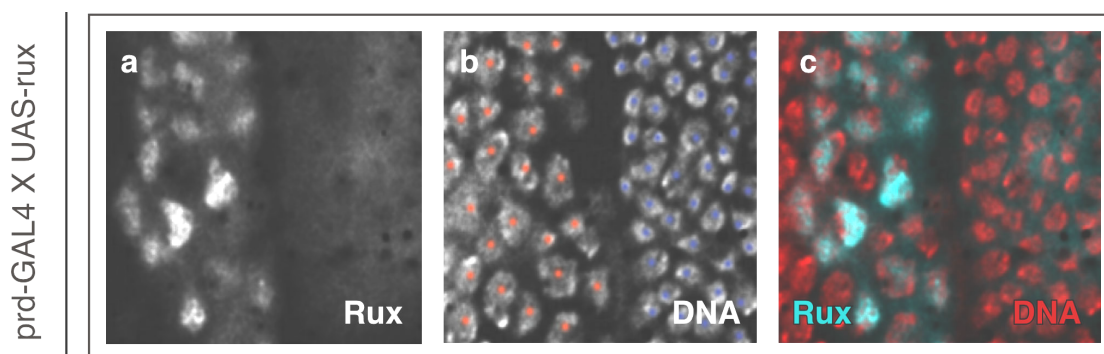


Fig. 2.6: Rux overexpression prevents mitosis.

Rux was over expressed in alternating segmental stripes of the embryonic epidermis from a UAS transgene (UAS-rux) by crossing UAS-rux flies to paired-GAL4 (*prdGAL4*) flies (a). The nuclear density in Rux-expressing cells is half of that in non-expressing cells (b), showing that Rux prevents execution of mitosis 15. DNA was visualized by staining with bisbenzidine and Rux with the anti-Rux antiserum. A merge of (a) and (b) is shown in (c) with Rux in blue and DNA in red.

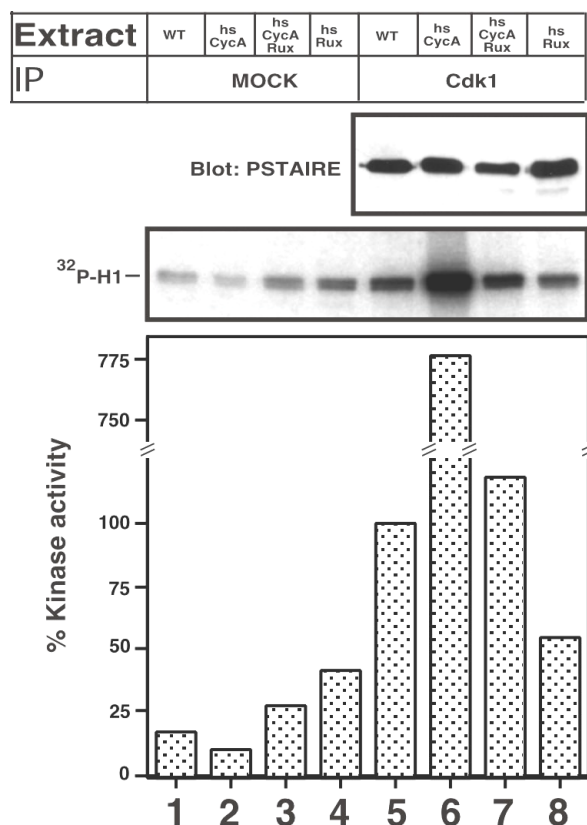


Fig. 2.7: Rux inhibits embryonic Cdk1 kinase activity.

Cdk1 was precipitated with a polyclonal anti-Cdk1 antiserum from embryonic extracts prepared from 3-5hr WT (lane 5), hs-cycA (lane 6), hs-cycA ; hs-rux embryos (lane 7) and hs-rux (lane 8) embryos. To confirm that equal amounts of Cdk1 were precipitated from each extract a sample was analyzed by Western blotting with an anti-PSTAIRE antibody (upper panel, PSTAIRE blot). Each precipitated sample was assayed for its ability to incorporate radiolabeled phosphate into the *in vitro* CDK substrate, histone H1 (central panel). The kinase activity of WT extract was set to 100% (lower panel, lane 5). The overexpression of CycA greatly enhances Cdk1 activity (lane 6) and this is reverted by co-expression of Rux (lane 7). Furthermore, overexpression of Rux inhibits Cdk1 activity close to background levels (lane 8). To determine background levels equal volumes of the same extracts were mock-precipitated with normal rabbit serum and assayed in H1 kinase assays (lanes 1-4).

Cdk is tightly regulated by the independent activity of several intrinsic and inducible cellular processes. A highly conserved means of inhibiting Cdk1 is phosphorylation of several conserved residues. Phosphorylation of Cdk1 on T14 and Y15 by wee and myt kinases inhibits CDK activity (Morgan, 1995). This is reversed by String ($Cdc25^{Stg}$), the *Drosophila* homologue of the Cdc25 phosphatase (Edgar and O'Farrell, 1989). $Cdc25^{Stg}$ mediated activation of Cdk1 is the rate-limiting step for initiation of mitosis (Edgar and O'Farrell, 1990). $cdc25^{Stg}$ levels are controlled by zygotic transcription which precedes mitosis by a couple of minutes and occurs asynchronously throughout the embryo. The expression of $cdc25^{Stg}$ and subsequent mitoses occur in 25 distinct domains in a symmetrical pattern along the anterior/posterior axis of the embryo. As CycA is destroyed upon progression through

mitosis the disappearance of CycA is a reliable reporter for completion of mitosis in the different domains.

A wild-type embryo is shown in Fig. 2.8Aa where mitosis has occurred in approx. half the embryo, as judged by the absence of CycA. In a *hs-rux* embryo CycA was present throughout the entire embryo (Fig. 2.8Ab). Using the extent of germband extension as a marker for age (Fig. 2.8Ab, arrowhead) approximately half of all cells in this embryo should have completed mitosis and degraded CycA. Thus, in agreement with previous reports and as described in Fig. 2.6 overexpression of Rux inhibited mitosis (Thomas et al., 1997). Overexpression of *stg* induced mitosis throughout the embryo (Fig. 2.8Ac) but mitosis did not occur in embryos where *stg* and *rux* were co-expressed (Fig. 2.8Ad). This experiment does not determine whether Rux downregulates Cdk1 by inducing an inhibitory phosphorylation of Cdk1 on T14 or Y15. To address this question *rux* was co-expressed with a Cdk1 where the inhibitory T14 and Y15 residues were replaced by an alanine and phenylalanine respectively (*cdc2^{AF}*). As this Cdk1 cannot be inhibited by wee and myt like kinases its activation does not require the presence of the Stg phosphatase. Therefore, a ubiquitous expression of *cdc2^{AF}* and *cycA* induces mitosis in all cells of the embryo (Fig. 2.8Ae). When *rux* was co-expressed in this background mitosis was once more inhibited (Fig. 2.8Af). Thus, Rux does not inhibit Cdk1 by inducing inhibitory phosphorylation of Cdk1, as it inhibits Cdk1 irrespective of the phosphorylation status of T14 and Y15.

Cdk1 was precipitated from *hscdc2^{AF}/hscycA* and *hscdc2^{AF}/hscycA/hsrux* embryos and Cdk1 activity was monitored in a H1 kinase assay (Fig. 2.8B). The H1 kinase activity of Cdk1 was reduced by almost 75% in *hscdc2^{AF}/hscycA/hsrux* embryos compared to *hscdc2^{AF}/hscycA* embryos. A second fraction of the Cdk1 precipitate was analyzed by Western blotting using SDS-PAGE conditions that allowed the separation of distinct phosphoisoforms of Cdk1 (Edgar et al., 1994). Under these conditions T14 or Y15 phosphorylated Cdk1 have the slowest mobility. Unphosphorylated Cdk1 has a slightly higher mobility and T161 phosphorylated Cdk1 displays the highest mobility (Fig. 2.8B). Cdk1 is activated by phosphorylation on T161 in the T-loop by CAK (Cdk Activating Kinase). Interestingly, the T161-phosphorylated isoform was barely present in *hscdc2^{AF}/hscycA/hsrux* embryos. Thus, the overexpression of Rux in embryos appears to inhibit mitosis by preventing both Cdk activation and activity.

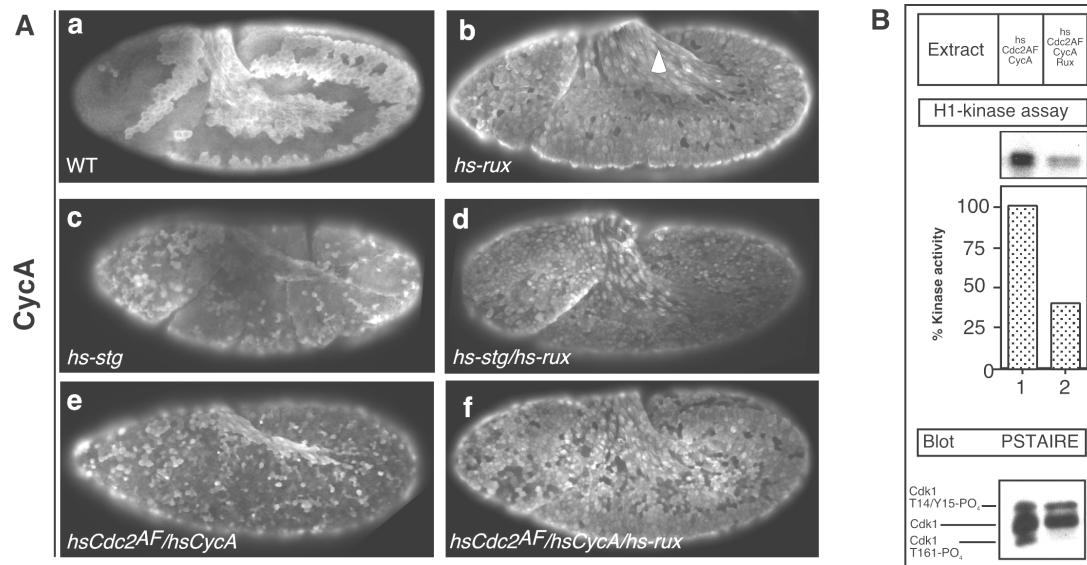


Fig. 2.8: Rux does not inhibit Cdk1 by regulating inhibitory phosphorylation of Cdk1.

(A) Mitosis 14 occurs in asynchronous domains on the embryonic epidermis, as can be distinguished by the stereotyped pattern of CycA disappearance (a). Overexpression of Rux in *hs-rux* embryos arrests cells before mitosis, preventing CycA destruction (b). Overexpression of *Cdc25^{Stg}* induces mitosis in most cells simultaneously. Arrowhead indicates the tip of the extending germband (c). This effect is inhibited by co-expression of Rux (d). The effect of *Cdc25^{Stg}* overexpression is mimicked by overexpression of CycA and a Cdk1 refractory to wee and myt-mediated inhibition (*Cdc2^{AF}*) (e). *Cdc2^{AF}/CycA* do not induce mitosis when co-expressed with Rux (f). Thus, Rux inhibits Cdk1 activity in a manner that does not rely on phosphorylation of T14 or Y15 on Cdk1. **(B)** Cdk1 precipitated from *hs-cdc2^{AF}*; *hs-cycA* has a high kinase activity (upper panel, lane 1 set to 100%) and is highly phosphorylated on T161 (lower panel, lane 1). In contrast, Cdk1 activity is reduced in a *hs-cdc2^{AF}*; *hs-cycA*; *hs-rux* extract (upper panel, lane 2) and is not phosphorylated on T161 (lower panel, lane 2).

In summary, Rux is a *Drosophila* cell cycle regulator with no obvious homologues. It is a nuclear protein and the nuclear localization of Rux is mediated by a bipartite NLS in the C-terminus of the protein. Rux physically associates with the mitotic cyclins A and B and triggers a nuclear accumulation of both when overexpressed. High level expression of Rux inhibits mitosis, independent of regulating Stg activity and reduces embryonic Cdk1. The reduction of Cdk1 activity is associated with a decrease in the extent of T161 phosphorylation on Cdk1.

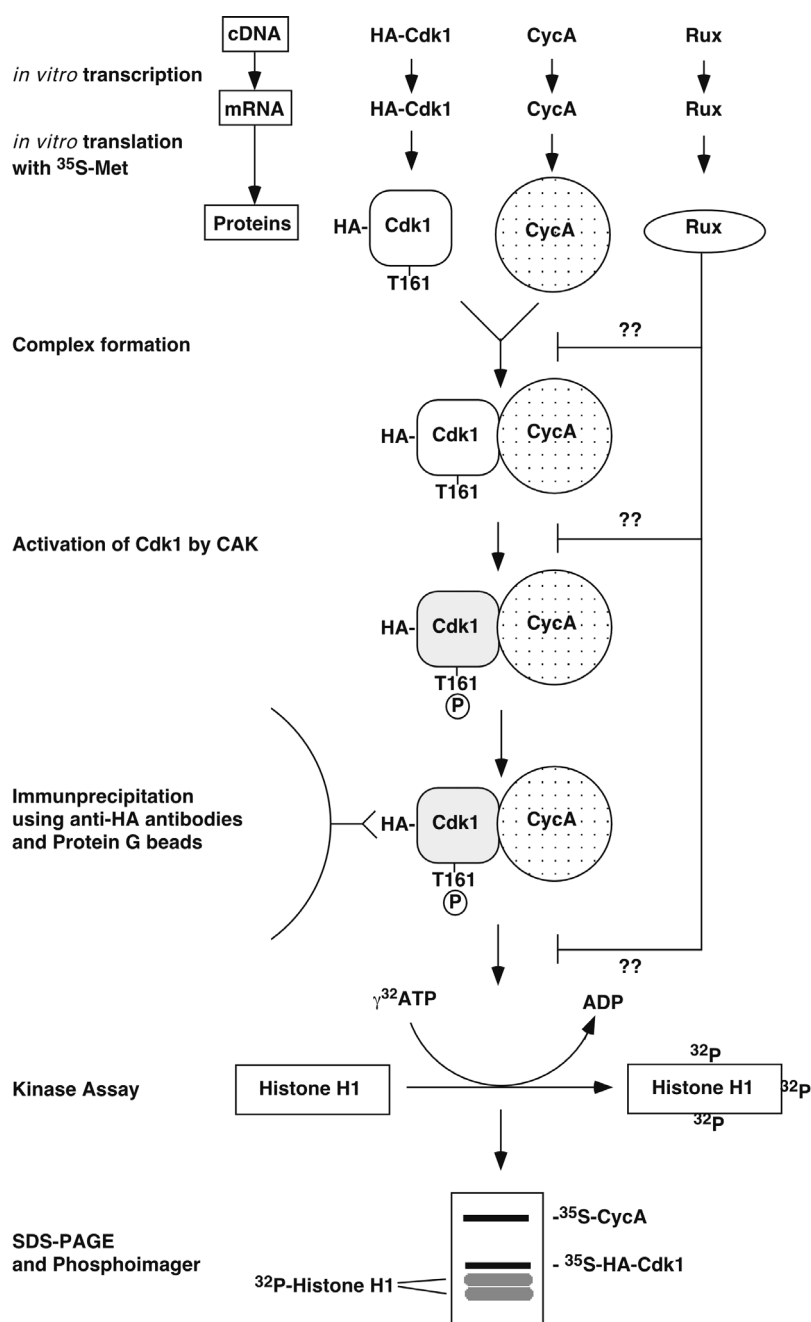


Fig. 2.9: An *in vitro* assay of CDK kinase activity.

HA-tagged CDKs, their cyclin partners and Rux were transcribed and translated *in vitro* using ³⁵S-Met as a radiolabel to allow monitoring of the individual proteins. Active Cdk/cyclin complexes were formed by mixing the correct proteins with a source of CDK Activating kinase (CAK). CAK phosphorylates Cdk1 on T161, thereby inducing a conformational change in the T-loop of the CDK and allowing access of CDK substrates to the active site. Either a crude embryonic extract or purified yeast Civ1p were used as CAK. After activation, HA-tagged CDK/cyclin complexes were precipitated with anti-HA antibodies and protein-G beads, washed and tested for their ability to phosphorylate histone H1. H1 phosphorylation was visualized by autoradiography and quantified with a phosphorimager.

Rux inhibits Cdk1/CycA and Cdk1/CycB complexes

Overexpression of Rux in embryos shows that Rux can inhibit Cdk1 activity. To analyze the biochemical nature of this effect, an *in vitro* assay was used in which the different steps of Cdk1 activation and activity can be monitored (Foley, 1997). cDNA coding for different CDKs and their respective cyclin partners were transcribed *in vitro* (Fig. 2.9). The resulting mRNAs were translated in a reticulocyte lysate and radiolabeled with ^{35}S -Met to allow visualization of distinct proteins. The CDKs were HA-tagged at the C-terminus to allow their purification. CDKs were mixed with their cyclin partners and co-incubated with a source of CAK to activate CDKs by phosphorylation on T161. The CDK/cyclin complexes were immunoprecipitated with an anti-HA antibody, washed several times and monitored for their ability to incorporate radiolabeled phosphate in H1. This assay has several advantages. The relative amounts of different proteins can be experimentally controlled, the order in which different complexes are assembled and the time point at which Rux is added can also be decided. As all proteins are radiolabeled it is possible to determine covalent modifications such as inhibitory or activating phosphorylations on CDKs.

In the first experiment the effect of Rux on Cdk1/CycA, Cdk1/CycB and Cdk2/CycE was monitored. HA-tagged Cdk1 and Cdk2, CycA Δ 170, CycB Δ 46, CycE and Rux were translated in the presence of ^{35}S -Met (see Figure 2.10A for translation products). The proteins were co-incubated with a 0-1hr embryonic extract which served as a source of CAK. CDKs alone were incubated with extract as a negative control. CDKs and cyclins were co-incubated as positive controls. The N-terminal truncations of CycA (CycA Δ 170) and CycB (CycB Δ 46) were used as they are stable in an embryonic extract and are capable of activating CDKs *in vitro*. After incubation the complexes were purified by anti-HA immunoprecipitation and tested in H1 kinase assays. Cdk1 alone had minimal kinase activity (Fig. 2.10D and E, lane 1). Co-incubation of Cdk1 with either CycA or CycB led to an increase in H1 kinase activity (Fig. 2.10D and E, lanes 2 and 4, respectively). The activity of Cdk1/CycA was set to 100%. Similarly Cdk2 alone is essentially inactive (Fig. 2.10D and E lane 6) and Cdk2/CycE complexes had strong kinase activity (Fig. 2.10D and E lane 7).

The kinase activity of Cdk1/CycA or Cdk1/CycB was greatly reduced after co-incubation with Rux (Fig. 2.10D and E lanes 3 and 5 respectively). Cdk1 kinase activity was inhibited to almost background levels in the presence of Rux. On the other hand, Rux did not inhibit Cdk2/CycE. Cdk2/CycE was an equally potent kinase in the absence or presence of Rux (compare Fig. 2.10D and E, lanes 7 and 8 respectively). Therefore, Rux specifically inhibits the *in vitro* kinase activity of Cdk1.

This is in agreement with previous reports, where Rux inhibits Cdk1, but not Cdk2 in an *in vivo* context.

A second fraction of the Cdk1 precipitates was monitored using SDS-PAGE under conditions that allow distinction of CDK phosphoisoforms. The incubation of Rux with Cdk1 and CycA or Cdk1 and CycB reduced the level of T161 phosphorylation on Cdk1 when compared to Cdk1/CycA and Cdk1/CycB alone (Fig. 2.10C, lanes 2-5). In contrast no reduction in the T163 phosphorylation of Cdk2 is seen after addition of Rux (compare Fig. 2.10C, lanes 7 and 8). T163 on Cdk2 is the equivalent residue to T161 on Cdk1.

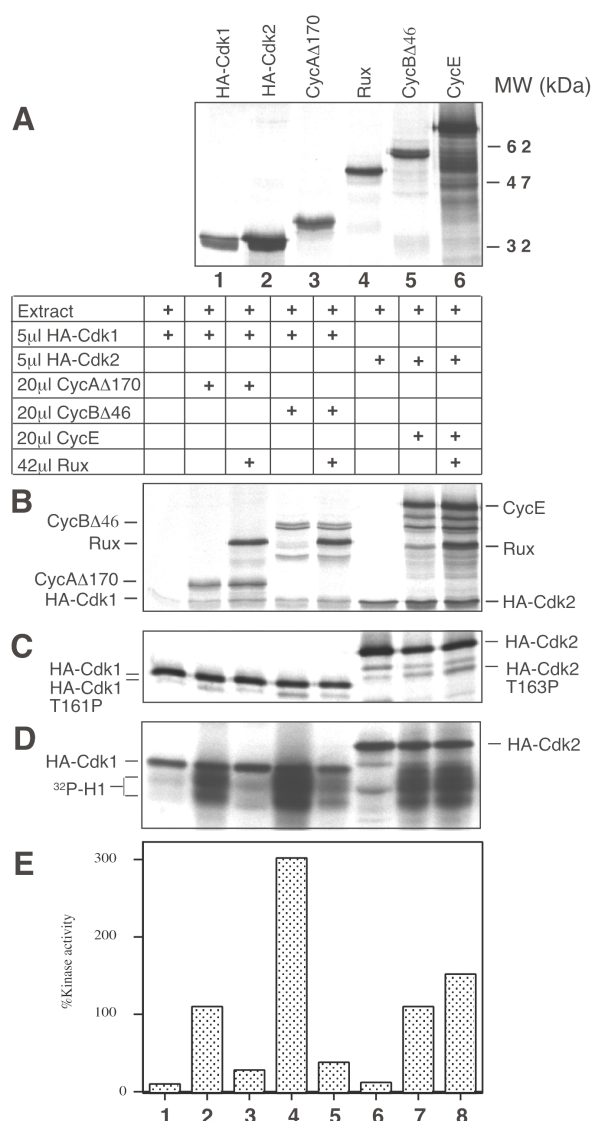


Fig. 2.10: Rux specifically inhibits Cdk1 *in vitro* kinase activity.

(A) A representative example of ^{35}S -Met labeled *in vitro* translated cell cycle proteins separated by SDS-PAGE. Rux migrates with an electrophoretic mobility of approx. 50kDa (lane 4). (B) Cdk1 was incubated alone (lane 1), with CycA (lane 2), CycB (lane 4), CycA and Rux (lane 3) or CycB and Rux (lane 5). Similarly, Cdk2 was incubated alone (lane 6), with CycE (lane 7) or CycE and Rux (lane 8). Each reaction was filled to an equal volume with reticulocyte lysate. CDKs were activated with embryonic extract as a source of CAK. After activation a sample was taken from each reaction and analyzed by SDS-PAGE as an input control. (C) CDK/cyclin complexes were precipitated with anti-HA antibodies and half the precipitate was analyzed by SDS-PAGE to separate CDKs into their constituent phosphoisoforms. Cdk1 is less T161 phosphorylated after co-incubation with Rux and CycA (lane 3) or Rux and CycB (lane 5) than after incubation with CycA (lane 2) or CycB (lane 4) alone. Rux does not diminish the extent of T163 phosphorylation of Cdk2. The T163 phosphoisoform is equally represented in Cdk2/CycE samples (lane 7) and Cdk2/CycE/Rux samples (lane 8). (D) A second half of the CDK/cyclin precipitate was monitored for its ability to phosphorylate H1. Cdk1 (lane 1) and Cdk2 (lane 6) are relatively inert kinases, which are activated by the addition of the correct cyclin partner; CycA and B for Cdk1 and CycE for Cdk2 (lanes 2, 4 and 7 respectively). CycB is more potent at stimulating Cdk1 (lane 4) than CycA (lane 2). Rux inhibits the H1 kinase activity of Cdk1/CycA (lane 3) and Cdk1/CycB (lane 5), whereas it does not inhibit the H1 kinase activity of Cdk2/CycE (compare lanes 7 and 8). (E) A graphical representation of the phosphorimaging of the H1 kinase activity in (D). The kinase activity of Cdk1/CycA was set as 100%.

The effect of Rux on the activity of different Cdk1/Cyc complexes was then analyzed in greater detail. The experimental setup employed was the same as described above. The effect of different amounts of Rux on fixed amounts of single Cdk/cyclin complexes was assayed. In these assays Rux had a relatively predictable effect on Cdk1/CycB complexes. Cdk1 alone was an inert kinase (Fig. 2.11D and E, lane 1). CycB considerably stimulated Cdk1 kinase activity (Fig. 2.11D and E, lane 2). This activity diminished as increasing amounts of Rux were used (Fig. 2.11D and E, lanes 3-6). Large amounts of Rux reduced kinase activity to background levels (compare Fig. 2.11D and E, lanes 1 and 6). A reduction in the extent of T161 phosphorylation on Cdk1 also accompanied Rux-mediated inhibition (Fig. 2.11C). The precipitated Cdk1 samples were analyzed by SDS-PAGE and Western Blotting for the relative levels of co-precipitating CycB (Fig. 2.11B). Equal amounts of CycB precipitated with Cdk1 irrespective of the amount of Rux added, indicating that Rux does not function by disrupting the Cdk1/CycB complexes.

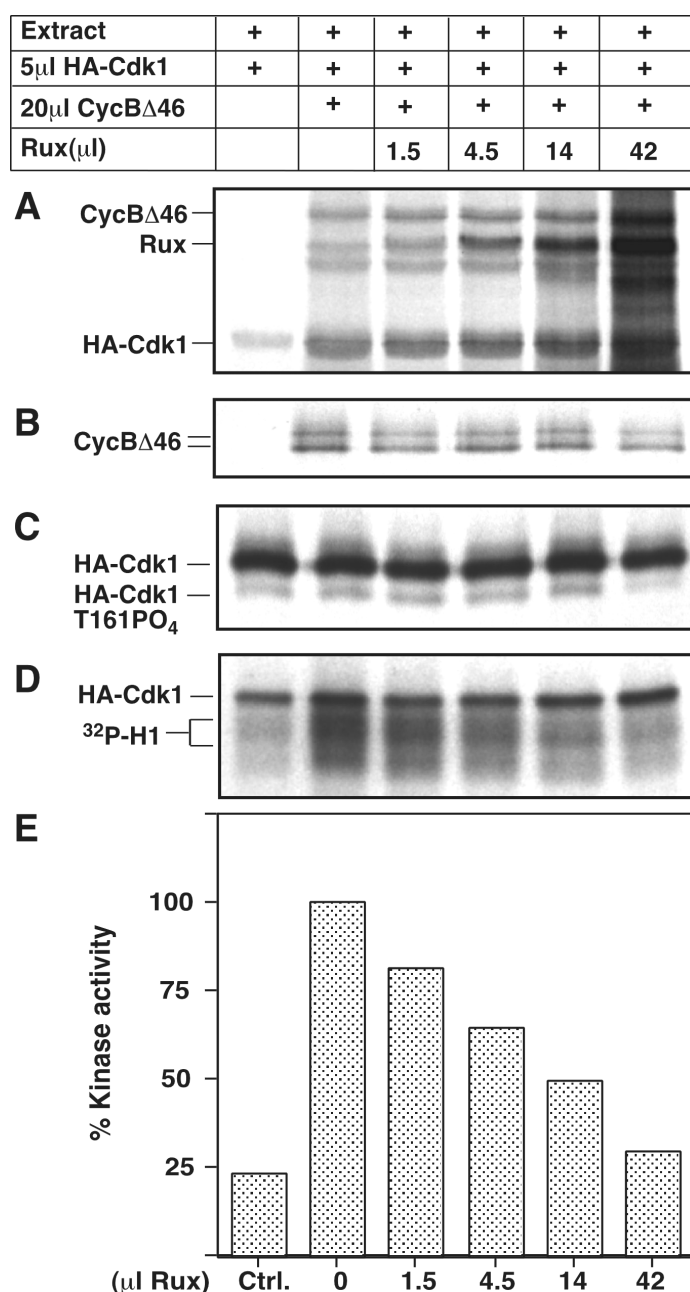


Fig. 2.11: Rux inhibition of Cdk1/CycB kinase activity *in vitro*.

(A) Equal amounts of Cdk1 and CycB were co-incubated with extract and increasing amounts of Rux. Each reaction was brought to an equal volume by the addition of reticulocyte lysate where necessary. An aliquot was taken from each sample after the activation of Cdk1/CycB by CAK to monitor input levels of the different proteins. **(B)** HA-Cdk1 was immunoprecipitated and the amount of co-precipitating CycB for the different samples determined by SDS-PAGE. CycB separates into two separate phosphoisoforms under these conditions. Regardless of the amount of Rux added approx. equal amounts of CycB co-precipitate with Cdk1. **(C)** Similarly, Cdk1 phosphoisoforms were distinguished by SDS-PAGE. A faint T161 phosphoisoform of Cdk1 is distinguishable in the absence of added cyclin (lane 1). This probably reflects the partnering of Cdk1 to cyclins provided in the extract. A consistent drop in the extent of T161 phosphorylation is discernible upon addition of large amounts of Rux (lane 6). **(D)** The H1 kinase activity of a fraction of the HA-immunoprecipitate was measured by autoradiography. Increasing amounts of Rux lead to a drop in the intensity of phosphorylation by Cdk1 (lanes 3-6). This experiment was repeated three separate time and identical results observed. **(E)** A graphical representation of the phosphorimaging of the H1 kinase activity in (D) confirms that as Rux levels increase H1 kinase activity decreases. The kinase activity of Cdk1/CycB was set to 100%.

Extract	+	+	+	+	+	+
5 μ l HA-Cdk1	+	+	+	+	+	+
20 μ l CycA Δ 170		+	+	+	+	+
Rux(μ l)			1.5	4.5	14	42

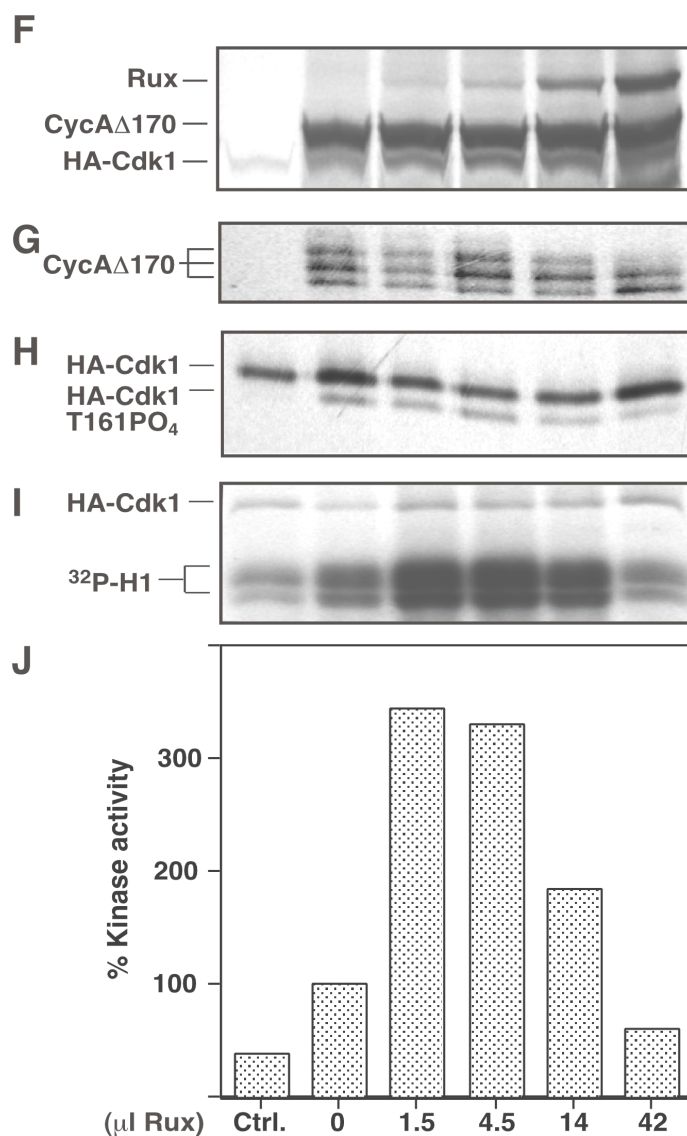


Fig. 2.12: Rux is a bimodal regulator of Cdk1/CycA *in vitro* kinase activity.

(A) Equal amounts of Cdk1 and CycA were co-incubated with extract and increasing amounts of Rux. Each reaction was brought to an equal volume by the addition of reticulocyte lysate where necessary. A sample was taken after the activation of Cdk1/CycA by CAK to monitor input levels of the different proteins and resolved by SDS-PAGE. (B) HA-Cdk1 was immunoprecipitated and the amount of co-precipitating CycA for the different samples determined by SDS-PAGE. CycA separates into several distinct phosphoisoforms under these conditions. The number of different isoforms are regularly proportional to the extent of Cdk1 activity (not shown). Irrespective of the amount of Rux added approx. equal amounts of CycA co-precipitate with Cdk1. (C) Cdk1 phosphoisoforms were distinguished by SDS-PAGE. A consistent drop in the extent of T161 phosphorylation is distinguishable upon addition of large amounts of Rux (lane 6). Although small amounts of Rux enhance Cdk1/CycA activity there is not a corresponding increase in the extent of T161 phosphorylation on Cdk1 (compare lanes 2 and 3). (D) The H1 kinase activity of a fraction of the HA-immunoprecipitate was measured by autoradiography. Large amounts of Rux lead to a drop in the intensity of phosphorylation by Cdk1 (lane 6), while low amounts of Rux greatly stimulate Cdk1/CycA activity (lane 3). This experiment was repeated five separate time and identical results observed. (E) A graphical representation of the phosphorimaging of the H1 kinase activity in (D). The kinase activity of Cdk1/CycA was set to 100%.

A surprising difference was observed when the experiments were repeated for Cdk1/CycA. As already described, Cdk1 alone displayed little kinase activity (Fig. 2.12D and E, lane 1) and was stimulated by the provision of a cyclin partner, in this case CycA (Fig. 2.12D and E, lane 2). Contrary to the results observed for Cdk1/CycB small amounts of Rux did not mildly reduce Cdk1/CycA activity. Instead, low levels of Rux enhanced Cdk1/CycA kinase activity by a factor greater than three (Fig 2.12D and E lanes 3 and 4). Only large amounts of Rux inhibited Cdk1/CycA kinase activity to background levels (Fig. 2.12D and E lanes 6). This inhibition was accompanied by a decrease in the extent of T161 phosphorylation on Cdk1 (Fig. 2.12C, compare lanes 2 and 6). However, the enhancement of Cdk1/CycA activity by low amounts of Rux did not have a corresponding increase in the extent of T161 phosphorylation (Fig. 2.12C, compare lanes 2 and 3). Thus, Rux does not appear to stimulate Cdk1 by enhancing the T161 phosphorylation of Cdk1. Enhancement of Cdk1/CycA activity does also not appear to arise as a result of enhancing Cdk1/CycA complex formation. Equal amounts of CycA precipitate with Cdk1 in the absence or presence of small amounts of Rux (Fig. 2.12B, compare lanes 2 and 3 respectively). Similarly, inhibition does not rely on disturbing Cdk1/CycA complex formation (Fig. 2.12B compare lanes 2 and 6).

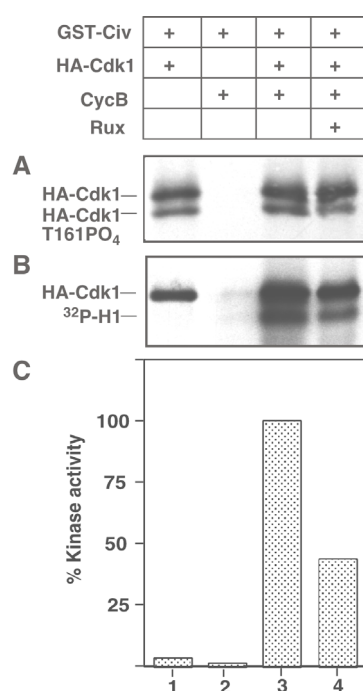


Fig. 2.13: Rux does not require additional *Drosophila* factors to inhibit Cdk1.

(A) The crude extract used in Figs. 9-11 was replaced with bacterially expressed and purified GST-Civ1p. Civ1 phosphorylates monomeric Cdk1 (lane 1) making it impossible to distinguish effects of Rux on T161 phosphorylation in this assay (lane 4). **(B)** Monomeric Cdk1 is inactive (lane 1), as is CycB (lane 2). Civ1 is a potent stimulator of Cdk1/CycB kinase activity (lane 3) and this is reduced by almost 60% upon co-incubation of Rux. **(C)** A graphical representation of the phosphorimaging of the H1 kinase activity in (B).

There is no obvious explanation for Rux enhancement of Cdk1/CycA activity. However, similar effects have been observed for other cell cycle regulators, such as *rum1* from *S. pombe* and mammalian p21 (Correa-Bordes and Nurse, 1995; Zhang et al., 1994). Interestingly, both of these proteins are Cyclin-dependent Kinase

Inhibitors (CKIs). CKIs have been identified in a large number of eukaryotes. Although there are no clearly conserved sequence motifs in all CKIs they have a defined set of functional characteristics. CKIs physically associate with CDKs, cyclins or both. They inhibit CDKs and prevent CDK activation, without covalently modifying CDKs. Based on the results presented above Rux fulfills these criteria. However, the inhibition of Cdk1 activity and activation was either observed in embryos or an *in vitro* system that used an embryonic extract as a source of CAK. Therefore, it cannot be excluded that Rux is a mediator protein that activates an unidentified CKI in *Drosophila* embryos.

To rule this possibility out the *in vitro* assay described above was repeated eliminating the embryonic extract and instead using GST-Civ1p as a source of CAK. CIV is the *S. cerevisiae* CAK. It is a monomeric protein of approximately 40kDa and has no homology to the *Drosophila* CAK; Cdk7/CycH. GST-Civ1p was expressed in bacteria and purified using glutathione-agarose beads. This was used to activate reticulocyte translated Cdk1/CycB. No additional *Drosophila* factors are required in this experiment, meaning that any effects observed are *Drosophila*-independent. Civ1p phosphorylated monomeric Cdk1 on T161 (Fig. 2.13A lane 1), (Kaldis et al., 1998). This monomeric Cdk had no kinase activity (Fig. 2.13B and C, lane 1). Upon addition of CycB, Cdk1 displayed strong H1 kinase activity (Fig. 2.13B and C, lane 3). When Rux was co-incubated with Cdk1 and CycB the kinase activity dropped to almost 40% of that for Cdk1/CycB alone (Fig. 2.13B and C, compare lanes 3 and 4). Thus, Rux directly inhibits Cdk1 in the absence of all other *Drosophila* factors.

Inhibition of Cdk1 by Rux in the assays described above always had a concomitant reduction in the level of T161 phosphorylation on Cdk1, raising the possibility that Rux inhibits Cdk1 by preventing the initial CAK-dependent activation. This question was addressed in a two-step assay. Cdk1 was activated by incubation with CycA and Civ1p (Fig. 2.14A and B, lane 3). In a second step, Rux was incubated with the activate Cdk1/CycA complexes. As a control, activate Cdk1/CycA was incubated with reticulocyte lysates. A fraction of each sample was removed and directly assayed for their ability to phosphorylate H1. The addition of Rux in the second step greatly diminished Cdk1 activity (Fig. 2.14A and B, compares lane 3 without Rux and lane 6 with Rux). Thus, Rux inhibited pre-activated Cdk1/CycA complexes. Precipitation of the individual samples with anti-HA antibodies and subsequent analysis of aliquots of the precipitate fractions confirmed that the Cdk1 had been successfully phosphorylated on T161 in the initial step. The Cdk1 incubated with CycA and Rux is as extensively phosphorylated on T161 as the Cdk1 incubated with CycA alone (Fig. 2.14C, compare lanes 12 and 9 respectively). Thus, inhibition by Rux did not depend

on regulating CAK activity and Rux did not recruit a phosphatase to inactivate Cdk1. Therefore, Rux does not solely rely on preventing T161 phosphorylation of Cdk1 as a means of inhibiting Cdk1 activity, rather Rux also inhibits T161-phosphorylated Cdk1/cyclin complexes.

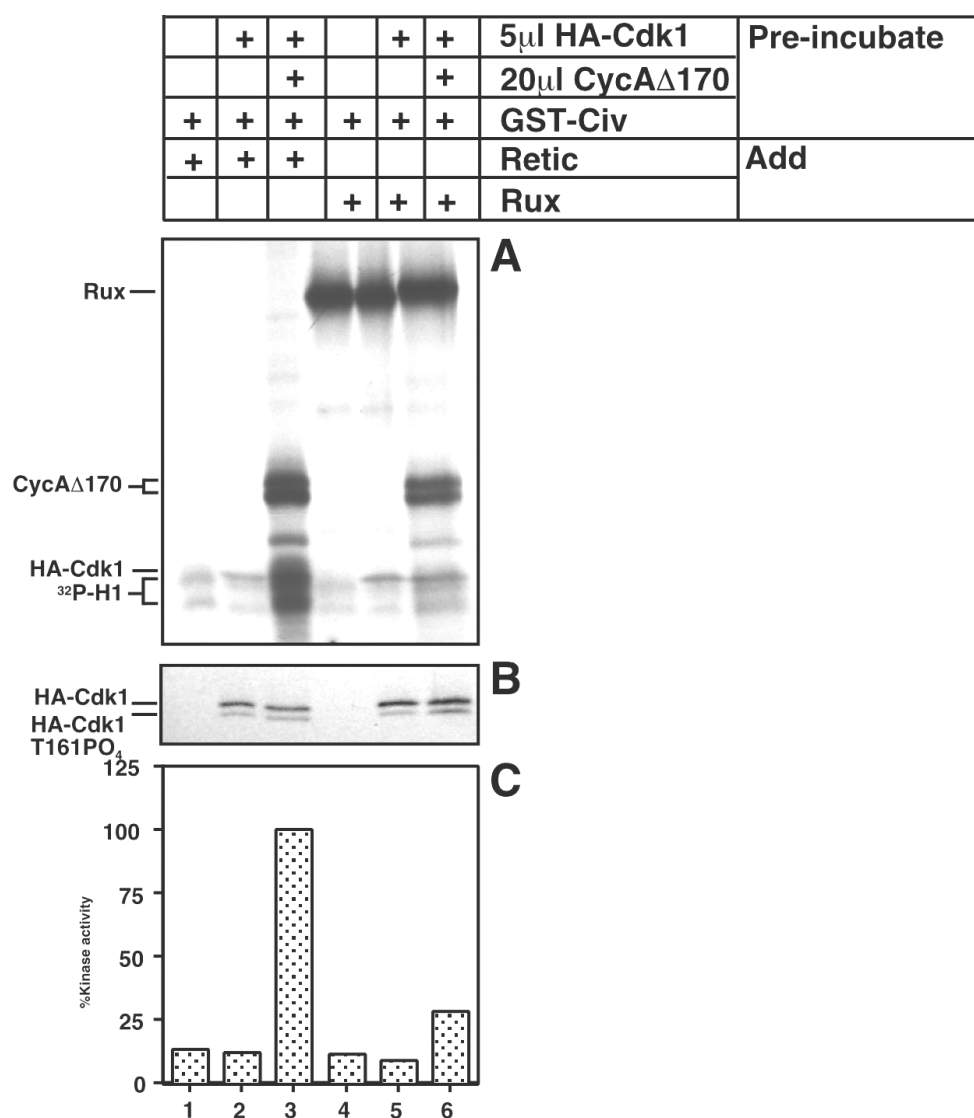


Fig. 2.14: Rux inhibits active Cdk1/CycA complexes.

(A) In a two-step experiment Cdk1 was activated by incubation with CycA and GST-Civ1p (lanes 3 and 6) for 20min. After activation Cdk1/CycA complexes were incubated with either reticulocyte lysate (lane 3) or an equal volume of Rux (lane 6) for an additional 20min. The H1 kinase activity of these samples was then directly assayed. As controls the activity of Cdk1 alone (lanes 1 and 4) or Cdk1 and Civ1p (lanes 2 and 5) were measured. The addition of Rux to activated Cdk1/CycA greatly diminishes Cdk1 activity (compare lanes 3 and 6). **(B)** The remainder of each sample was immunoprecipitated with anti-HA antibodies. A fraction was analyzed by SDS-PAGE to monitor T-161 phosphorylation. Cdk1 is as equally T161 phosphorylated in lane 3 as in lane 6, confirming that the Cdk1/CycA complexes had been activated before addition of Rux and that Rux did not diminish this phosphorylation. **(C)** A graphical representation of the phosphorimaging of the H1 kinase activity in (A).

The simplest interpretation of the result above is that Rux specifically inhibited Cdk1. Another potential interpretation is that the inhibition observed was not specific, rather that Rux is a substrate for Cdk1 and consequently functioned as a competitor with H1 for radiolabeled phosphate in the kinase assays. To exclude this possibility the endogenous kinase activity of an embryonic extract was assayed in the presence or absence of HA-Rux. As expected, an embryonic extract had high H1 kinase activity due to the presence of endogenous CDK/cyclin complexes (Fig. 2.15B and C, lane 1). Similar to the result described for Fig. 13, Rux inhibited embryonic CDK/cyclin activity (Fig. 2.15B and C, lane 2). Inhibition was not a result of diminishing T161 phosphorylation of Cdk1, as the T161 phosphoisoform was equally present either in the absence or presence of Rux (Fig. 2.15A, compare lanes 1 and 2 respectively). Furthermore, inhibition was not caused by Rux acting as a competitor with H1, as no

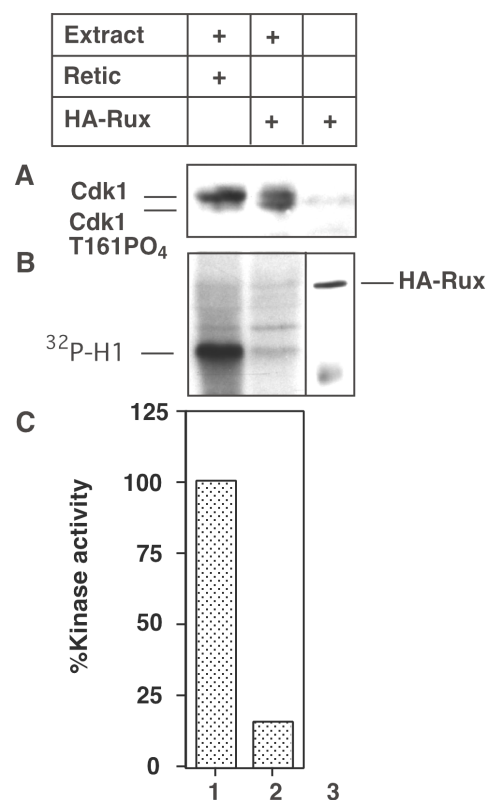


Fig. 2.15: Rux does not compete with *in vitro* substrates for phosphates.

(A) Extracts from 0-1hr embryos were incubated with reticulocyte lysate (lane 1) or non-radiolabeled HA-Rux (lane 2). Cdk1 analysis with anti-PSTAIR Western blotting showed that Rux did not reduce the extent of T161 phosphorylation on Cdk1 (compare lanes 1 and 2). **(B)** Both samples were analyzed directly in a H1 kinase assay. In lane 3 a Western blot of reticulocyte-translated HA-Rux is loaded as a control to mark the position of the HA-Rux in lane 2. The addition of HA-Rux reduced kinase activity to almost 14%, although no phosphorylation of Rux was observed. **(C)** Quantification of the H1 kinase activity in (B) by phosphorimaging. The kinase activity of extract without added Rux was set to 100%.

phosphorylation of Rux was observed (Fig. 2.15A, compare lanes 2 and 3). Therefore, Rux directly inhibits active Cdk1/cyclin complexes.

In conclusion, Rux specifically inhibits Cdk1 associated with either CycA or CycB. Rux directly inhibits Cdk1 activity and inhibits the initial Cdk1 activation step. These functions of Rux do not require additional *Drosophila* factors and are not caused by Rux competing with other substrates for Cdk1. Based on these results I propose that Rux is a novel *Drosophila* CKI. Rux is the first CKI to be characterized in a multicellular organism with specificity for mitotic cyclins. All other multicellular CKIs characterized to date inhibit G1 CDK/cyclin complexes. Both *S. cerevisiae* and *S. pombe* have CKIs specific for mitotic cyclins; SIC1 and *rum1* respectively. Therefore, the possibility arises that there is an evolutionarily conserved requirement for CKIs that regulate the activity of mitotic cyclins.

Rux interacts with CycA via two distinct RXL motifs.

As Rux has no obvious homologues in the databases it is difficult to deduce key amino acids from the primary sequence. Nonetheless, there are several short amino acid sequences in the Rux protein which have been identified as critical in other CKIs. One such sequence is the cyclin-binding, Cy or RXL motif (Adams et al., 1996; Chen et al., 1996). This motif has been identified in numerous proteins as mediating interactions with cyclins and consists of the amino acids arginine-X-lysine, where X is any amino acid. Recent three-dimensional structural analysis of the human CKI p27 revealed that the RXL motif inserts into the cyclin box of CycA (Russo et al., 1996). There are three RXLs in the Rux protein (Fig. 2.1B). Point mutations were introduced into the RXLs separately converting each motif to a KXK. The individual RXL mutant constructs were tested in three separate assays for their ability to interact with *Drosophila* CycA.

The first assay is based upon the observations described in Fig. 2.3 that overexpression of Rux leads to a nuclear accumulation of Rux and CycA. As Rux physically associates with CycA, it is possible that Rux RXL mutants with an impaired ability to interact with CycA will be less efficient at triggering a redistribution of CycA to the nucleus. RNA encoding a point mutation in the C-terminal RXL (HA-Rux Δ RXL3) motif was injected into pre-blastoderm embryos. A representative example is shown in Fig. 2.16. The RNA has been injected into the anterior of the embryo. HA-Rux Δ RXL3 has the same subcellular localization as wild-type Rux, i.e. it is a nuclear protein (Fig. 2.16b and f). Similar to wild-type Rux, HA-Rux Δ RXL3 directs a nuclear accumulation of CycA. CycA displays a nuclear localization in the anterior part of the embryo (Fig. 2.16e) and is exclusively cytoplasmic in interphase cells at the posterior of the embryo (Fig. 2.16i). The nuclear accumulation of CycA in the anterior of the embryo is not a consequence of cell cycle state of these cells. DNA staining reveals that all anterior cells are in interphase (Fig. 2.16d). At this stage of the cell cycle CycA is normally cytoplasmic (Fig. 4A, interphase). Thus, both wild-type Rux and HA-Rux Δ RXL3 are equally competent at driving a nuclear accumulation of CycA.

The embryo depicted is in the process of germband extension (Fig. 2.16a arrowhead). This is a process which begins early during mitosis 14. As mentioned above mitosis 14 occurs in a stereotyped pattern of domains over the embryo surface. In a wild-type embryo at this stage of germband extension mitosis 14 is ongoing in the anterior domains 1,2,5,6 and 7, as well as domain 4. Domain 4 is

located at the anterior tip of the extending germband. A number of condensed metaphase chromosomes can be detected in domain 4 (Fig. 2.16h, arrowheads and 2.16j). A correlating change in CycA subcellular localization occurs in the same mitotic cells (Fig. 2.16i and j), indicating that mitosis 14 occurs normally at the posterior of the embryo. No mitotic figures are visible at the anterior of the embryo where Rux Δ RXL3 is expressed, although at this stage mitosis occurs in domains 1,2 and 5 in WT embryos (Fig. 2.16d). Thus, identical to what has been described for wild-type Rux (Fig. 2.3), Rux Δ RXL3 is a nuclear protein, which when overexpressed drives a nuclear accumulation of CycA and inhibits mitosis.

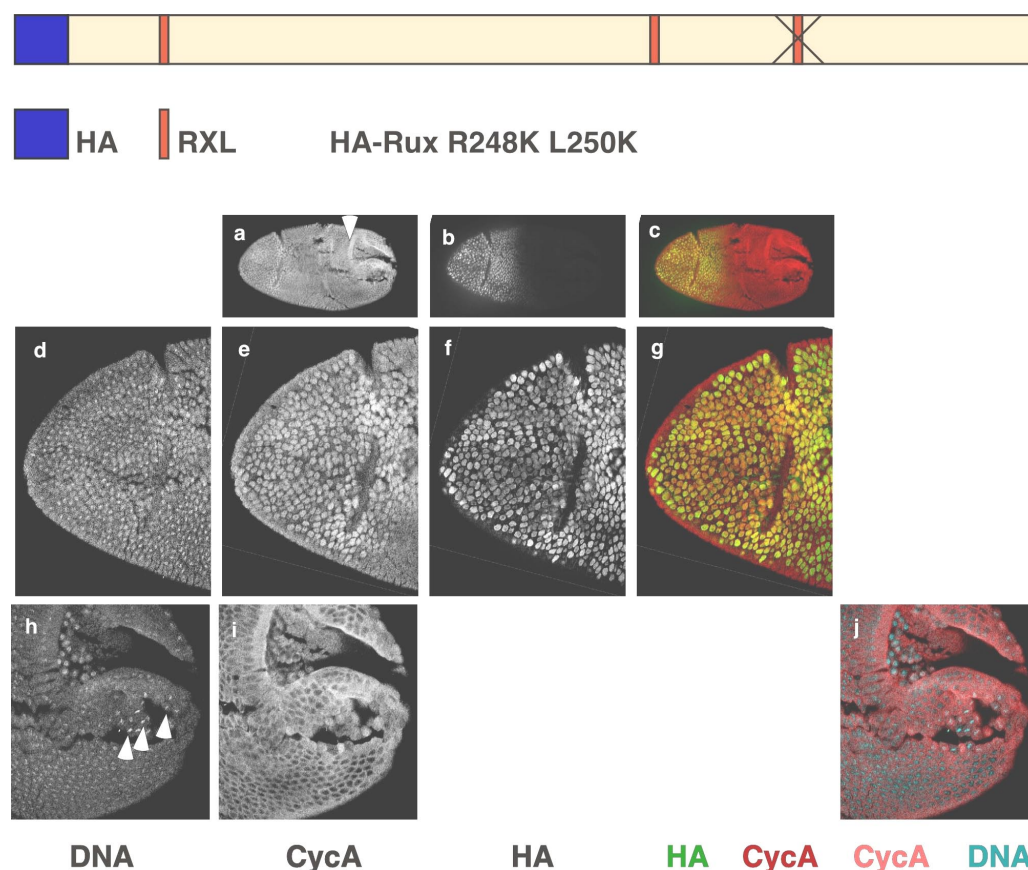


Fig. 2.16: The C-terminal RXL in Rux is not required for Rux-CycA *in vivo* interactions.

mRNA encoding HA-tagged Rux Δ RXL3 was injected into the anterior of an embryo and the protein visualized with anti-HA antibodies (b). The embryo depicted is at the start of mitosis 14, as determined by germband extension (a, arrowhead). An overlay of the CycA and Rux staining is shown in (c) with CycA in Red and Rux in green. Higher magnification of HA-Rux Δ RXL3 expressing cells (f) shows that DNA is in a decondensed interphase state (d), CycA accumulates in the nucleus (e) and HA-Rux Δ RXL3 is a nuclear protein. An overlay of the CycA and Rux staining is shown in (g) with CycA in Red and Rux in green. Mitosis 14 occurs in a WT manner in non HA-Rux Δ RXL3 expressing cells. Metaphase cells are detectable in domain 4 (h, arrowheads) and CycA is cytoplasmic in interphase cells (i). An overlay of the DNA and CycA staining is shown in (j), with CycA in pink and DNA in blue. DNA was visualized by staining with bisbenzidine, CycA with anti-CycA antiserum and HA with anti-HA antiserum.

Introducing point mutations into the central RXL (HA-Rux Δ RXL2) had a different effect on the ability of Rux to interact with CycA in blastoderm embryos. HA-Rux Δ RXL2 is a nuclear protein (Fig. 2.17b and e). However, in contrast to wild-type Rux, the mutant isoform is unable to direct a nuclear accumulation of CycA. The embryo presented here is in interphase of cycle 14 and the RNA has been injected into the anterior part. In this part of the embryo CycA is entirely cytoplasmic, despite a large accumulation of HA-Rux Δ RXL2 (Fig. 2.17a and d). Thus removing RXL2 severely impairs the ability of Rux to interact with CycA *in vivo*, suggesting that this is a key motif for mediating Rux-CycA interactions. Embryos expressing HA-Rux Δ RXL2 also display a WT pattern of cell divisions (data not shown), demonstrating that HA-Rux Δ RXL2 does not inhibit Cdk1 *in vivo*.

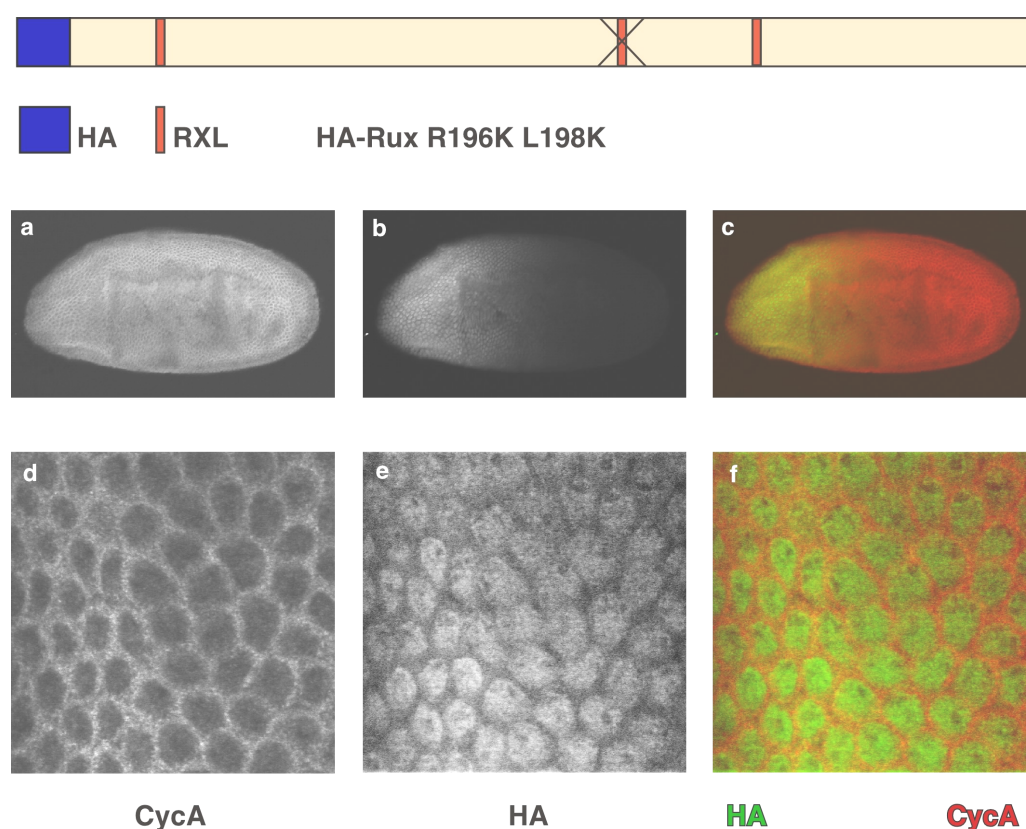


Fig. 2.17: Mutations in the central RXL motif abrogate Rux-CycA *in vivo* interactions.

mRNA encoding HA-tagged Rux Δ RXL2 was injected into the anterior of an embryo and the protein visualized with anti-HA antibodies (b). This embryo is in interphase 14 and no cell are undergoing mitosis (a). An overlap of the HA-Rux Δ RXL2 and CycA staining is shown in (c) with CycA in red and HA-Rux Δ RXL2 in green. Higher magnification of HA-Rux Δ RXL2 expressing cell confirms that it is a nuclear protein (e). HA-Rux Δ RXL2 does not trigger a nuclear accumulation of CycA, as cycA is strictly cytoplasmic in the same cells (d). An overlay of (d) and (e) is shown in (f) with HA-Rux Δ RXL2 in green and CycA in red. DNA was visualized by staining with bisbenzidine, CycA with anti-CycA antiserum and HA- with anti-HA antiserum.

A point mutation converting the N-terminal RXL to KXK (HA-Rux Δ RXL1) produces results intermediate to HA-Rux Δ RXL2 and HA-Rux Δ RXL3. The embryo depicted in Fig. 2.18 was injected in the posterior half. HA-Rux Δ RXL1 is detected in the dorso-central part of the embryo because posterior cells move forward during germband extension. HA-Rux Δ RXL1 is a nuclear protein in all cells where it is expressed (Fig. 2.18b). CycA is present only in the cytoplasm of cells expressing low amounts of HA-Rux Δ RXL1 (Fig. 2.18e, closed arrowheads) (Fig. 2.18d and f, closed arrowheads). Cells expressing higher amounts of HA-Rux Δ RXL1 (Fig. 2.18d, open arrowheads) have an even distribution of CycA throughout the cell. Thus, it appears that HA-Rux Δ RXL1 is only moderately able to interact with CycA and that high levels of HA-Rux Δ RXL1 expression are required to induce a partial nuclear accumulation of CycA. In the embryo presented here the nuclear accumulation of CycA in some cells may merely arise from the particular cell cycle state of those cells. It is possible that these cells are in prophase, which is a cell cycle stage where CycA normally accumulates in the nucleus. Some of the cells expressing HA-Rux Δ RXL1 are approximately half the size of other cells, demonstrating that HA-Rux Δ RXL1 does not prevent progress through the cell cycle.

In a second series of assays all three deletion constructs were tested for their ability to moderate the *in vitro* kinase activity of Cdk1/CycA. As observed above, Cdk1 alone is essentially inert as a H1 kinase (Fig. 2.19A and B, lane 1). Addition of CycA as a regulatory subunit greatly enhances Cdk1 kinase activity (Fig. 2.19A and B, lane 2). Large amounts of WT Rux inhibit Cdk1/CycA activity to almost background levels (Fig. 2.19A, lane 3), whereas low amounts of Rux stimulate Cdk1/CycA kinase activity (Fig. 2.19B, lane 3). In contrast, Rux Δ RXL1 only mildly inhibits Cdk1/CycA (Fig. 2.19A, lane 4) and low amounts of Rux Δ RXL1 enhance Cdk1/CycA to almost wild-type levels (Fig. 2.19B, lane 4). Rux Δ RXL2 does not inhibit Cdk1/CycA. Instead, large amounts actually enhance Cdk1/CycA activity by more than 50% (Fig. 2.19A, lane 5). Furthermore, low levels of Rux Δ RXL2 do not stimulate Cdk1 kinase activity as well as wild-type (Fig. 2.19B, lane 5). Finally, Rux Δ RXL3 influences Cdk1/CycA activity in a manner almost identical to wild-type Rux. A large amount of Rux Δ RXL3 potently inhibits Cdk1/CycA (Fig. 2.19A, lane 6) and lower amounts of Rux Δ RXL3 enhance Cdk1/CycA activity by a factor of 2 (Fig. 2.19B, lane 6).

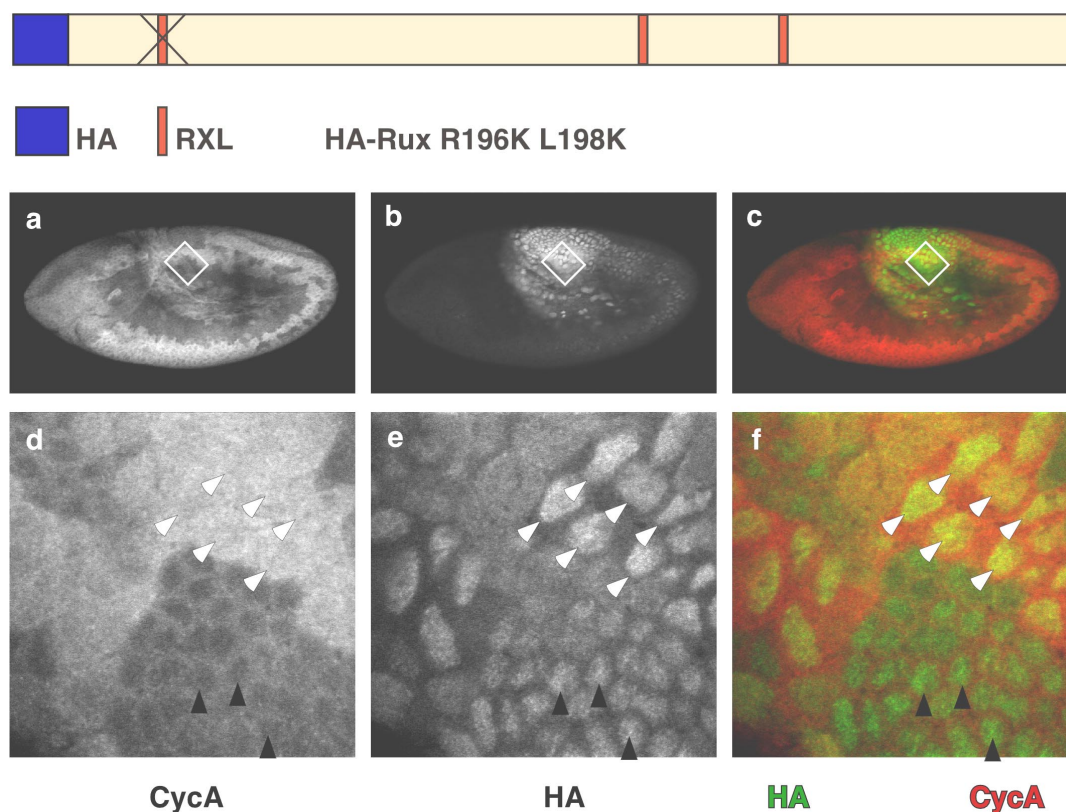


Fig. 2.18: Mutations in the N-terminal RXL motif diminish Rux-CycA *in vivo* interactions.

mRNA encoding HA-tagged Rux Δ RXL1 was injected into the posterior of an embryo and the protein visualized with anti-HA antibodies (b). This embryo is in cell cycle 14, as judged by the extent of germband extension (a). Mitosis 14 occurs in a normal pattern as determined by the orderly disappearance of CycA, demonstrating that HA-Rux Δ RXL1 does not inhibit progression through mitosis (a). An overlap of the Rux and CycA staining is shown in (c) with CycA in red and Rux in green. Higher magnification of HA-Rux Δ RXL1 expressing cell confirms that it is a nuclear protein (e). HA-Rux Δ RXL1 only triggers a partial nuclear accumulation of CycA in cells expressing high amounts of HA-Rux Δ RXL1 (d and e, open arrowheads). CycA remains cytoplasmic in cells where low amounts of HA-Rux Δ RXL1 are expressed. HA-Rux Δ RXL1 does not inhibit mitosis as cell expressing lower amount have a higher nuclear density than cells expressing large amounts (e, compare open and closed arrowheads). A merge of (d) and (e) is shown in (f) with Rux in green and CycA in red. DNA was visualized by staining with bisbenzidine, CycA with anti-CycA antiserum and HA with anti-HA antiserum.

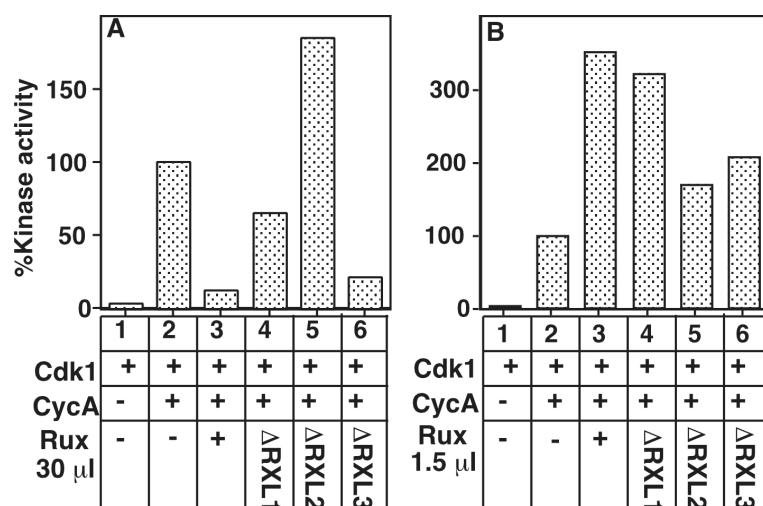


Fig. 2.19: RXL1 and RXL2 are important for inhibiting Cdk1/CycA kinase activity.

(A) The average results for three separate experiments are presented graphically. In each case kinase assays were performed as described for Fig. 9 using extract as a source of CAK. The kinase activity of Cdk1/CycA was set to 100% (lane 2) and all reactions were performed in an identical volume. As a negative control the activity of Cdk1 was determined (lane 1) and as a control for Rux activity Cdk1/CycA was incubated with WT Rux (lane 3). Large amounts of Rux Δ RXL1 only mildly inhibits Cdk1 activity (lane 4), while large amounts of Rux Δ RXL2 actually enhance Cdk1/cycA activity (lane 5). In contrast, Rux Δ RXL3 inhibits Cdk1/CycA as effectively as WT Rux (lane 6). **(B)** Low amount of WT Rux enhance Cdk1/CycA kinase activity (lane 3). Rux Δ RXL1 enhances Cdk1/CycA to almost the same extent as WT Rux (lane 4), whereas Rux Δ RXL2 (lane 5) and Rux Δ RXL3 (lane 6) display a slightly diminished ability to do so.

To confirm that RXL2 is essential for Rux-CycA interactions HA- Rux Δ RXL2 was transiently expressed in WT embryos and precipitated from an extract prepared from the embryos. As a control WT HA-Rux was translated in embryos and precipitated. Whereas, WT HA-Rux precipitates large amounts of CycA from cellularized embryos (Fig. 2.20, lane 1), HA- Rux Δ RXL2 does not (Fig. 2.20, lane 2).

In summary, Rux Δ RXL1 is greatly impaired in its ability to regulate CycA localization *in vivo* and inhibit Cdk1/CycA *in vitro*. Rux Δ RXL2 does not direct a nuclear accumulation of CycA and does not inhibit Cdk1/CycA *in vitro*. Furthermore, Rux Δ RXL2 is incapable of precipitating CycA from embryos, whereas WT Rux does. The effects of Rux Δ RXL3 on CycA *in vivo* and Cdk1/CycA *in vitro* are identical to wild-type Rux. These results strongly argue that RXL2 in Rux is essential for interaction with CycA and inhibition of Cdk1/CycA, RXL1 is important for both functions and RXL3 is dispensable in both regards.

Fig. 2.20: Rux Δ RXL2 does not interact with CycA *in vivo*.

mRNA encoding either HA-Rux or HA-Rux Δ RXL2 was injected into approximately 300 pre-blastoderm embryos respectively. After a 2hr recovery period embryos were homogenized and the homogenate precipitated with anti-HA antibodies. As a control for the amount of recovered HA-tagged protein a sample of both homogenates was analyzed for the presence of the HA tag (upper panel, HA blot). A second sample was analyzed by Western blotting with anti-CycA antiserum for the co-precipitation of CycA (lower panel, CycA blot). HA-tagged Rux transiently expressed in *Drosophila* embryos binds and precipitates CycA (lane 1), whereas HA-Rux Δ RXL2 does not (lane 2), demonstrating that the central RXL motif in Rux is essential for Rux-CycA interactions.

A role for Rux in exit from mitosis

Endogenous *rux* is expressed at low level and cannot be detected by *in situ* hybridization. To determine the stages during which the *rux* gene is transcribed total mRNA was isolated from different developmental stages and amplified by RT-PCR using oligonucleotides specific for the *rux* transcript. No transcript was detected in 0-2hr embryos, indicating the absence of maternally provided mRNA (Fig. 2.21A). Zygotic transcription started in 2-hr embryos and persisted in 12-24hr embryos. No transcript was detected in L1 larvae. This may be due to inadequate preparation of mRNA, as the control transcript for the ribosomal protein rp49 is also underrepresented. Transcription occurs in older larvae, pupae and adult flies.

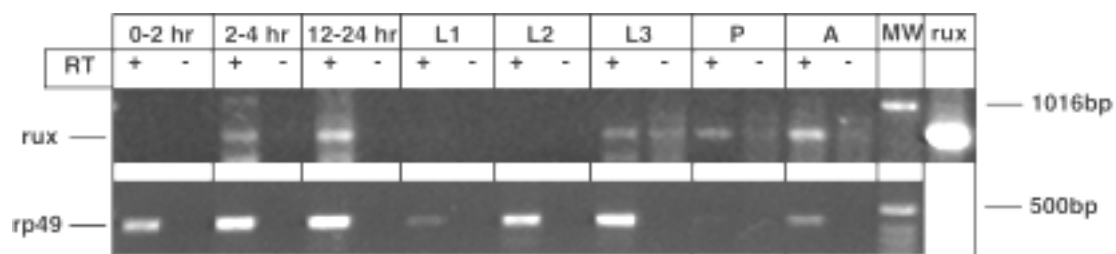


Fig. 2.21: Rux is expressed during most stages of *Drosophila* life.

Poly-adenylated mRNA was isolated from different staged embryos, larvae, pupae and adults. Rux transcript was amplified from each stage by RT-PCR (upper panel lanes marked '+'). The primer RT1 was used for the RT reaction and the primers RT1 and RT2 were used for the PCR reaction. As a negative control isolated mRNA was amplified by PCR, without a preceding reverse transcription step (upper panel, lanes marked '-'). As a control for transcript length 1ng plasmid DNA containing the Rux ORF was amplified using the PCR primers RT1 and RT2 ('rux'). As a control for the quality of mRNA preparation the purified mRNA was assayed for the presence of the ribosomal protein transcript, rp49. rp49 mRNA was amplified with the primer rp491 and the subsequent PCR reaction performed with the primers rp491 and rp492. The *rux* transcript is absent from 0-2hr embryos, indicating the absence of a maternal provision of transcript. *rux* mRNA is present in embryos from 2hr onward, as well as larvae, pupae and adults. Transcript is not detected in L1 larvae, although this may be due to a poor preparation of mRNA, as the rp49 transcript is underrepresented in the same sample.

Interestingly, *rux* is transcribed in 2-4hr embryos. At this stage embryos are in interphase or early mitosis 14. These cycles occur without any G1 stage. However, the initial characterization of *rux* mutants indicated that Rux is required for establishing a G1.

To determine whether Rux functions at this period progression through mitosis 14 was compared for *rux*³ mutant and WT embryos. Mitosis 14 occurs in a series of domains over the embryonic epidermis (Fig. 2.22A) and (Foe, 1989). An antibody raised against phosphorylated histone H3 (PH3) is a reliable reporter for mitosis in many species including *Drosophila*. This antibody binds PH3 during all stages of mitosis from DNA condensation in prophase, through chromosome alignment at the

metaphase plate, chromatid separation at anaphase and chromosome decondensation during telophase (Fig. 2.22B). Therefore, this antibody is a reliable tool for recognizing all stages of mitosis in the distinct mitotic domains. Fig. 2.22C shows a dorsal view of WT embryos stained with the PH3 antibody at different stages of mitosis 14. The temporal order of the mitotic domains agrees with those described previously (compare Fig. 2.22A and C). This pattern is reproducible between individual embryos and between different WT strains. Higher magnification allows the identification of distinct stages for the individual domains (Fig. 2.22D shows the different stages of mitosis 14 for domain 4). Mitosis 14 generally starts as a thin wisp of 1-2 cell widths for a particular domain. This rapidly expands by another 2-3 cell widths and then takes on a very defined structure. Mitosis is completed in the central cells first giving each domain a hollowed-out appearance, before completion of mitosis for the entire domain.

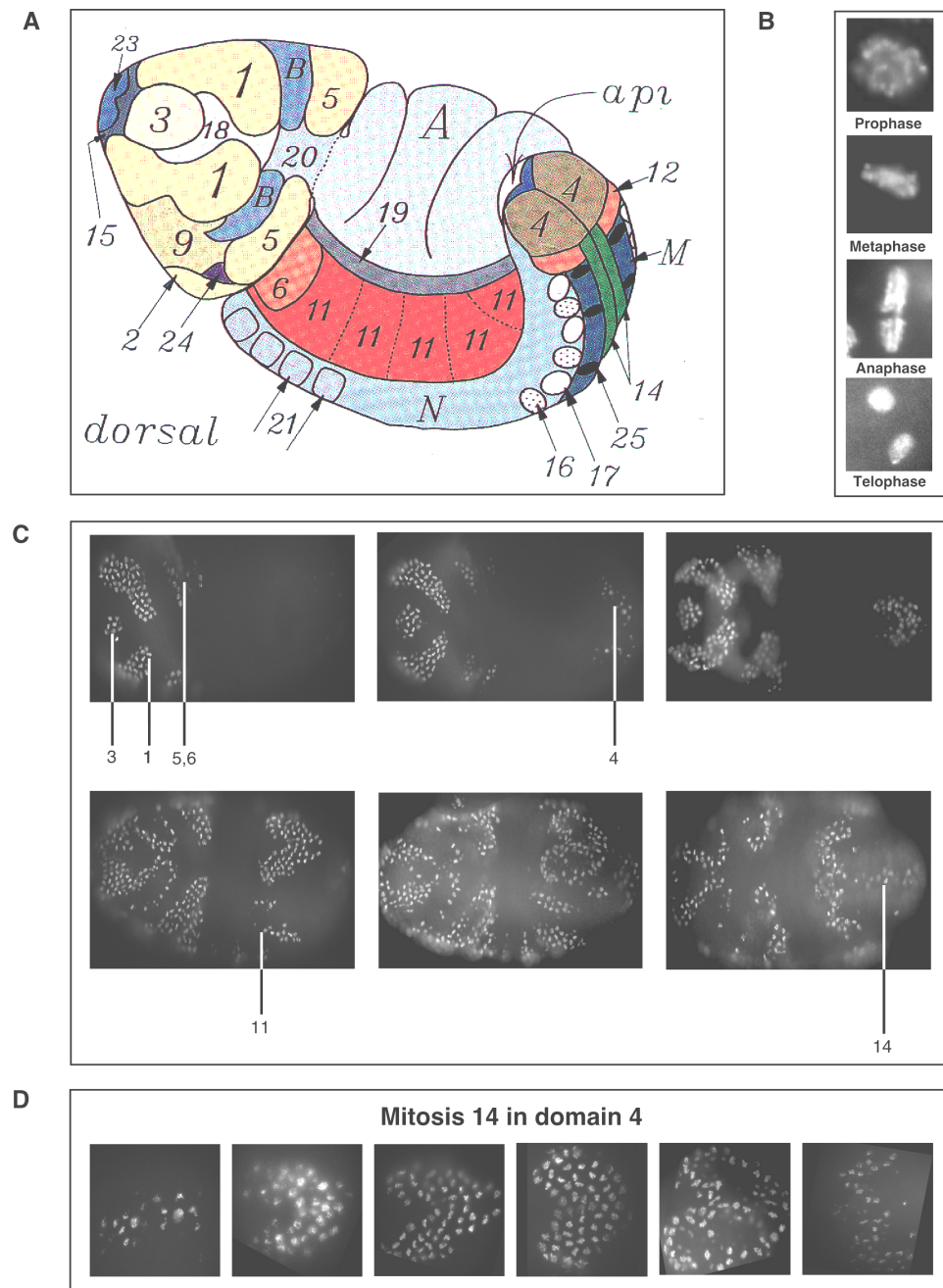


Fig. 2.22: Mitosis 14 occurs in a stereotyped pattern of domains.

(A) Schematic representation of the domains of mitosis 14. Mitosis 14 occurs as a series of domains with bilateral symmetry along the anterior-posterior axis. The later domains M and N are not synchronous and the anterior domains A (amnioserosa) and B do not divide. Presented is a dorso-lateral view of an embryo taken from (Foe, 1989). (B) An antibody raised against a phosphorylated form of histone H3 (PH3) specifically recognizes H3 during mitosis and reveals DNA conformation during prophase, metaphase, anaphase and telophase. (C) The anti-PH3 antibody reliably reproduces the domain pattern of mitosis 14. Presented is an dorsal view of an embryo early in gastrulation and germband extension. Anterior is to the left. Individual domains are numbered. Domain 4 is intimately associated with the tip of the extending germband and is a reliable reporter of developmental stage. (D) Higher magnification of individual domains reveals that mitosis 14 can be divided into stages for each domain. A dorsal view of domain 4 is presented here with anterior to the left. Mitosis starts as a thin wisp of cells, which rapidly expands laterally, hollows out in the center and completes for peripheral cells. The central cells exit mitosis first, as they are the first to enter. The shape of the domain changes during progression through mitosis as a result of cell movements during germband extension.

Using this staging technique the rates of progression through mitosis 14 were compared for WT and *rux*³ mutant embryos. As *rux*³ mutants are not male sterile it is possible to compare a homozygous WT population with a homozygous mutant population. A WT embryo and *rux*³ embryo were aligned, such that domain 1 was at the same stage for both embryos (Fig. 2.23A and B). The other domains were then compared to determine whether the synchrony was maintained. The order in which the domains enter mitosis was identical for both populations (data not shown). However, when domain 1 was at the same stage in WT and mutant embryos the later

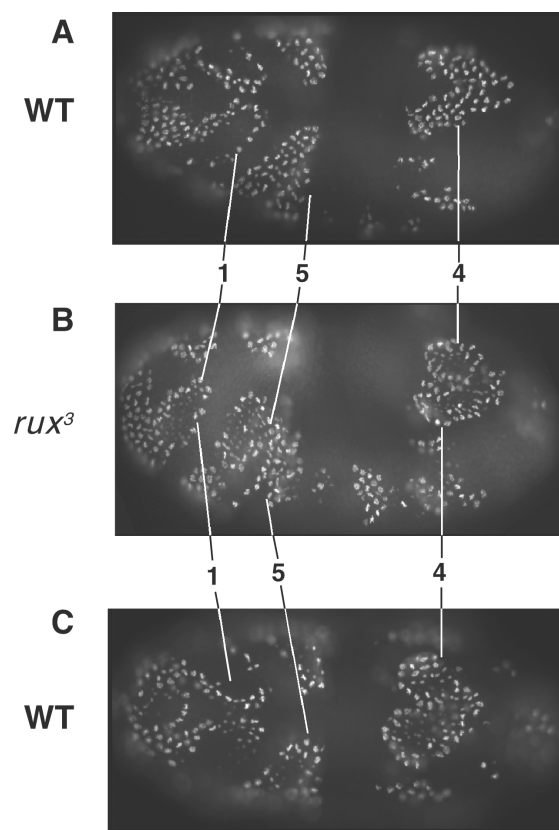


Fig. 2.23: Mitosis 14 is prolonged in *rux*³ mutants.

To compare the duration of mitosis 14 between WT and *rux*³ mutants, individual embryos were chosen where domain 1 had progressed equally far in WT (A) and mutant embryos (B). In the embryos presented in A and B domain 1 has a hollow appearance, indicating that mitosis is approx. half completed for this domain. A comparison between later domains shows that mitosis is further advanced in mutant than WT embryos. For example, whereas all cells of domain 4 are still in metaphase in the WT embryo (A) many have completed mitosis in the mutants (B). In a similar comparison a WT embryo was chosen where domain 4 is at an identical stage for a *rux*³ mutant (B) and a WT embryo (C). In this case, domain 1 is further advanced in the WT than mutant embryo.

domains were further advanced in the mutants. For example, whereas domain 4 was in a synchronous metaphase in WT embryos, most cells were in anaphase, telophase or had exited mitosis in *rux*³ mutants. Similarly when domain 4 was set at an identical stage for WT and mutant embryos (Fig. 2.23B and C), domain 1 was more advanced in WT than *rux*³ mutants. In the WT embryo shown in 2.23C, domain 1 had almost completely exited mitosis. A single line of cells were in anaphase/telophase. The *rux*³ embryo in 2.23B was half way through mitosis 14 in domain 1, as can be seen by the large number of peripheral prophase cells and the central anaphase/telophase cells.

The same comparison described in Fig. 2.23 was performed for homozygous *rux*² mutant embryos and a heteroallelic combination of *rux*³ and *rux*⁸ embryos. In all tested mutant combinations mitosis was prolonged in mutants in comparison to WT embryos, indicating that the phenotype observed is linked to the *rux* locus (Fig. 2.24). Domain 1 was set at the same stage in all embryos in Fig. 2.24. All later domains are further advanced in mutants embryos than in the WT embryo Therefore, The effect described in Fig. 2.23 is not specific to the *rux*³ allele and is not the result of a background mutation in the *rux*³ genotype.

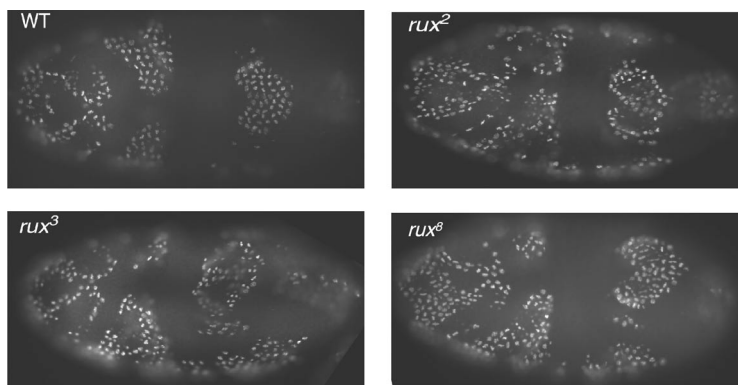


Fig. 2.24: mitosis 14 is prolonged in all *rux* mutants

To confirm that the prolonging of mitosis observed in Fig. 2.23 is specifically caused by mutations in the *rux* locus mitosis 14 was compared between WT and different *rux* alleles. Embryos were staged such that domain 1 is at the same stage in WT, *rux*², *rux*³ and *rux*⁸ mutants. Close examination revealed that mitosis is further advanced in all mutants in later domains, such as 4, 5 and 11. Furthermore mitosis 14 is approx. equally advanced in the different mutant embryos.

Mitosis was followed in living embryos to further analyze the mitotic phenotype of *rux*³ mutants. A transgene expressing GFP-tagged histone H2 (GFP-His2AvD; (Clarkson and Saint, 1999) was crossed into the *rux*³ mutant background, producing *rux*³; GFP-His2AvD flies. Using fluorescence microscopy images were taken of developing embryos at 10s intervals over a period from shortly before gastrulation until the

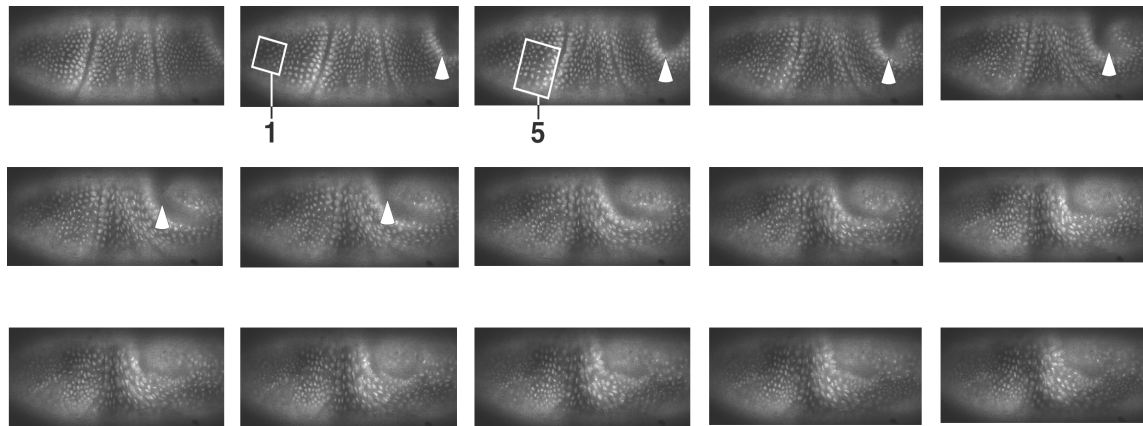


Fig. 2.25: Following mitosis 14 in living embryos.

Presented are individual frames from live observations of a single *rux*³; GFP-His2AvD embryo. Anterior is to the left and dorsal is up. The arrowhead marks the position of the tip of the germband. DNA condensation during metaphase reveals the individual mitotic domains at lower magnification. Domains 1 and 5 are presented as boxed regions. Mitosis 14 begins within minutes of the initiation of germband extension. Pictures were taken every 10s after the beginning of germband extension to follow mitosis 14.

completion of germband extension. This period covers the bulk of mitosis 14 and is therefore suitable for following mitosis in individual domains (Fig. 2.25).

Higher magnification allows resolution of mitosis for individual cells to an extent that prophase, metaphase, anaphase and telophase can be satisfactorily distinguished (Fig. 2.26).

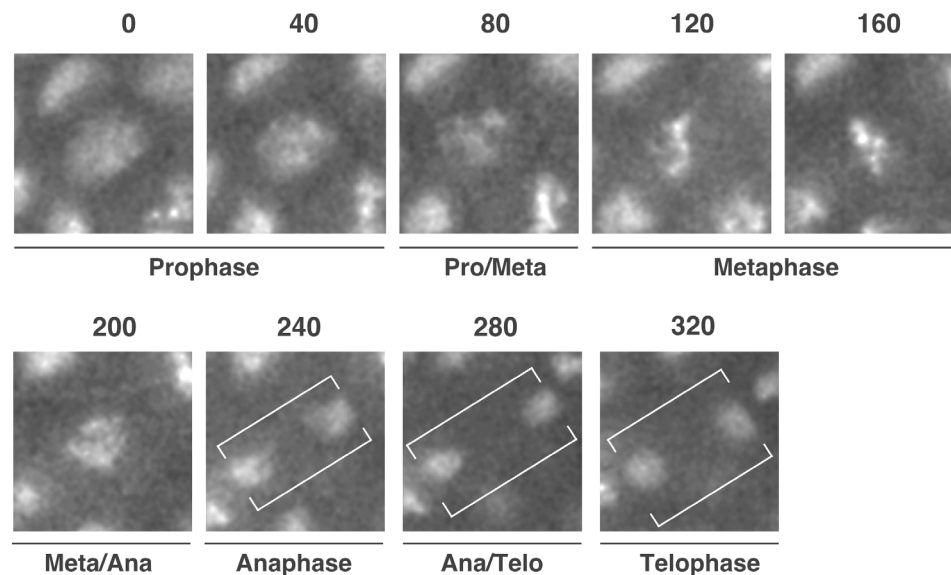


Fig. 2.26: Higher magnification of mitosis 14 in a single cell.

Individual pictures of mitosis 14 in an individual cell of domain 5 of a *rux*³; GFP- His2AvD. At this magnification the individual stages of mitosis are discernible. At time 0 DNA is in a decondensed prophase state. After 80s DNA begins to condense and align on the metaphase plate. Metaphase is visible as the time of maximal alignment of sister chromatids on the interphase plate. After 200s sister chromatids are pulled to opposite poles. By telophase sister chromatids reach opposite poles and DNA starts to decondense.

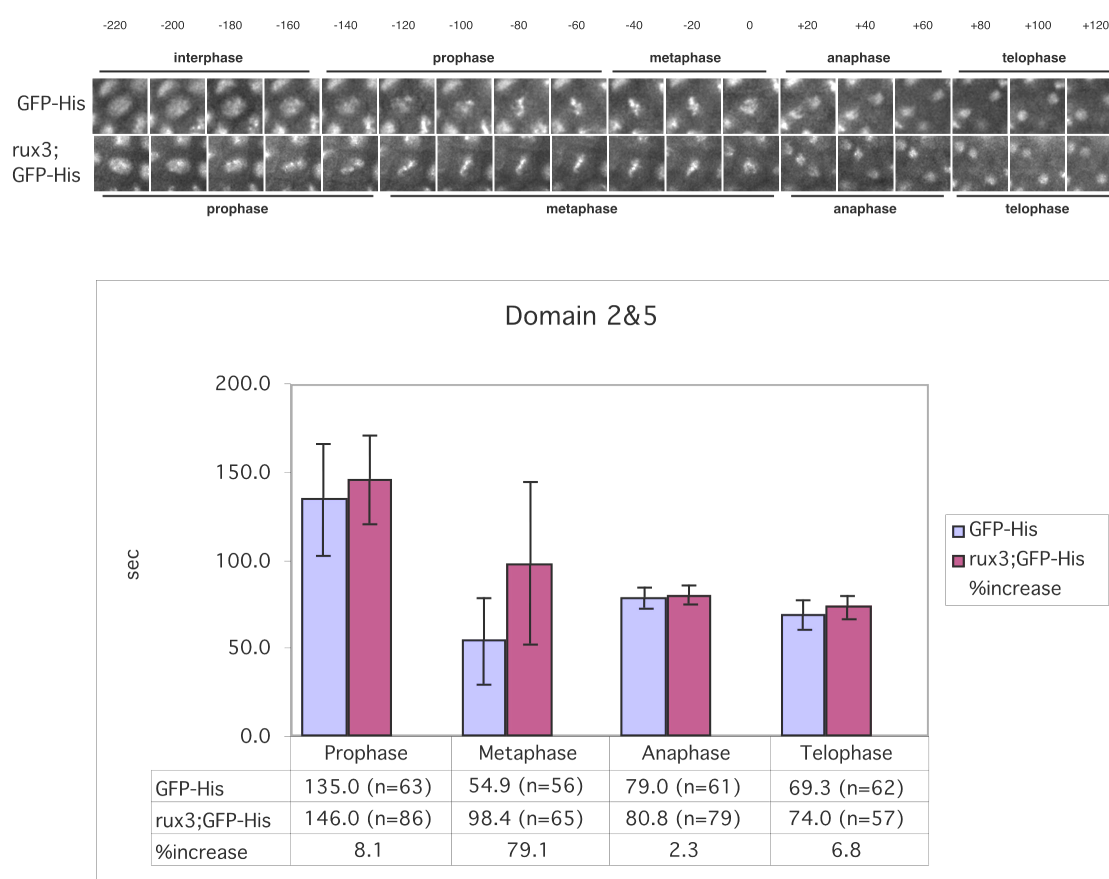


Fig. 2.27: Metaphase is significantly longer in *rux*³ mutants.

(A) Mitosis was followed for individual cells of GFP- His2AvD and *rux*³ ; GFP- His2AvD embryos in domains 2 and 5. Individual frames for a WT and a *rux*³ mutant are presented in the upper series of panels. Although prophase, anaphase and telophase occur at equal rates in both genotypes metaphase is almost twice as long in the mutant cell (metaphase). The total results are represented graphically in the lower panel. (B) Prophase anaphase and telophase are approx. equally long in WT and mutant embryos. In contrast, metaphase is significantly longer in mutant cells. Metaphase is on average 79% longer in mutant embryos than in WT embryos. Numbers in parentheses indicate the number of observations made for the individual mitotic stages for both genotypes. Times of the individual stages are given in seconds.

Mitosis was timed for individual cells in specific domains at 10s intervals. As a control the experiment was repeated using the parent GFP-His2AvD strain. The cells of domains 2 and 5 were concentrated on, as they are most amenable to live observations. These observation revealed that metaphase is significantly longer in mutants than WT embryos for both domains (Fig. 2.27A and B). Metaphase is prolonged by almost 80% in *rux*³ mutants (Fig. 2.27A and B). Prophase, anaphase and telophase, in contrast, are not significantly changed in mutant embryos. A representative example is shown in 2.27A, where there is a dramatic lengthening of metaphase in *rux*³ mutants, while all other stages of mitosis proceed at WT pace. In summary, analysis of fixed, and living *rux* mutant embryos demonstrates that mitosis is prolonged in comparison to WT embryos. Specifically, metaphase is considerably

longer in mutants, indicating that a wild-type function of the Rux protein is to contribute to mitotic exit by downregulating Cdk1/CycA activity at metaphase. A potential interpretation of these results is that Rux mediated inhibition of Cdk1/CycA cooperates with APC/C dependent destruction of CycA during metaphase. The combined effects of these activities suppress Cdk1/CycA activities to a level where a transition to anaphase is possible. In the absence of Rux protein CycA is only downregulated by proteolysis alone, lengthening metaphase.

To test if Rux can downregulate Cdk1/Cyclin activity during metaphase the effects of Rux induction on cells expressing an indestructible CycA (CycA Δ 170) were followed. *prd-GAL4 X UAS-CycA Δ 170* embryos express CycA Δ 170 in stripes in the epidermis of the embryo resulting in a metaphase arrest in these stripes. *rux* expression was induced from a second transgene under the control of a heat-inducible promoter (*hs-rux*) to determine whether Rux induces an exit from mitosis in the CycA Δ 170 expressing cells. This experiment has several potential drawbacks: Densely packed mitotic DNA is only poorly accessible to transcription factors and nascent transcripts are aborted during mitosis. As the experiment requires induction of transcription during mitosis by administration of a heat pulse the effects of a heat-shock on mitosis were first examined.

Mild heat pulses affect the mitotic program in *Drosophila* embryos.

Embryos fixed immediately after administering a 5min heat-shock have normal mitotic figures (Fig. 2.28A), where various stages such as metaphase (Fig. 2.28Aa, white arrowheads) and anaphase (Fig. 2.28Ab, black arrowhead) are distinguishable. 5min after heat shock no mitotic figures are visible (Fig. 2.28B). Using germband extension as a timer (Fig. 2.28Ba), mitosis 14 should be occurring in domains 1 and 5 in the anterior section of the embryo depicted in Fig. 2.28Ba. Close examination of this region reveals that the DNA has a uniform decondensed morphology, reminiscent of interphase/early prophase. The pattern of mitosis 14 returns to the embryo 10 min. after heat shock. Mitosis 14 is visible in domains 1,4 and 5 of the embryo depicted in Fig. 2.28Ca. A higher magnification of domain 1 (Fig. 2.28Cb) reveals that the mitotic pattern for domain 1 is also comparable to a WT embryo. Peripheral cells enter mitosis (Fig. 2.28Cb, white arrowheads metaphase), while more central cells exit mitosis (Fig. 2.28Cb, black arrowheads anaphase). Furthermore, cells from domain 5 are initiating mitosis (Fig. 2.28Cb, circles) confirming that domain 1 is more advanced than domain 5.

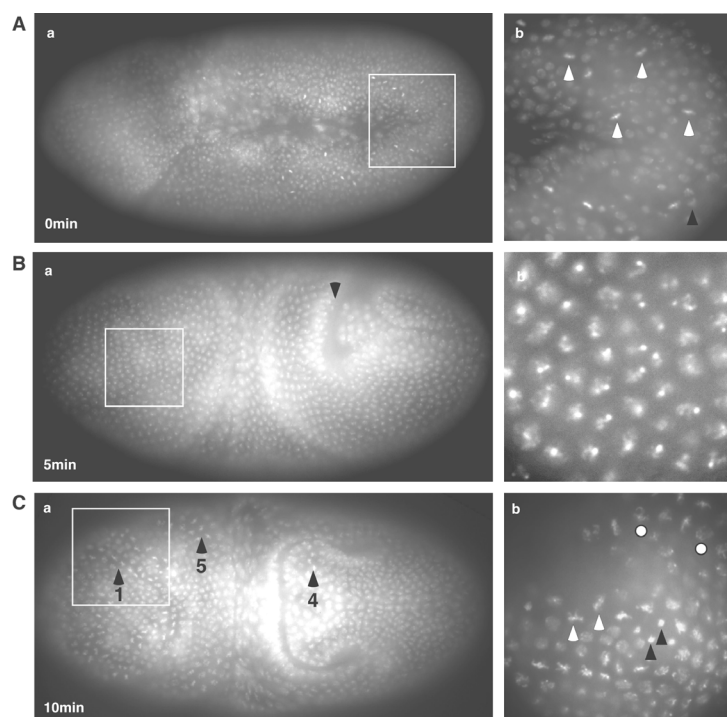


Fig. 2.28: A mild heat-shock disturbs mitosis.

WT embryos were submitted to a 5min heat pulse by floating them on a thin apple juice-agar plate on a 37°C water bath. Embryos were fixed immediately (A), 5min (B) or 10min (C) after the heat pulse. DNA morphology was visualized by staining embryos with bisbenzidine. Embryos are oriented with dorsal surface up and anterior to the left. Mitosis proceeds as normal during a heat pulse. A higher magnification of the embryo in Aa reveals the presence of metaphase (open arrowheads) and anaphase chromosomes (closed arrowheads) (Ab) immediately after a heat pulse. No mitotic figures are visible 5min after a heat pulse. The embryo shown in Ba is undergoing germband extension (arrowhead). At this stage mitosis occurs in domains 1 and 5 (boxed region) in a WT embryo. DNA has a uniform morphology in heat shock embryos (Bb). 10 min after a heat pulse the mitotic program resumes. Mitotic figures are visible in domains 1, 4 and 5 of a WT embryo (Ca). Higher magnification of domain 1 (Cb) confirms that mitosis 14 is asynchronous in domain 1. Peripheral cells are in metaphase (open arrowheads) and central cells are in anaphase (closed arrowheads). Meanwhile, cells of domain 5 are at the prophase/metaphase transition (open circles).

5min after administration of a 5min heat shock all cells appear to be in interphase. To determine if this is the case other known markers of mitosis, such as nuclear envelope breakdown (NEB), histone H3 phosphorylation and mitotic spindle formation were examined. Embryos were stained for β -tubulin and with a fluorescently tagged wheat-germ agglutinin (WGA) as a marker for mitotic spindle formation. No mitotic spindle was apparent 5 min after heat shock, as the β -tubulin staining was entirely cytoplasmic (Fig. 2.29C). Surprisingly, the pattern of PH3 staining suggested that mitosis 14 continued after a heat shock. In the embryo in Fig. 2.29B a PH3 staining pattern was detectable which overlaps with the expected pattern of mitotic domains. However, higher magnification of either the DNA or PH3 staining suggested that the DNA in all cells was in a decondensed interphase/prophase state. The germband was extending in the embryo shown (Fig.

2.29Aa, arrowhead). In a WT embryo of this stage domain 1 of mitosis 14 is near completion (compare Fig. 2.29A and Fig. 2.23A). However, all cells in the region of the embryo in Fig. 2.29 corresponding to domain 1 stained positive for PH3 and had a decondensed, non-mitotic DNA morphology. PH3 positive cells are not always in mitosis. Therefore, it is not possible to deduce from a persistence of PH3 staining after a heat pulse regime that the cells are still in mitosis.

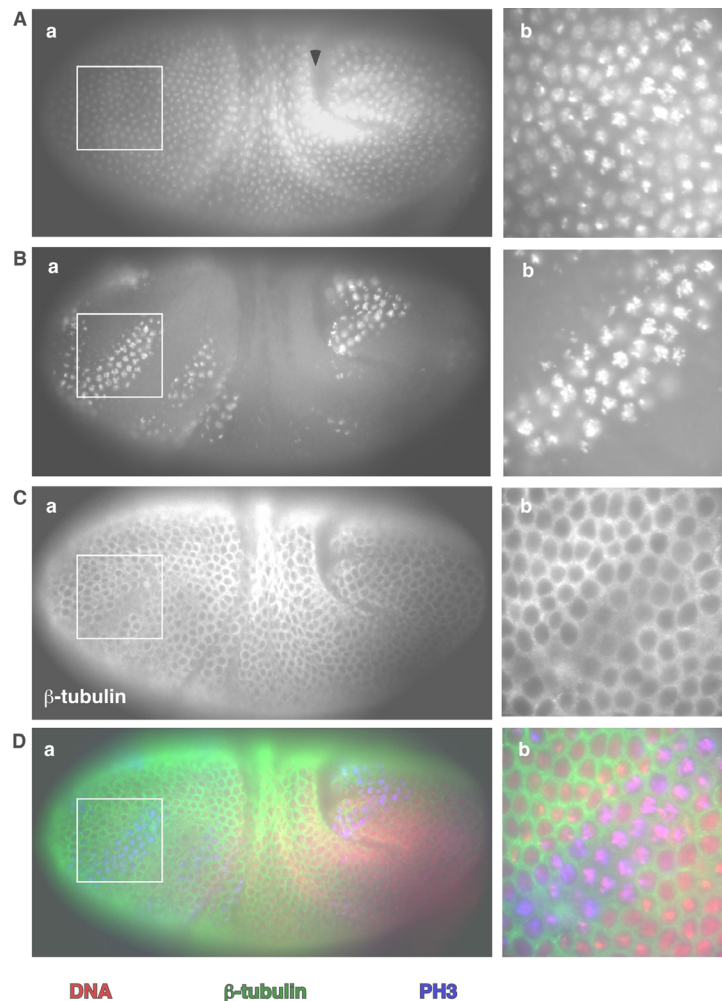


Fig. 2.29: No mitotic spindles are visible 5min after a heat pulse.

Embryos were fixed 5min after a 5min heat shock. The embryo presented is in a dorso-lateral orientation.

(A) DNA is visualized by staining with bisbenzidine, confirming the absence of mitotic figures 5min after a heat pulse. **(B)** Despite the apparent absence of mitotic figures many cells stain positive for PH3 in a manner that resembles the WT pattern of mitotic domains. **(C)** β -tubulin is visualized by staining with an anti- β -tubulin antibody. No mitotic spindles are detected 5min after a 5min heat pulse. **(D)** The three images are merged with DNA in red, β -tubulin in green and PH3 in blue. All DNA is in an interphase/prophase configuration (Aa), although many cells stain positive for PH3 (Ba). Furthermore, mitotic spindles are not discernible, as β -tubulin is associated with the cell cortex (Ca). Thus, 5min after a heat pulse all cells appear either in prophase or interphase.

The heat shock protocol also had effects on the nuclear envelope. A heat-shock embryo is shown in Fig. 2.30 with an extending germband (Fig. 2.30Aa, arrowhead). At this point in a WT embryo mitosis 14 occurs throughout the anterior and all stages of mitosis are visible. NEB starts at the prophase/metaphase transition and persists until telophase (Fig. 2.4). The nuclear envelope is fully intact in heat shock embryos (Fig. 2.30Ca and b) 5min after the heat pulse despite the presence of numerous PH3 positive cells (Fig. 2.30Ba and C) in the anterior of the embryo. Higher magnification of DNA or PH3 staining suggests a prophase-like morphology for all mitotic cells.

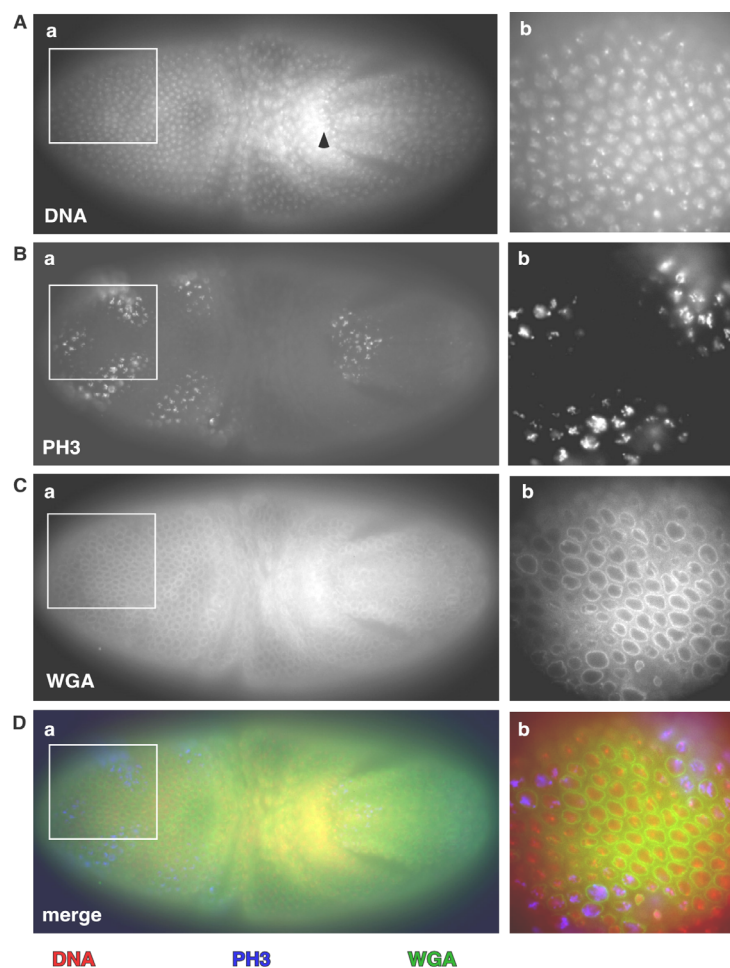


Fig. 2.30: Nuclear envelope breakdown is not detectable 5min after a heat pulse.

Embryos were fixed 5min after a 5min heat shock. The embryo presented is in a dorsal orientation with anterior to the left. (A) DNA is visualized by staining with Hoechst. (B) A mitotic domain pattern of PH3 positive cells is detected despite the decondensed structure of the DNA. (C) The nuclear membrane is detected by staining cells with a fluorescently labeled WGA. All nuclear envelopes are intact 5min after a heat pulse. (D) The three images are merged with DNA in red, WGA in green and PH3 in blue. Based on the extent of germband extension (Aa, arrowhead) and the number of PH3 positive cells in the anterior of the embryo (Ba) a large portion of cells should be in metaphase, anaphase and telophase. Nuclei are not distinguishable during these stages of mitosis. Nonetheless the nuclei are intact in almost all cells of a heat shock embryo, as one finds in interphase/prophase cells.

In summary, the mitotic program is affected 5min after administration of a mild heat shock. DNA has a uniform morphology, mitotic spindles are not detected and all nuclear envelopes are intact. The DNA morphology is particularly interesting, as it has a decondensed form, reminiscent of interphase/early prophase. It is possible that a heat shock induces a stress response which involves DNA decondensation, spindle disassembly and reassembly of interphase structures, such as the nuclear envelope. In this model all prophase and metaphase cells will appear as prophase after a heat shock. Individual embryos were observed where the asynchrony within individual domains was clearly disturbed as a result of the heat shock. The central cells of a WT domain enter mitosis first, followed by the peripheral cells (Fig. 2.22C). Thus, individual WT domains are distinguishable where central cells are in anaphase (Fig. 2.31c, circle), surrounded by metaphase (Fig. 2.31c, black arrowheads) and prophase (Fig. 2.31c, white arrowheads) cells. Heat shock embryos of the same stage were observed where all peripheral cells had an apparent early prophase structure (Fig. 2.31b, white arrowheads). Only one central cell appeared in metaphase (Fig. 2.31b, blue arrowhead). All other central cells did not stain for PH3, suggesting that they were not in mitosis. Thus, it appears a mild heat shock interferes with mitosis in such a way that DNA decondenses, and cells adopt either a transitory prophase or interphase nature. Mitotic cells retain their mitotic nature, despite the absence of NEB or spindle formation, as can be deduced from the persistence of PH3 staining and the fact that the arrest observed is transitory.

To confirm that the administration of a 5min heat pulse caused a decondensation of metaphase DNA a heat shock was administered to GFP-His2AvD embryos early in mitosis 14 and the effects on DNA morphology followed by time lapse microscopy. Similar to Fig. 2.28 no mitotic figures were visible in living cells several minutes after heat pulsing. In particular, nuclei were observed where the DNA was in metaphase after completion of the heat-shock, retained a metaphase morphology for an unusually long period (5min compared to the expected 2min) and then decondensed, without execution of anaphase or telophase. A time course is shown for a cell of domain 1 in Fig. 2.32. The DNA was in metaphase immediately after administration of a heat pulse (Fig. 2.32, 0s). Metaphase persisted for an additional 5min (Fig. 2.32, 300s). The DNA slowly decondensed for the following 5min, without completing mitosis. Instead, it assumed an interphase-like morphology, without any intervening anaphase or telophase (Fig. 2.32, 600s). Therefore, administration of a mild heat-pulse induces a rearrangement of DNA morphology for a brief period, where all cells adopt an interphase-like structure. This is a transitory effect, as the mitotic program is reinitiated after a brief recovery period.

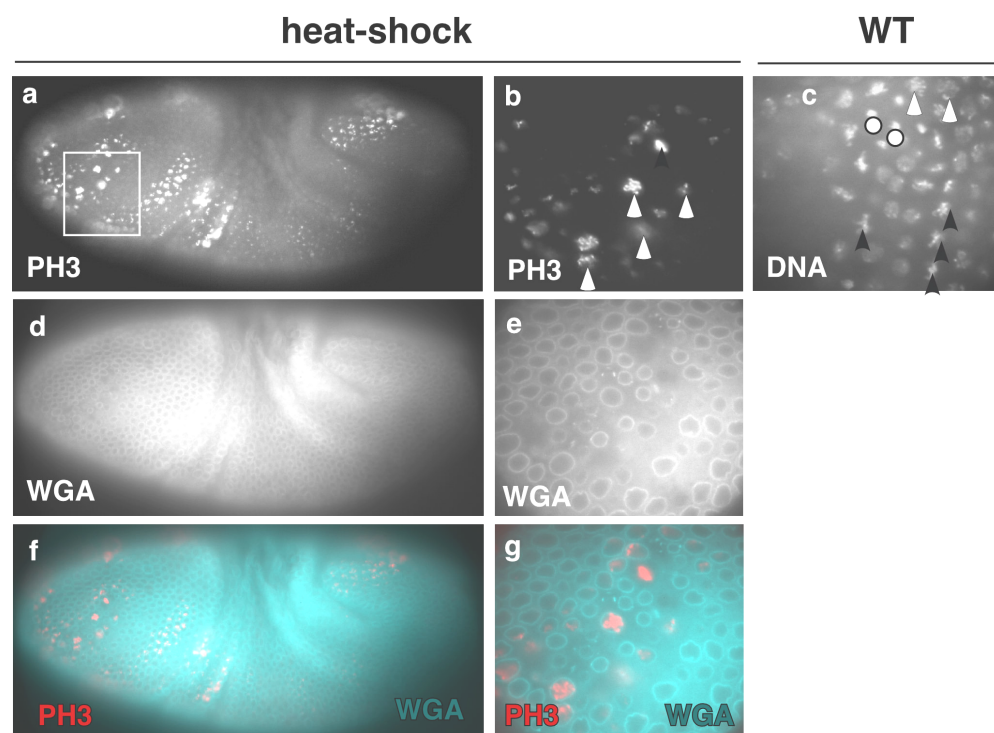


Fig. 2.31: Heat pulses transiently disturb the PH3 pattern of individual domains.

Mitosis 14 occurs asynchronously within a particular domain. A typical WT domain 1 is shown in (c). Central cells are in anaphase (circles), while external cells are in metaphase (black arrowheads) and prophase (white arrowheads). In a WT embryo 5min after administration of a 5min heat pulse external cells have a prophase-like PH3 staining (b, white arrowheads), while only one metaphase cell is distinguishable in the center of the domain (blue arrowhead). The WGA staining is shown for the corresponding embryo in (d) and (e). A merge of the two staining is shown in (f) and (g) with PH3 in red and WGA in blue.

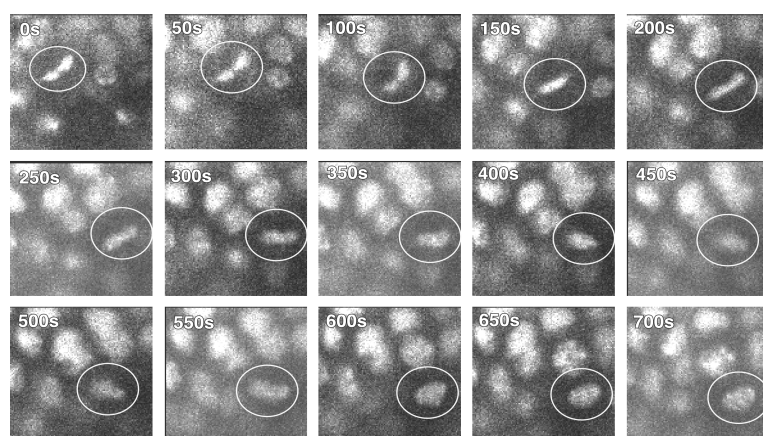


Fig. 2.32: A 5min heat pulse transiently leads to a decondensation of metaphase DNA.

A GFP-His2AvD embryo was exposed to a 5 min heat shock at the beginning of mitosis 14 for domain 1. Progression through mitosis for an individual cell from domain 1 was followed by time lapse fluorescence microscopy. A single picture was taken every 10s. Stills from every 50s are presented here. A single cell is outlined. Immediately after mitosis at $t=0s$ the cell is in metaphase. This state persists for almost 6min, in comparison to the normal metaphase, which lasts only 2min. Afterwards, the DNA begins to decondense and assume an interphase/prophase like morphology without any apparent anaphase or telophase.

Rux expression drives cells from metaphase to interphase.

The same heat-shock protocol was applied to *prd-GAL4 X UAS-CycA Δ 170 ; hs-rux* embryos. The heat-shock was applied to embryos in late mitosis 15. At this stage expression of UAS-CycA Δ 170 was sufficiently high to arrest cells in metaphase in stripes in the embryo (data not shown). The heat-shock did not abrogate UAS-CycA Δ 170 function, as the metaphase arrest was re-established after the heat-shock in control *prd-GAL4 X UAS-CycA Δ 170* embryos (Fig. 2.33A). The heat-shock protocol was sufficient to induce expression of *rux* from the *hs-rux* transgene in all cells, including those expressing CycA Δ 170. *In situ* hybridization with a *rux* RNA probe showed a uniform level of *rux* expression in both stripes and interstripes (Fig. 2.33B). Rux protein was detected 15 min after induction (data not shown). CycA Δ 170-expressing cells exited mitosis 20 min after induction of Rux. Stripes of telophase cells were visible in *prd-GAL4 X UAS-CycA Δ 170 ; hs-rux* embryos (Fig. 2.33Cb, brackets). An hour after *rux* induction almost all cells were arrested in interphase (Fig. 2.33D), demonstrating that Rux induced a mitotic exit. As nuclear density was equally high in the paired expressing stripes and the interstripes (Fig. 2.33D) this exit from mitosis must have involved completion of mitosis. Thus, expression of *rux* was sufficient to induce an exit from mitosis in cells expressing an indestructible CycA.

Examination of the *prdGAL4 X UAS-CycA Δ 170* embryos at later developmental stages showed that the metaphase arrest induced by expression of CycA Δ 170 was transitory. The DNA of most cells in *prdGAL4 X UAS-CycA Δ 170* embryos was in a decondensed metaphase state approx. 2hr after initiation of UAS-CycA Δ 170 expression (Figure 2.34a-b). The nuclear density of CycA Δ 170-expressing stripes was half of that for interstripes, suggesting that cells expressing CycA Δ 170 exited mitosis with a 4n DNA content. If Rux is involved in mitotic exit it is likely that Rux was one of the factors which downregulated CycA Δ 170 and induced a metaphase exit in these embryos. Therefore, *rux³ ; prdGAL4 X rux³ ; UAS-CycA Δ 170* embryos of the same developmental stage were examined. Numerous cells expressing stable CycA in a *rux* mutant embryo remained trapped in metaphase (Figure 2.34a-d). Whereas almost all cells in the embryo depicted in 2.34a-b were in interphase, approximately half the cells in the *rux* mutant were in metaphase. Thus, *rux* mutants are impaired in their ability to overcome a CycA Δ 170 induced cell cycle arrest, as Rux activity is required to downregulate CycA activity during metaphase. This is very similar to an observation made previously in budding yeast. Low level overexpression

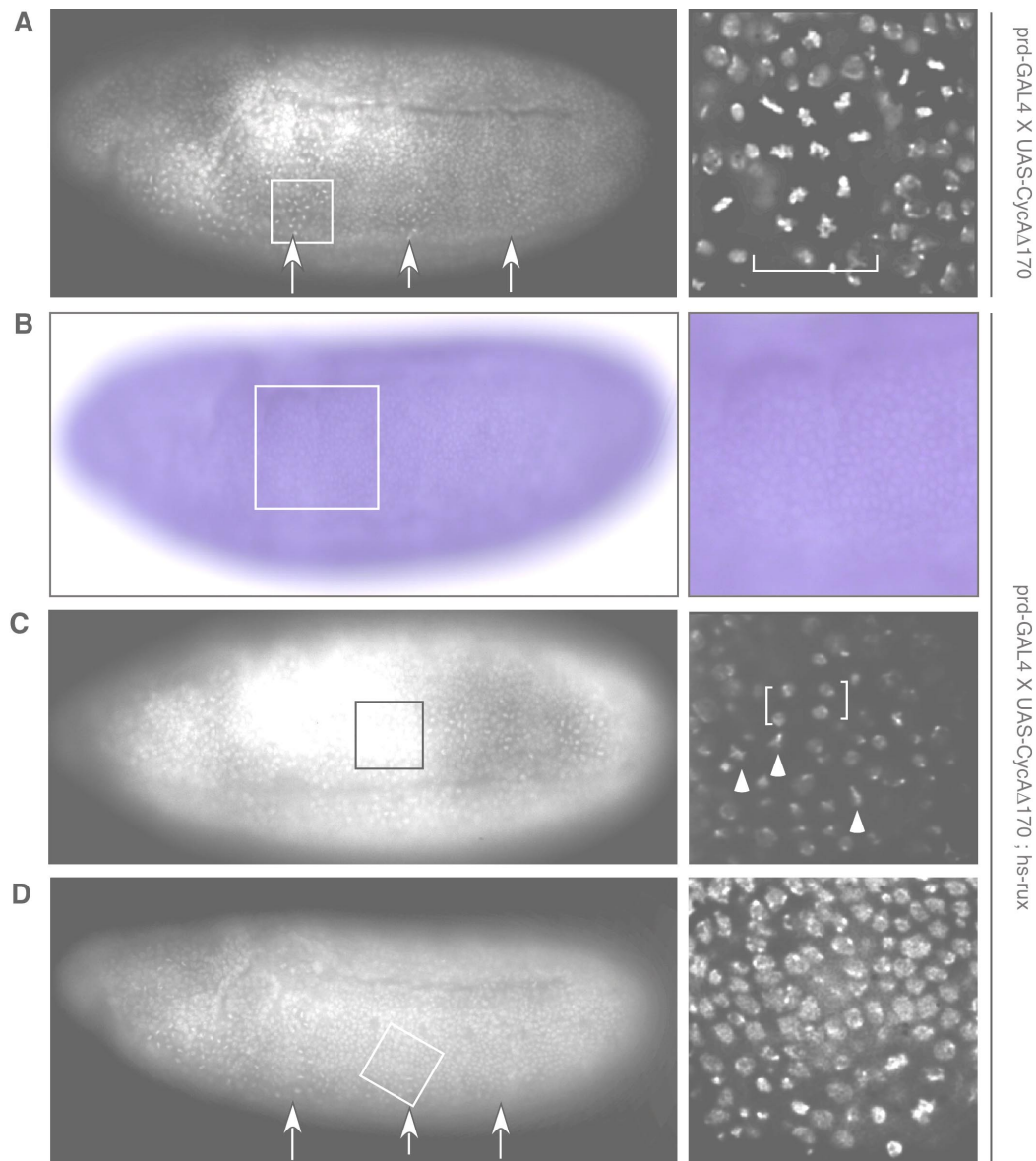


Fig. 2.33: Rux overexpression is sufficient to drive cells from metaphase into interphase. (A) A control *prdGAL4 X UAS-CycA Δ 170* was exposed to a 5min heat pulse and fixed 20 min later. The heat-pulse does not reverse a metaphase arrest induced by overexpression of *CycA Δ 170*, as cells arrest in metaphase in stripes of the embryo after the heat pulse (A, arrows). A magnification of the boxed region in A confirms that the cells have arrested in metaphase (brackets). (B) *rux* expression is induced throughout the embryo by a 5min heat pulse in a *prd-GAL4 X UAS-CycA Δ 170 ; hs-rux* embryo. The embryo presented in B is at the same developmental stage as the embryo in A and was fixed 10min after a heat pulse. *rux* expression is visualized by *in situ* hybridization with a *rux* RNA probe. The gene is expressed to equal extents in *CycA Δ 170*-expressing and non-expressing cells. (C) 20min after administration of a heat pulse to *prdGAL4 X UAS-CycA Δ 170 ; hs-rux* embryos cells in paired stripes start to exit metaphase. As well as a reduction in the number of metaphase cells (arrowheads) a number of cells are discernible that are in anaphase/telophase (brackets). (D) 1hr after *rux* induction all cells are in interphase.

of a stable cyclin in *S. cerevisiae* leads to a transitory metaphase arrest (Amon et al., 1994). Cells eventually exit metaphase as the yeast CKI, Sic1p downregulates cyclin activity.

In summary, Rux is a CKI specific for mitotic cyclins. Rux overexpression inhibits mitosis and mitosis is prolonged in *rux* mutants. In particular, metaphase is significantly longer in *rux* mutants and expression of *rux* is sufficient to force cells trapped in metaphase into interphase. CycA is required for execution of metaphase and CycA must be downregulated to exit metaphase, as expression of an indestructible CycA leads to a metaphase arrest (Sigrist et al., 1995). The data presented above strongly argue for a role for Rux in contributing to exit from mitosis by downregulating Cdk1/CycA activity. In *rux* mutants CycA proteolysis alone is responsible for downregulation of Cdk1/CycA, leading to a prolonging of metaphase.

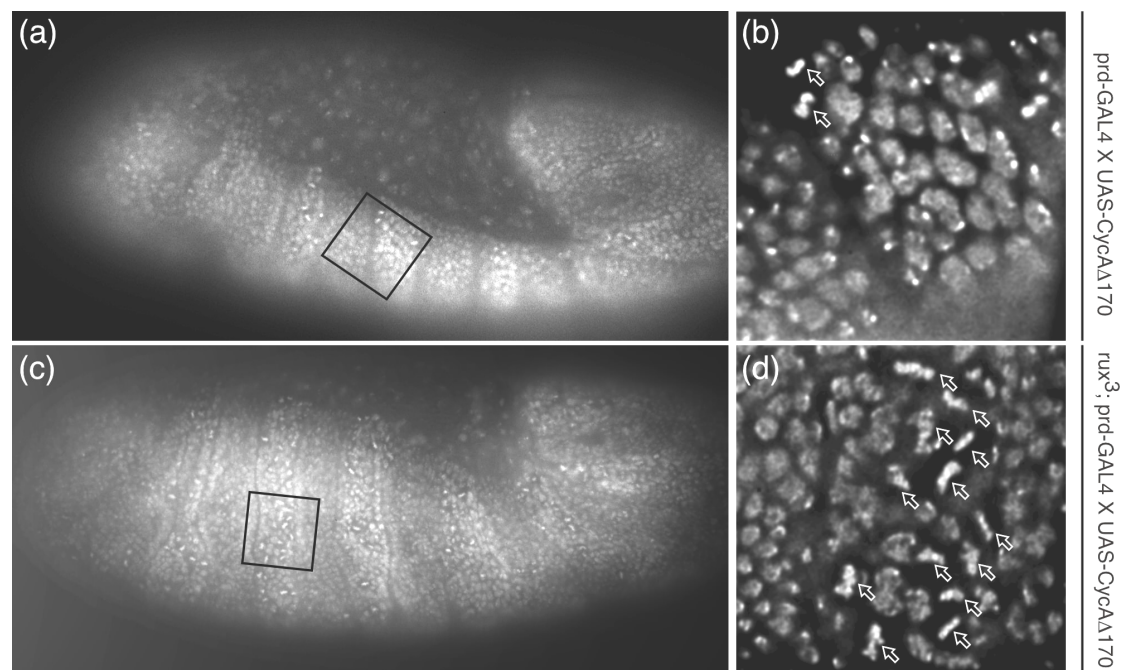


Fig. 2.34 *rux* mutants display an impaired ability to overcome a transient metaphase arrest induced by CycA Δ 170.

(A) The metaphase arrest induced by CycA Δ 170 in Fig. 2.23 is not permanent. Approximately 2hr after metaphase arrest cells exit mitosis with separating sister chromatids (a), resulting in stripes of cells with half the nuclear density of interstripes. Most cells in the CycA Δ 170 expressing stripes are in interphase after 2 hr (b). **(B)** In a *rux* mutant embryo expressing CycA Δ 170 a greater number of cells are arrested in metaphase at the same developmental stage (c). A higher magnification shows that almost half of the *rux* mutant cells are still in metaphase (d). Therefore, Rux activity is required to downregulate CycA Δ 170 during metaphase.

SIC1 functions as a CKI in *Drosophila* embryos

SIC1 from *S. cerevisiae* is the only CKI known with a role in exit from mitosis. The data presented above and in previous reports reveal a number of similarities between Rux and SIC1. Both are CKIs specific for mitotic cyclins, with a role in G1 establishment. Both interact directly with target cyclins via RXL motifs and are downregulated toward the end of G1. There are no obvious similarities between the two proteins at the level of the amino acid sequence. However, it is possible that both proteins function in a similar manner. To test this SIC1 was assayed for its ability to inhibit *Drosophila* cell cycle proteins *in vivo* and *in vitro*. SIC1 mRNA was transiently expressed by injecting mRNA into pre-blastoderm embryos. The embryos were aged for a further 2 hours and analyzed for cell cycle progression. A typical embryo is presented in Fig. 2.35. SIC1 mRNA was injected into the anterior half of the embryos (Fig. 2.35Ab). Based on the extent of germband extension (Fig. 2.35a, arrowhead) most cells in a WT embryo of this stage have undergone mitosis 14. However, cells expressing SIC1 mRNA arrest in G2 of cycle 14. The nuclear density in the SIC1 expressing part of the embryo is approx. half of that in the remainder of the embryos (Fig. 2.35c). Higher magnification of SIC1 expressing cells confirms that they are in interphase as the DNA is decondensed (Fig. 2.35Af). CycA is also present in all SIC1 expressing cells (Fig. 2.35Aa) and is exclusively cytoplasmic (Fig. 2.35Ae), confirming that these cells have arrested in G2 of cell cycle 14. The identical DNA morphology and CycA staining pattern was observed for all embryos examined. In each case SIC1 arrested cells in G2 of cycle 14.

In a second series of experiments Sic1p was tested for its ability to modify the *in vitro* kinase activity of *Drosophila* CDK/cyclin complexes. The experimental setup was identical to that described in Fig. 10. CDKs, cyclins, and Sic1p were translated *in vitro* and co-incubated using an embryonic extract as a source of CAK. CDK/cyclin complexes were then precipitated and tested for their ability to phosphorylate the *in vitro* substrate histone H1. Sic1p is a potent inhibitor of Cdk1/CycA (Fig. 2.36a) and Cdk1/CycB (Fig. 2.36b), but not of Cdk2/CycE. Cdk2/CycE activity was enhanced by a factor of 2.6 by the addition of Sic1p. Thus, identical to Rux Sic1p specifically inhibited the kinase activity of *Drosophila* mitotic CDK/cyclin complexes and induced a cell cycle arrest in G2 upon overexpression in *Drosophila* embryos.

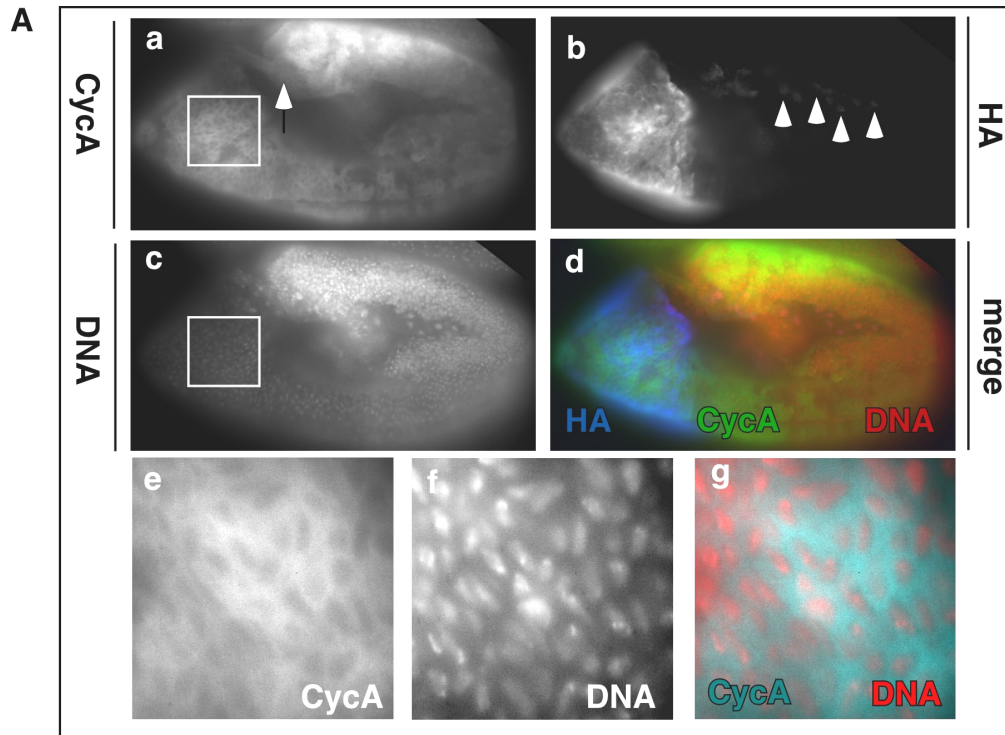
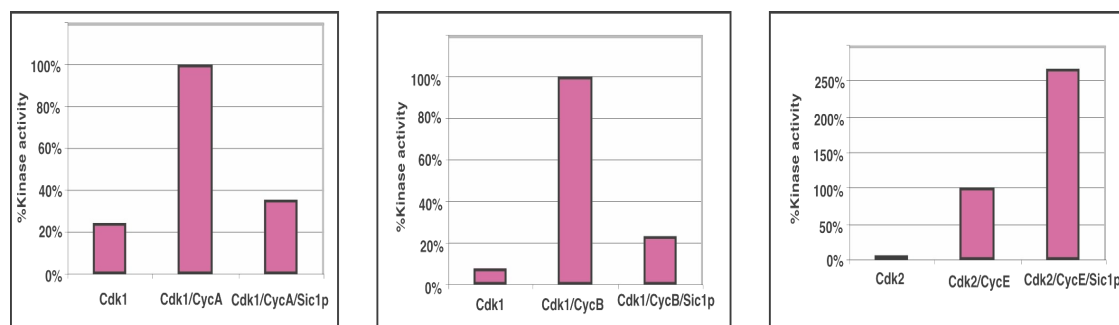


Fig. 2.35: SIC1 overexpression in *Drosophila* embryos arrests cells in G2.

mRNA for HA-tagged SIC1 (HA-SIC1) was injected into the anterior of pre-blastoderm *Drosophila* embryos. HA-Sic1p was visualized by indirect immunofluorescence with anti HA antibodies (b). The protein is ubiquitously expressed in the anterior of the embryos. Sic1p is nuclear in cells of the amnioserosa (b, arrowheads). CycA was visualized by staining embryos with anti-CycA antiserum (a) and DNA was visualized by staining with bisbenzidine (c). The three images are merged in (d) with DNA in red, CycA in green and Sic1p in blue. The germband (a, arrow) is fully extended in the embryo depicted here, indicating that the embryo is undergoing mitosis 15. The boxed region in (a) and (c) is shown under higher magnification in (e-g). CycA is clearly cytoplasmic in all Sic1p expressing cells (e) and the DNA is in a decondensed interphase state (f). A merged image of (e) and (f) is shown in (g) with CycA in blue and DNA in red.



2.36: Sic1p specifically inhibits Cdk1 kinase activity.

The H1 kinase activity of Cdk1/CycA, Cdk1/CycB and Cdk2/cycE in the presence and absence of Sic1p was assayed. The results presented here are the averages of three individual experiment. As a negative control for kinase activity Cdk1 or Cdk2 was assayed in the absence of any cyclin partner. The activities of CDK/cyclin complexes was set to 100% for each individual experiment. Cdk1 and Cdk2 are relatively inactive kinases (columns 1, 4 and 7 respectively) that are enhanced by the addition of CycA or CycB for Cdk1 and CycE for Cdk2 (columns 2, 5 and 8 respectively). Cdk1/CycA activity is reduced by approx. 65% upon co-incubation with Sic1p (column 3). Similarly the activity of Cdk1/cycB is reduced by almost 80% (column 6). The activity of Cdk2/cycE is enhanced by a factor of greater than 2.

Rux was transiently expressed in U2OS carcinoma cells to test whether Rux also inhibits cell cycle progression in other species. As a positive control p27, a mammalian CKI known to elicit a G1 arrest, was expressed in cells of the same line. Rux induced a G1 arrest in cells to almost the same extent as the control CKI, p27, demonstrating that Rux also functions as a CKI in other organisms (Figure 2.37). The arrest induced in this case was in G1, not G2 as is observed in *Drosophila*. This probably reflects the fact that CycA is principally an S phase cyclin in mammals, whereas it is primarily a mitotic cyclins in *Drosophila*.

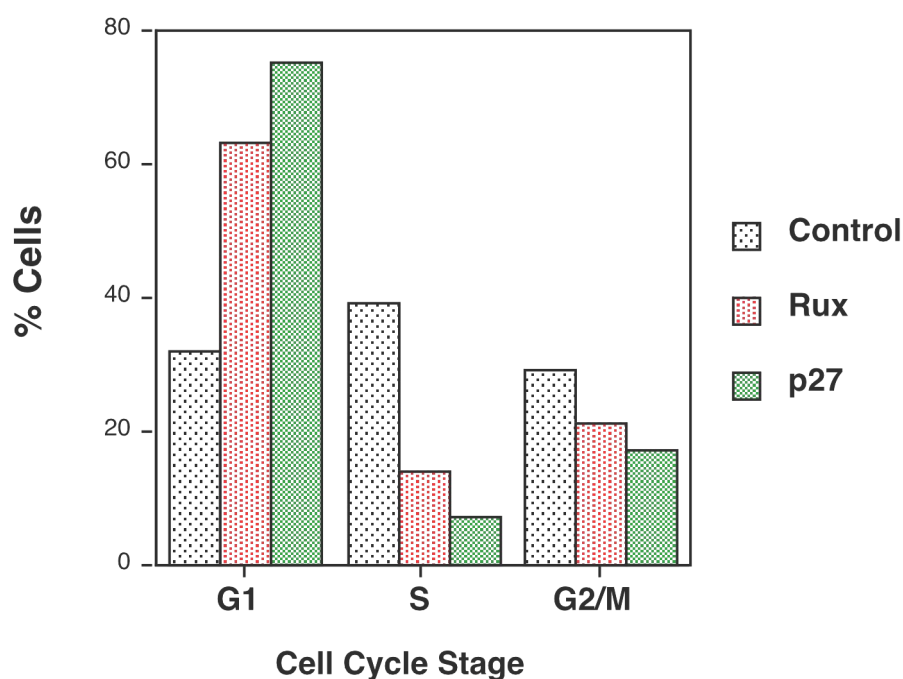


Fig. 2.37: Rux prevents cell cycle progression in U2OS cells.

Rux was transfected into U2OS cells and the cell cycle profile monitored after transfection. 62% of all cells transfected with Rux are in G1, whereas 27% of control cells transfected with vector alone are in G1, indicating that Rux induces a G1 arrest in human cells. In agreement with this 74% of all cells transfected with p27 are in G1. p27 is a CKI of the CIP/KIP family, known to induce a G1 arrest. These experiments were performed by Rene Medena at the University of Utrecht.

Downregulation of Rux activity during cell cycle progression

As Rux is a negative regulator of cell cycle progression it is likely that Rux is also negatively regulated at some point during the cell cycle to allow progression into the next phase. This phenomenon has been observed for numerous CKIs. Generally, CKIs are downregulated at discrete times, mainly before S phase by proteasome mediated degradation. The signal that triggers CKI destruction is often phosphorylation by specific CDK/cyclin complexes. It has been proposed that Rux is downregulated in such a manner (Thomas et al., 1997). A Rux-lacZ fusion protein is destroyed prior to S phase and this destruction is enhanced by overexpression of the S phase cyclin, CycE. Furthermore, Cdk2/CycE phosphorylates Rux *in vitro*. Thus, it was proposed that Cdk2/CycE targets Rux for destruction at S phase by phosphorylation.

High level overexpression of Rux in embryos arrested cells in G2 (Fig. 2.6), preventing analysis of Rux destruction during specific stages of the cell cycle. However, lower level overexpression of Rux did not completely inhibit cell cycle progression. Instead, the cell cycle was considerably slower. Virgin females that maternally provided GAL4 (matGAL4) induced low levels of Rux expression during interphase of cell cycle 14 when crossed to UAS-rux males (data not shown). These expression levels were not sufficient to elicit a cell cycle arrest. Nonetheless, cell cycle 14 was considerably slower in these embryos than in control WT embryos. A WT and matGAL4 X UAS-rux embryo are compared in Fig. 2.38. Both embryos were approximately at the same developmental stage, as determined by the extent of germband extension (Fig. 2.38a and b, arrowhead). In matGAL4 X UAS-rux embryos mitosis 14 had only begun in domains 1 and 5, whereas mitosis 14 was underway in approximately half the domains (1-11) in the WT embryo. Although mitosis 14 was delayed the overall pattern of mitosis was maintained in matGAL4 X UAS-rux embryos (Fig. 2.38b and data not shown). Cdc25^{Stg} activity is the limiting factor for entry into mitosis 14. *cdc25^{Stg}* is transcribed in most mitotic domains about 10 minutes in advance of entry into mitosis. In the matGAL4 X UAS-rux embryos mitosis was not delayed as a result of delaying *cdc25^{Stg}* transcription. *In situ* hybridization analysis with *cdc25^{Stg}* RNA probes revealed that *cdc25^{Stg}* was transcribed in the same domains in WT (Fig. 2.38e) and matGAL4 X UAS-rux embryos (Fig. 2.38f) at the same developmental stage (arrowheads in Fig. 2.38e and f indicate extent of germband extension).

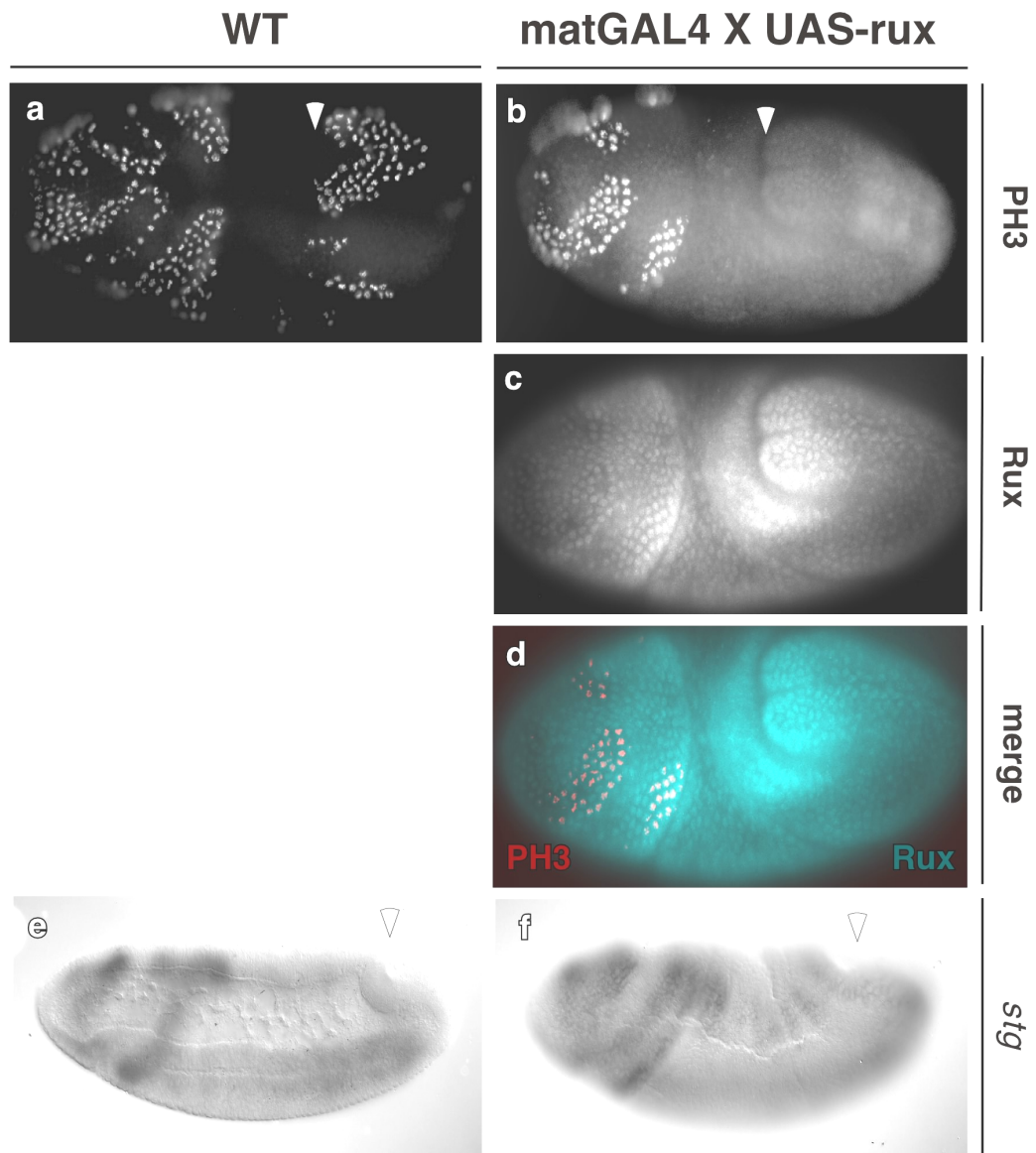


Fig. 2.38: Mild overexpression of Rux delays execution of mitosis.

Rux was expressed early during embryogenesis by crossing *matGAL4* virgins to *UAS-rux* males. Rux protein is first visible in interphase 14 of *matGAL4 X UAS-rux* embryos. The level of Rux expression is such that it does not completely inhibit mitosis, rather mitosis is delayed. A WT (a) and *matGAL4 X UAS-rux* (b) from similar developmental stages is shown (observe relative position of germband, marked with an arrowhead). Mitosis is visualized by staining embryos with anti-PH3. Whereas mitosis 14 is proceeding in domains 1-11 of the WT embryo (a) it is only detectable in domains 1, 2, 3 and 5 of the *matGAL4 X UAS-rux* embryo (b). The temporal order of mitosis 14 is preserved in the *matGAL4 X UAS-rux* embryo (b). The expression levels of Rux are shown in (c) and a merge of (b) and (c) is shown in (d) with Rux in blue and PH3 in red. Rux does not delay mitosis at the level of regulating *cdc25^{stg}* transcription. *In situ* hybridization with a *cdc25^{stg}* RNA probe are shown for a WT (e) and a *matGAL4 X UAS-rux* (f) embryo. Both embryos are at the same stage of mitosis 14 (arrowhead indicates position of germband) and transcription patterns for *cdc25^{stg}* are the same in both.

As Rux overexpression does not prevent $cdc25^{Stg}$ transcription the observed delay in mitosis must be downstream of $cdc25^{Stg}$ transcription. There are several possible explanations for this observation. One possibility is that Rux prevents Cdk1 from phosphorylating its substrate molecules, thereby delaying entry into mitosis (Fig. 2.39B). It has also been proposed that a positive feed-back loop exists between Cdk1 and $Cdc25^{Stg}$. Low levels of Cdk1 activity are proposed to activate $Cdc25^{Stg}$ by phosphorylation. $Cdc25^{Stg}$ increases Cdk1 activity further through removal of inhibitory phosphates on Cdk1, thereby precipitating an entry into mitosis (Fig. 2.39B). In this case Rux overexpression would inhibit both the feedback loop and the phosphorylation of downstream targets of Cdk1. The result in this case is a reduction in both Cdk1 activation and activity, whereas the first model simply predicts a

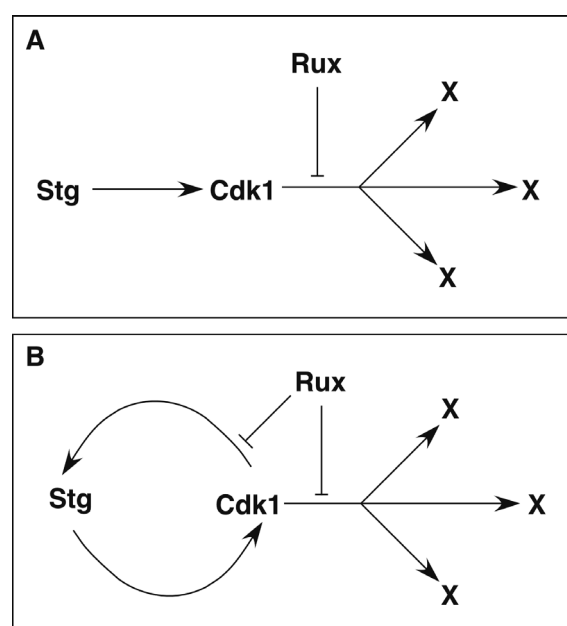


Fig. 2.39: Two potential explanations for the delay of mitosis in *matGAL4 X UAS-rux* embryos.

(A) Stg activates Cdk1 by dephosphorylating it on T14 and Y15. Cdk1 activity rises to a critical threshold level and triggers entry into mitosis by phosphorylating downstream targets. Moderate levels of Rux brake this process, thereby slowing the rate of entry into mitosis for individual domains. (B) $Cdc25^{Stg}$ activates Cdk1 by dephosphorylating it on T14 and Y15. A positive feedback is established as Cdk1 hyperactivates $Cdc25^{Stg}$ by phosphorylation. Rux delays entry into mitosis by braking the feedback loop as well as the phosphorylation of downstream targets of Cdk1. Entry into mitosis is delayed as a result of the hypoactivation of $Cdc25^{Stg}$.

reduction in Cdk1 activity.

Rux directly inhibits Cdk1 activity (Fig. 2.13) and does not inhibit $Cdc25^{Stg}$ activity (Fig. 2.8). Therefore, overexpression of $Cdc25^{Stg}$ should not alter the ability of Rux to delay execution of mitosis in the case of the former model, as $cdc25^{Stg}$ *in situ*

analysis confirms that $Cdc25^{Stg}$ levels are high enough to induce mitosis in *matGAL4 X UAS-rux* embryos (Fig. 2.38f). In the case of the latter model overexpression of $Cdc25^{Stg}$ would enhance the feedback stimulation of Cdk1, thereby at least partially overcoming the mitotic delay observed in *matGAL4 X UAS-rux* embryos. This hypothesis was tested by crossing *UAS-rux ; UAS-cdc25^{Stg}* males to *matGAL4* virgin females. Overexpression of $Cdc25^{Stg}$ in control *matGAL4 X UAS-cdc25^{Stg}* embryos resulted in replacement of the standard pattern of mitotic domains with simultaneous mitoses throughout the embryo (Fig. 2.40a). Co-expression of Rux and Stg using a *matGAL4* driver also abolished the standard pattern of mitotic domains and led to mitoses throughout the embryo (Fig. 2.40c-e). Whereas there are less mitoses in *matGAL4 X UAS-cdc25^{Stg} ; UAS-rux* embryos than in *matGAL4 X UAS-rux* embryos the number is high enough to conclude that overexpression of $Cdc25^{Stg}$ overcomes the mitotic delay elicited by *matGAL4 X UAS-rux*. These data support a model where *matGAL4 X UAS-rux* delay mitosis by inhibiting Cdk1 activity and indirectly preventing Cdk1 activation by $Cdc25^{Stg}$.

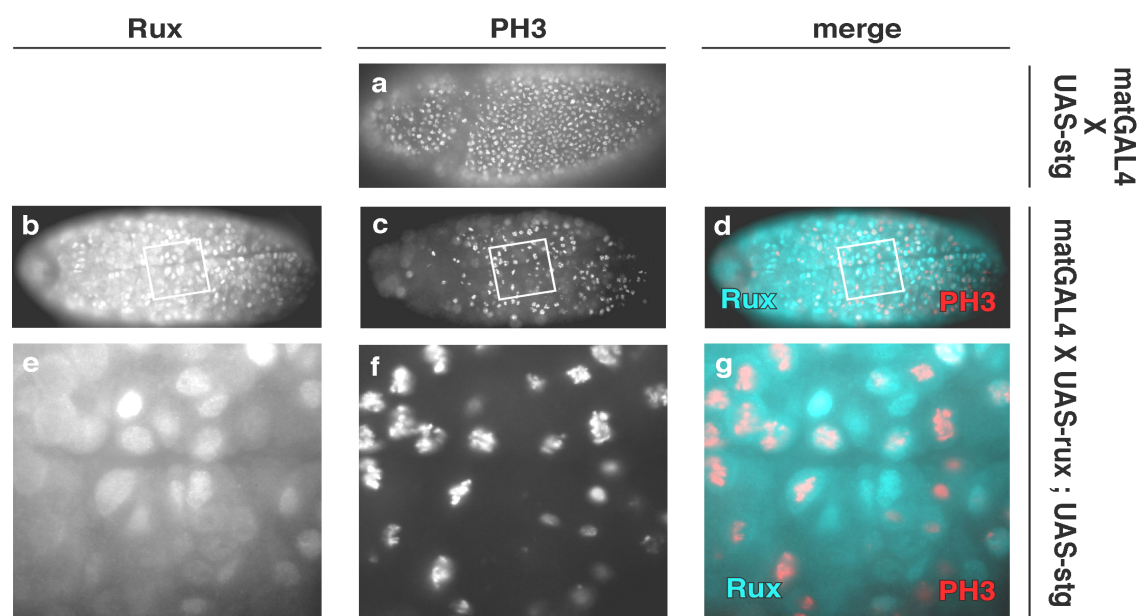


Fig. 2.40: Co-expression of $Cdc25^{Stg}$ and Rux reverses the mitotic delay observed in *matGAL4 X UAS-rux* embryos.

Ubiquitous expression of $Cdc25^{Stg}$ (a) induces mitosis 14 throughout the embryo. Mitosis is visualized with anti PH3 antibodies. Mitosis 14 occurs throughout *matGAL4 X UAS-rux ; UAS-Cdc25^{Stg}* embryos in a manner that deviates from the classical domain pattern (c). The Rux staining for the *matGAL4 X UAS-rux ; UAS-Cdc25^{Stg}* embryo is shown in (b) and a merge of (b) and (c) is shown in (d) with Rux in blue and PH3 in red. The boxed region in b-d is shown at a higher magnification in e-f. Rux expressed in all cells by the *matGAL4* driver (e). In contrast to control *matGAL4 X UAS-rux* embryos (Fig. 38) mitosis is not delayed in *matGAL4 X UAS-rux ; UAS-Cdc25^{Stg}* embryos, rather it occurs throughout the embryo to a slightly lesser extent than in *matGAL4 X UAS-stg* embryos.

Disappearance of CycA mirrors progression through mitosis as a result of CycA destruction during metaphase (Fig. 2.41a,d,g and j). Interestingly, it was observed that Rux disappears in a very similar manner in *matGAL4 X UAS-rux* embryos. Rux destruction occurred in a manner that directly reflects the mitotic domains of mitosis 14 (Fig. 2.41b and e). Rux destruction also mirrored that of CycA in cell cycle 15 (Fig. 2.41g and h) with the exception of the amnioserosa (Fig. 2.41h, bracketed area). The amnioserosa is a specialized group of cells that arrests division in G2 of mitosis 14 with a DNA content of 4n. Rux was destroyed in mitosis 15 and did not accumulate in G2 of cell cycle 16 (Fig. 2.41k), presumably due to a diminishment of *matGAL4* activity. The Rux protein that accumulated in the amnioserosa during cell cycle 14 was stable for a long time, as the signal can still be detected in embryos of cell cycle 16 (Fig. 2.41k arrowhead). Thus, it appears that Rux is stable in G2 cells and is turned over in dividing cells.

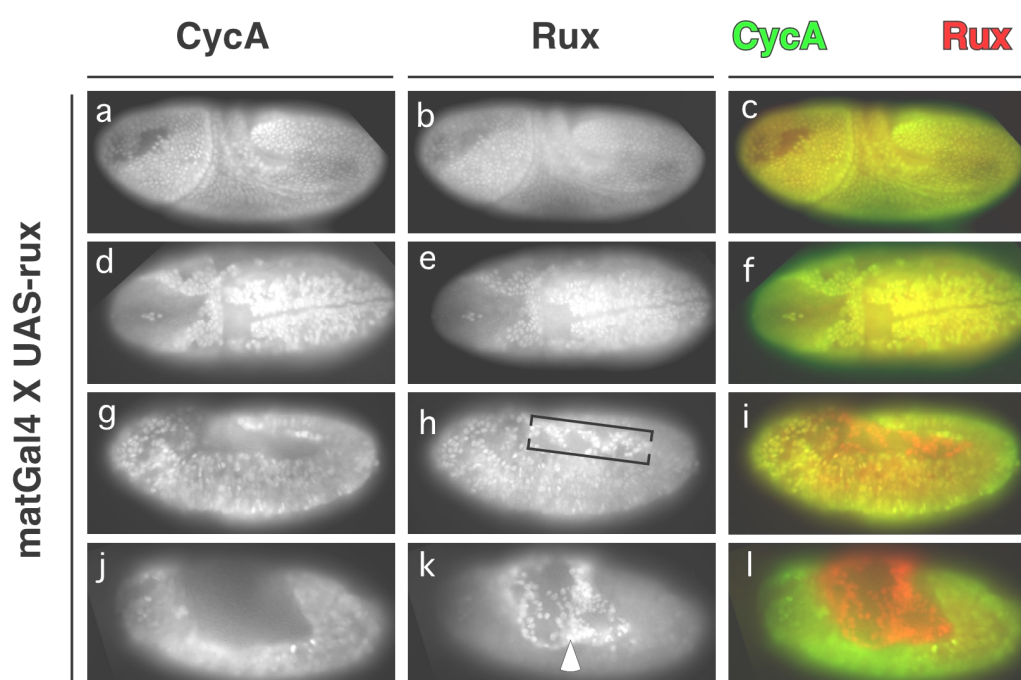


Fig. 2.41: Rux is degraded in dividing cells in the embryo.

CycA (a, d, g and j) and Rux (b, e, h and k) are shown in *matGAL4 X UAS-rux* embryos during mitosis 14 (a-f), mitosis 15 (g-i) and mitosis 16 (j-l). A merge of the corresponding Rux and CycA staining are shown in c, f, i and l with Rux in red and CycA in green. CycA is degraded during metaphase (Fig. 4). Therefore, the pattern of CycA degradation reflects the course of progression through the different mitoses. CycA disappears in a manner that reflects the pattern of mitotic domains in mitosis 14 (a, d). The pattern of Rux disappearance is almost identical in the same embryos (b, e). Similarly, the pattern of Rux destruction (h) almost mirrors that of CycA (g) during mitosis 15, with the exception of the amnioserosa (h, brackets), a specialized group of cells that arrest in G2 of mitosis 14. No new Rux protein is translated during the 16th cell division, due to a lack of activity of the *matGAL4* driver (k). Nevertheless, the Rux protein in the amnioserosa since the 14th cycle is still present (k, arrowhead).

Higher magnification revealed that Rux and CycA are destroyed in a distinct temporal order. Whereas CycA was destroyed at the metaphase to anaphase transition (Fig. 2.4 and Fig. 2.42e-h), Rux was stable in metaphase (Fig. 2.42j) and anaphase cells (Fig. 2.42k). Rux protein first disappeared as cells exited mitosis at the telophase to interphase boundary (Fig. 2.42l). It is important to emphasize that these observations were made with cells in mitosis 14.

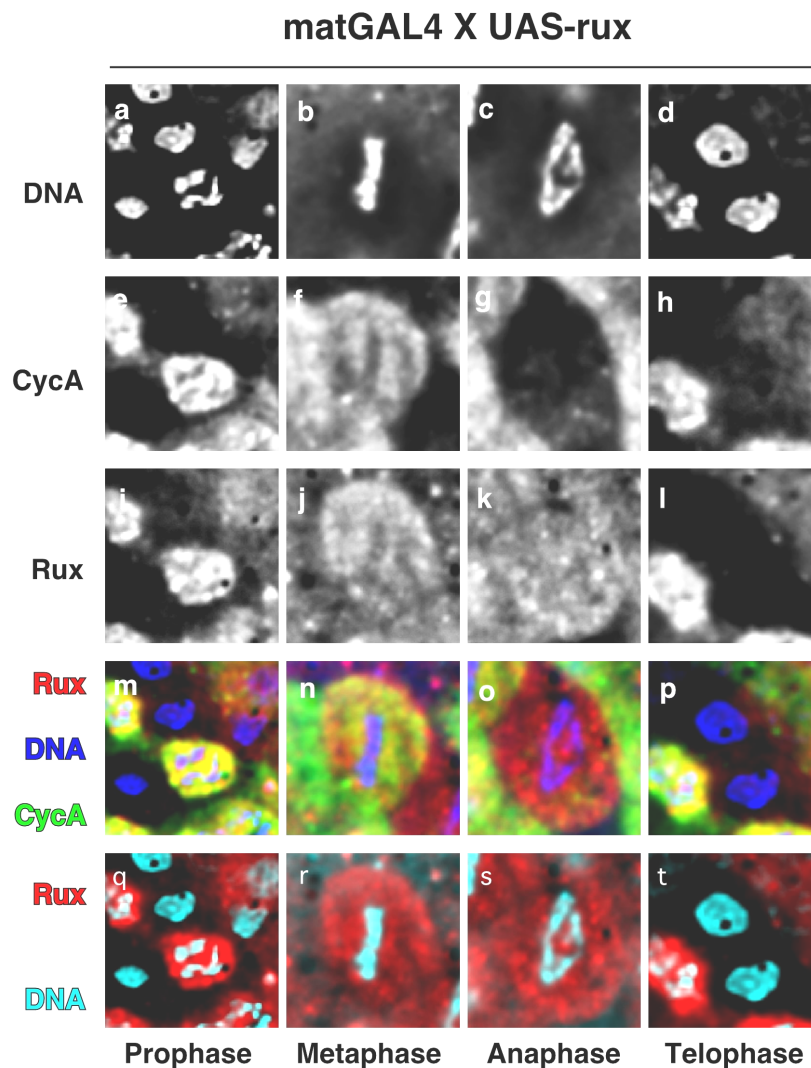


Fig 2.42: Rux is degraded after anaphase in dividing cells.

CycA (e-h) and Rux (i-l) were visualized in single cells from matGAL4 X UAS-rux embryo at different stages of the cell cycle. Cell cycle stage was determined by staining for DNA with bisbenzidine (a-d) and cells were scored as prophase (a), metaphase (b), anaphase (c) or telophase/interphase (d). CycA is destroyed during metaphase (e-h) in agreement with previous observations. Rux is a nuclear protein during interphase and prophase (i). The protein is spread throughout the entire cell after nuclear envelope breakdown in metaphase (j) and Rux persists during anaphase (k). Rux protein is destroyed during or after telophase (l). A merge of the three images is shown in m-p with Rux in red, DNA in blue and CycA in green. A merge of the Rux and DNA channels alone is shown in q-t with Rux in red and DNA to blue to confirm that Rux persists throughout metaphase and anaphase.

The first 16 divisions occur without any G1 phase. S phase 15 follows within 5 minutes of mitosis 14 (Edgar and O'Farrell, 1990). It is therefore not possible to deduce from the above data whether Rux was destroyed as cells exited mitosis or as cells entered S phase. To test this possibility directly it is necessary to express Rux prior to mitosis 16. Mitosis 16 is followed by a prolonged G1. If Rux persists in G1 one can deduce that Rux destruction occurs prior to S phase. If, however, Rux is destroyed after mitosis 16 then the destruction described above is a mitotic event. To perform this experiment it is necessary to express levels of Rux prior to mitosis 16 that are not high enough to prevent mitosis. A heat shock of 10 minutes produced sufficient amounts of Rux to induce a brief mitotic delay during mitosis 14, similar to that seen with *matGAL4 X UAS-rux* embryos. Mitosis 14 proceeded within 1 hour after the heat-shock and Rux was degraded in a pattern similar to CycA (Fig. 2.43a-c). Furthermore, Rux was stable in the amnioserosa (Fig. 2.43b) and higher magnification confirmed that Rux was degraded after CycA (data not shown). Thus, a 10min heat pulse of *hs-rux* embryos sufficiently recapitulated the Rux expression levels and cell cycle effects observed in *matGAL4 X UAS-rux* embryos. The same heat shock protocol was applied to embryos prior to mitosis 16 and the presence of Rux was determined after completion of mitosis 16 and entry into G1 of cycle 17. Rux was not destroyed in G1 as all cells showed high levels of Rux protein (Fig. 2.43d and e). Thus, Rux is stable throughout mitosis and G1 and is degraded as cells enter S phase. These data are in agreement with a function for Rux as a CKI with a role in triggering an exit from mitosis and maintaining subsequent G1 phases.

The results described above suggest that Rux and CycA are degraded in distinct manners. Rux is stable in the amnioserosa, whereas CycA is not and Rux is destroyed before S phase, whereas CycA is destroyed during metaphase. To confirm that two separate mechanisms exist for Rux and CycA degradation the levels of both proteins were compared in *prdGAL4 X UAS-rux* embryos. As described above cells expressing Rux in these embryos arrest division before mitosis 15 (Fig. 2.6). Rux protein levels persisted for several hours afterwards (Fig. 2.44a and d), whereas CycA disappeared. (Fig. 2.44b and e). Interestingly, CycA is destroyed in non-metaphase cells, as Rux induces a G2 arrest. Thus, a cell-cycle independent developmental program appears to ensure CycA destruction in embryos of this stage. The most likely explanation is that CycA destruction is a result of a rise in the levels of *fizzy-related (fzr)* transcription. Fzr is a component of the APC E3 ligase and triggers the destruction of target proteins such as CycA in G1 (Sigrist and Lehner, 1997). As Rux is not degraded in these cells it appears that Rux is destroyed in a different manner to CycA.

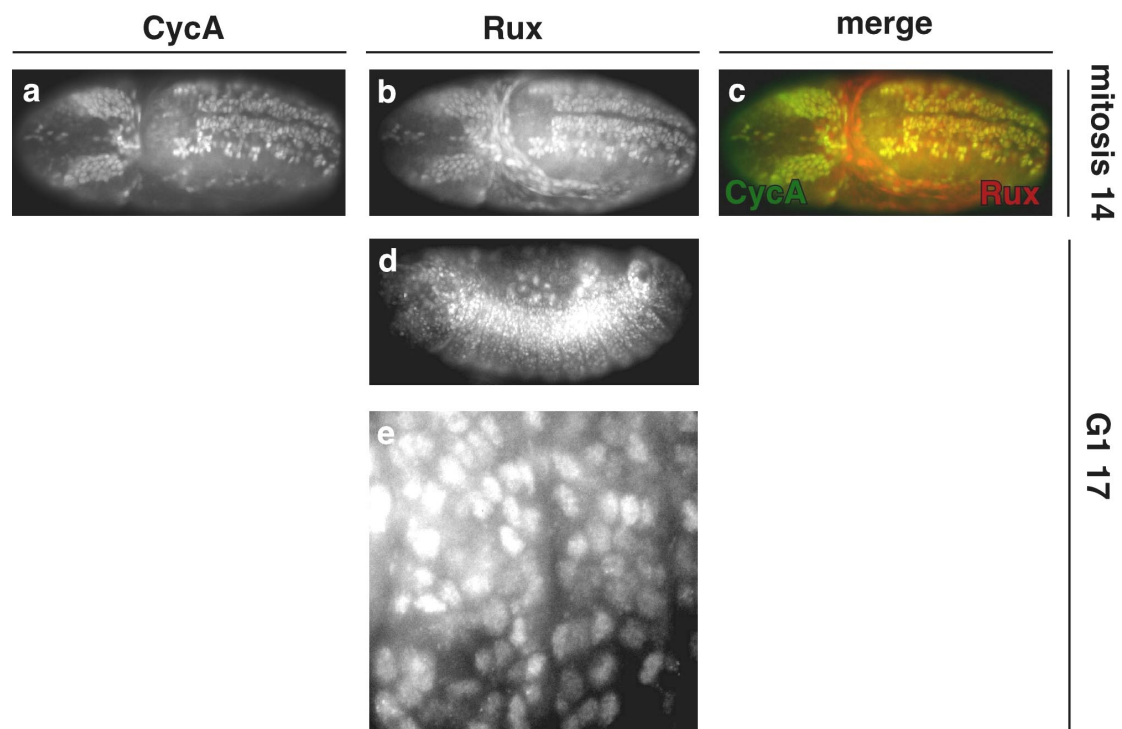


Fig. 2.43: Rux is stable in G1.

A 10min heat pulse followed by a 1hr recovery period, reproduces the *rux* expression levels observed in mat-GAL4 X UAS-*rux* embryos. A hs-*rux* embryo was subjected to a 10min heat pulse and fixed after 1hr. The embryo was stained for CycA (a) and Rux (b). The levels of Rux produced are not sufficient to completely prevent mitosis, however they do delay execution of mitosis. CycA and Rux disappear in a classical mitotic domain pattern, as observed in matGAL4 X UAS-*rux* embryos. Furthermore, Rux is not degraded in the amnioserosa of hs-*rux* embryos (b). A merge of the embryos in (a) and (b) is shown in (c) with Rux in red and CycA in green. Rux protein is shown in hs-*rux* embryos 1hr after a 10min heat pulse (d). The epidermal cells of this embryo are in a prolonged G1 state. A magnification of a region of the embryo in (d) is shown in (e). *rux* protein is not turned over in G1 cells 1hr after expression (d-e), whereas it is turned over in dividing cells (b-c). Thus, Rux destruction occurs prior to DNA replication at S phase and not after mitosis.

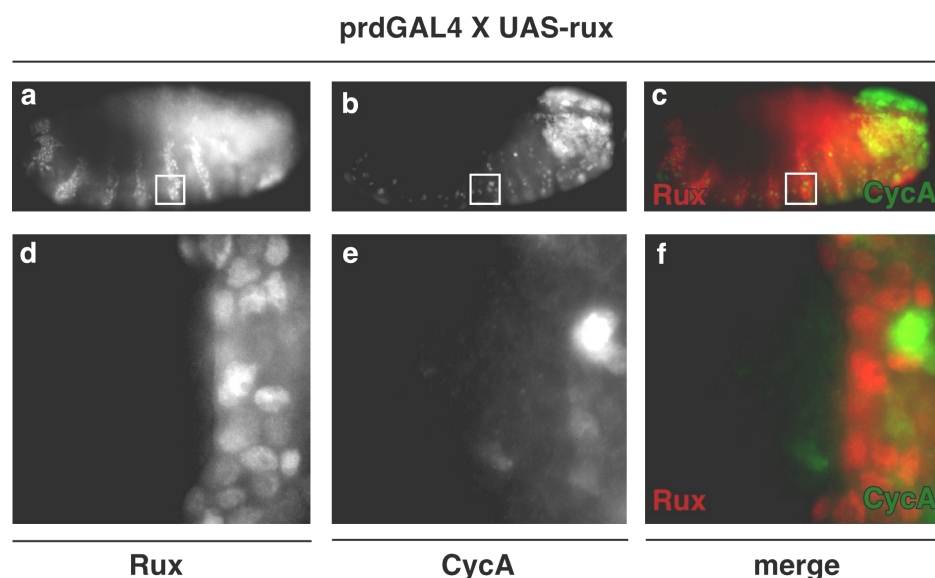


Fig. 2.44: Rux and CycA are destroyed in distinct manners.

Expression of Rux from a UAS-transgene by the prdGAL4 driver arrests cells in G2 of the 15th cell cycle (Fig. 6). The Rux protein is stable for several hours after expression in these cells (a, an embryo is shown with fully retracted germband). CycA, on the other hand is almost completely gone from these cells (b), although CycA destruction normally occurs at mitosis and these cells do not divide. A merge of (a) and (b) is shown in (c) with Rux in red and CycA in green. The boxed region in a-c is magnified in d-f. CycA is almost completely absent in Rux expressing cells, although these cells fail to divide. The cell expressing CycA in (e) and (f) is in a different focal plane to the Rux-expressing cells and probably belongs to the nervous system. These cells are still mitotically active, whereas most WT epidermal cells of this stage are in G1.

These data are in agreement with previous reports that Rux is degraded at the G1-S transition in the eye imaginal disc (Thomas et al., 1997). It was suggested that this destruction is mediated by Cdk2/CycE, presumably through phosphorylation of Rux. This hypothesis was tested in two separate experiments. prdGAL4 females were crossed to UAS-CycE ; hs-rux males. The prd-GAL4 driver line induces high levels of CycE in alternating stripes of the epidermis. Rux was expressed at high levels throughout 3-4hr old embryos by subjecting them to a 15min heat pulse. The levels of Rux protein were then monitored as a function of time. Rux protein was ubiquitously present an hour after the heat shock (data not shown) and started to subside slightly by 2hr (Fig. 2.45a and d). 3hr after heat shock Rux levels had dropped further in all cells and was gone entirely in some (Fig. 2.45b and e). By 4hr Rux was absent throughout almost the entire embryo (Fig. 2.45c and f) with the exception of cells of the nervous system (Fig.45c, arrowheads). Interestingly Rux disappeared at equal rates from CycE overexpressing cells and WT cells (compare prd-expressing and non-expressing stripe in Fig. 2.45e), indicating that overexpression of CycE in the embryonic epidermis is not sufficient to induce Rux destruction.

prdGAL4 X UAS-cycE ; hs-rux

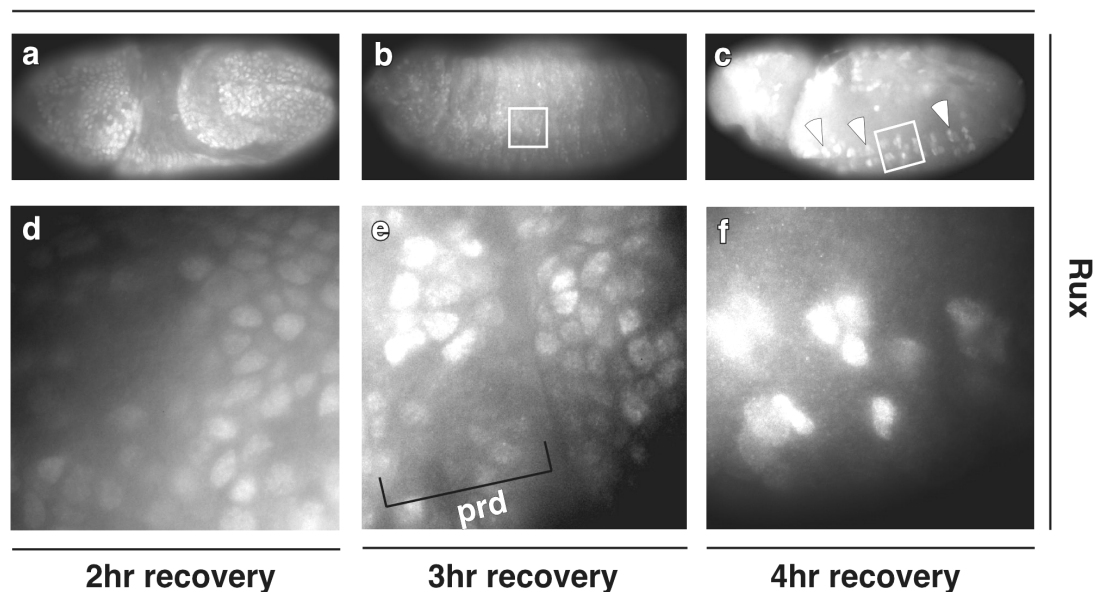


Fig. 2.45: CycE overexpression does not accelerate the rate of Rux destruction.

Rux was overexpressed in prdGAL4 X UAS-cycE ; hs-rux embryos through administration of a heat pulse. The disappearance of Rux was monitored over a fixed period. 2hr after overexpression the protein is present to relatively high levels throughout the embryo (a, d). 3hr after induction Rux levels decline in all cells and disappear in some (b, boxed region magnified in (e)). There is no apparent difference in the total amounts of Rux in CycE overexpressing cells (e, bracket) to cells from interstripes. 4hr after induction Rux has disappeared from almost the entire embryo in both prd stripes and interstripes (c). The protein persists in a subset of cells of the nervous system (c, arrowheads), which are probably in G1. A magnification of the boxed region in (c) is shown in (f).

To directly test whether CycE activity is required for Rux destruction time course experiments were done in *cycE* mutant embryos overexpressing Rux. *cycE* null mutants are homozygous lethal. To construct homozygous mutant embryos heterozygous flies were crossed *inter se*. The parental wild-type chromosome was marked with a transgene that expresses β -galactosidase in 14 stripes of the epidermis. WT embryos expressing the transgene (Fig. 2.46a, arrowheads) are distinguishable from homozygous mutant embryos, which lack β -gal staining (Fig. 2.46d). Rux is still present 1hr after induction in WT embryos overexpressing Rux, and CycA accumulates in the nucleus (Fig. 2.46b). In contrast, Rux is almost completely degraded in *cycE* mutant embryos (Fig. 2.46e), except for the G2 population of amnioserosa cells (Fig. 2.46e, brackets). Therefore, CycE activity is not required for Rux destruction.

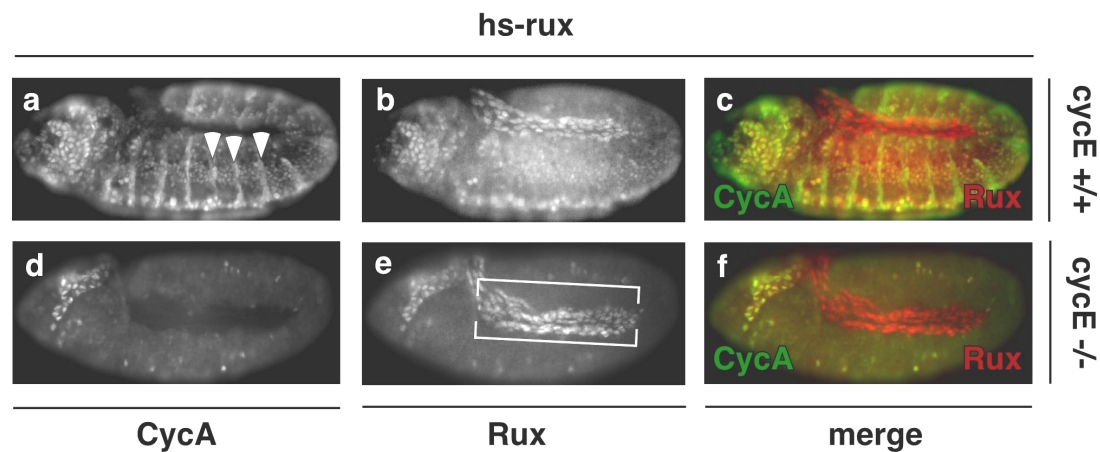


Fig. 2.46: Rux destruction does not depend on CycE activity.

Rux was overexpressed from a heat-inducible promoter in WT or *cycE*^{-/-} mutant embryos. For this experiment heterozygous *cycE* mutants were crossed *inter se*. The WT chromosome bore a transgene, expressing β -galactosidase in 14 stripes in the embryos. The embryos were homozygous for a heat-inducible *rux* transgene (*hs-rux*) on a different chromosome. One quarter of the embryos arising from this cross are mutant for *cycE*, while three quarters of all embryos will have either one or two wild-type copies of the *cycE* gene. WT embryos express β -galactosidase in stripes in the embryo (a, arrowheads) whereas mutant embryos do not (d). The levels of CycA (a and d) and Rux (b and e) were monitored for WT (a and b) and *cycE* embryos (d and e). No Rux is detectable in *cycE* embryos 1hr after induction (e) with the exception of the amnioserosa (brackets), whereas it persists in WT embryos (b). Furthermore, CycA is absent in *cycE* ; *hs-rux* embryos (d), while it is present in control *hs-rux* embryos (a). A merge of (a) and (b) is shown in (c) with Rux in red and CycA in green. A merge of (d) and (e) is shown in (f) with Rux in red and CycA in green.

Interestingly, CycA is also completely destroyed in *cycE* ; *hs-rux* embryos. One possible explanation for this observation is that Rux activity indirectly stimulates Fzr-mediated destruction of target proteins. Fzr is active in its unphosphorylated state and is inactivated by CDK/cyclin mediated phosphorylation. It is possible that CycE mediated phosphorylation prevents destruction of Rux and CycA in WT embryos (Fig. 2.47A). In a CycE mutant overexpressing Rux there is no CDK activity available to phosphorylate Fzr, as CycE is absent and Cdk1 is inhibited by overexpression of Rux. In this case, Fzr is dephosphorylated after completion of mitosis and CycA is rapidly degraded (Fig. 2.47B). It is not clear if the destruction of Rux observed here is Fzr-dependent, as Rux is stable in G1 cells and Fzr is active during G1 (Sigrist and Lehner, 1997). Furthermore, Rux and CycA destruction are distinct events and CycA destruction is mediated by Fzr.

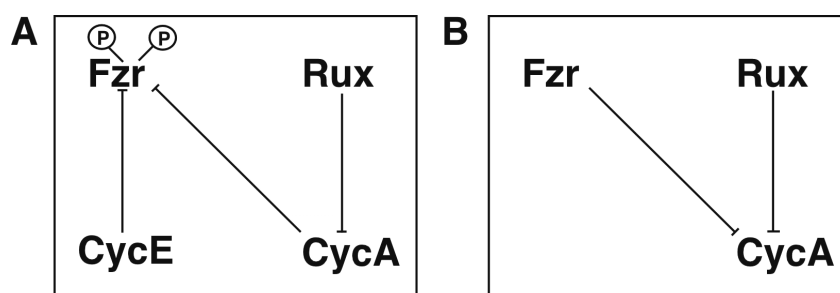


Fig. 2.47: A model to explain the disappearance of CycA in *cycE*; *hs-rux* embryos.

In a WT embryo the overlapping activities of CycE and CycA phosphorylate Fzr, keeping it in an inactive state. Overexpression of Rux inhibits CycA, however not CycE. Therefore, Fzr is maintained in an inactive state. In *cycE*; *hs-rux* embryos overexpressed Rux prevents Cdk1/CycA from phosphorylating Fzr and CycE is no longer present to inactivate Fzr. Thus, Fzr shifts to the active unphosphorylated form, triggering a rapid turnover of both Rux and CycA.

An *in vitro* assay was developed to further analyze Rux protein turnover. Radiolabeled, *in vitro* translated Rux was incubated in a 0-1hr embryonic extract and aliquots were removed at fixed time points and analyzed by SDS-PAGE. Wild-type Rux protein was rapidly degraded in this system, so that almost the entire protein was gone by 30mins (Fig. 2.48A). Addition of proteasome inhibitors, such as clasta-

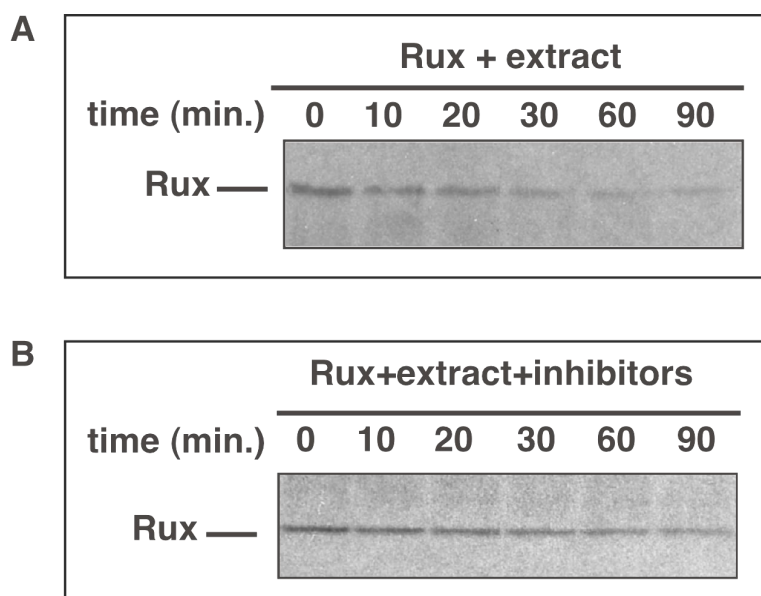


Fig. 2.48: Rux is degraded by the proteasome.

(A) An *in vitro* assay was developed to monitor Rux protein turnover. Rux was translated *in vitro* in reticulocyte lysate in the presence of ^{35}S -Met. The radiolabeled protein was then incubated in a crude 0-1hr embryonic extract and samples removed at the indicated times. The sample were resolved by SDS-PAGE to monitor total protein levels as a function of time. The Rux protein is rapidly degraded in extract. **(B)** Addition of 100 μM of the proteasome inhibitor clasto-lactocystin stabilized the Rux protein. The amount used was determined by the ability of clasto-lactocystin to inhibit the destruction of a fluourogenic peptide substrate of the proteasome in an embryonic extract.

lactocystin significantly stabilizes Rux in this degradation system (Fig. 2.48B). Approximately a half of the protein is still detectable after 30min and residual protein can still be determined after 90min. The same results were observed using a second proteasome inhibitor, NLVS. Thus, it appears that Rux is degraded in a proteasome-dependent manner in this system.

Several CKIs are destroyed at specific cell cycle stages by the proteasome. Traditionally, this destruction is triggered by CDK-dependent phosphorylation of the substrate CKI. Rux has four potential CDK phosphorylation sites with the consensus sequence TP (Fig. 2.1B). To determine whether phosphorylation on any of these sites was a prerequisite for Rux destruction in the assay described above a series of point mutations were introduced into the Rux protein. In each case potential phosphor-acceptor threonines were converted to alanines (Fig. 2.49). A total of seven different mutant constructs were made. All were degraded with kinetics identical to WT Rux. The results are summarized for six different construct graphically (Fig. 2.49A). A seventh mutant construct where all four threonines are mutated to alanines is shown in Fig. 2.49Bb. Removing all four threonines had no effect on the rate of Rux destruction (compare Fig. 2.49Ba and 49Bb), indicating that Cdk-mediated phosphorylation is not essential for Rux destruction. This is in agreement with the observation in live embryos where Rux is rapidly turned over in an *in vivo* context with low Cdk activity (Fig. 2.46).

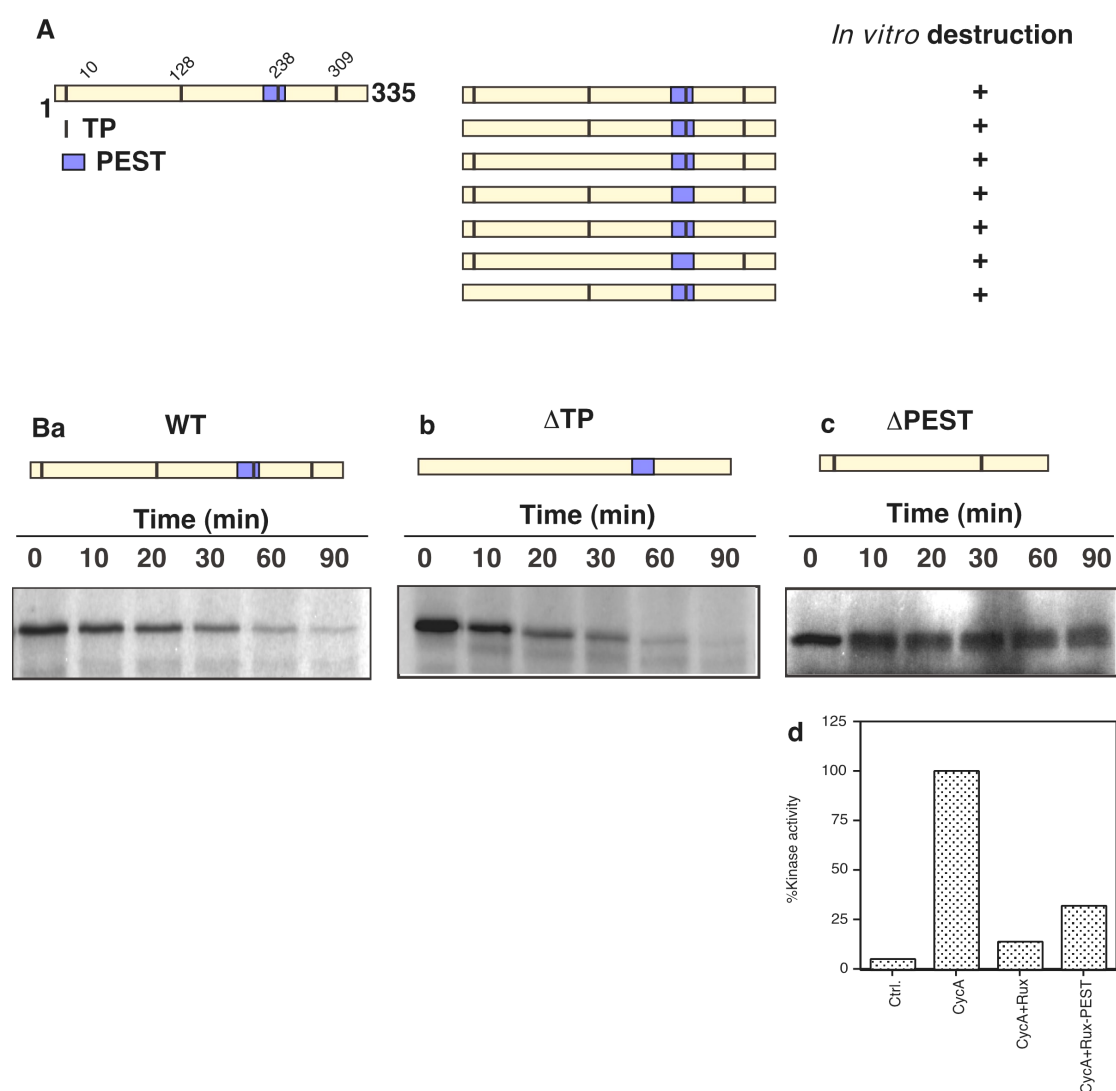


Fig. 2.49: Rux *in vitro* destruction is mediated by a C-terminal PEST sequence.

(A) A schematic representation of the WT Rux protein showing the relative positions of all potential CDK phosphorylation sites (TP) and the PEST motif (PEST). (B) A series of mutant constructs were made where different TPs had been replaced by APs. Protein destruction was monitored by incubating radiolabeled constructs in an extract, removing samples at specific times and assaying protein amounts as a function of time by SDS-PAGE and autoradiography. All constructs were destroyed with the same kinetics as WT Rux. A mutant construct where all four potential phosphorylation sites were removed (Bb, autoradiograph) was destroyed at the same rate as WT Rux (Ba, autoradiograph). A C-terminal deletion removing the PEST (Rux Δ PEST) sequence stabilizes the Rux protein (Bc). Rux Δ PEST inhibits Cdk1/CycA to the same extent as WT Rux. In a standard kinase assay, Cdk1/CycA was incubated with reticulocyte lysate (d, lane 2) WT Rux (d, lane 3) or Rux Δ PEST (d, lane 4). The kinase activity of Cdk1/CycA was set to 100%. Rux and Rux Δ PEST reduced kinase levels by almost 75%.

A commonly used signal for proteasome-mediated destruction is the PEST-motif, which is defined as a region of a protein with a high density of prolines, aspartates, serines and threonines (Rechsteiner and Rogers, 1996). A very strong PEST motif was found in the C-terminus of the Rux protein using the PESTfind algorithm (<http://emb1.bcc.univie.ac.at/embnet/tools/bio/PESTfind>). A C-terminal truncation protein where the candidate PEST sequence was completely removed (Rux Δ PEST)

was no longer degraded in the *in vitro* assay (Fig. 2.49Bc). This stability was not the result of a gross conformational rearrangement of the Rux protein, as Rux Δ PEST still inhibited Cdk1/CycA kinase activity as efficiently as WT Rux (Fig. 2.49Bd). HA-tagged Rux Δ PEST construct was also stable in late anaphase (Fig. 2.50a-c) and telophase (Fig. 2.50d-f) when injected into WT embryos. Thus, it does not appear that Rux destruction is mediated by CDK/cyclin dependent phosphorylation, rather it is mediated by PEST-dependent destruction. There is some degree of control to the temporal order of destruction, as Rux is stable in G1, G2 and until anaphase during mitosis.

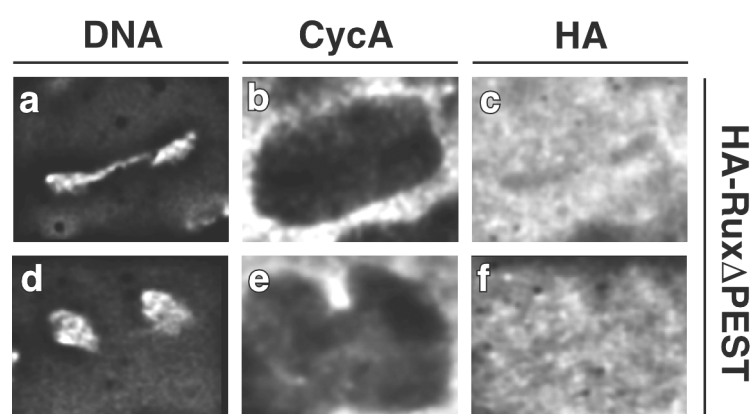


Fig. 2.50: Rux Δ PEST is stable in embryos.

mRNA encoding HA-Rux Δ PEST was injected into pre-blastoderm embryos. Rux Δ PEST was visualized by staining blastoderm embryos with anti-HA antibodies (c, f). DNA was visualized by staining with Hoechst (a, d) and CycA was visualized with anti-CycA antibodies (b, e). Two individual cells are shown in anaphase (a-c) and telophase/interphase. As opposed to WT Rux, Rux Δ PEST is present in telophase cells, indicating that it is not degraded in the same manner.

DISCUSSION.

Orderly progression through the cell cycle is a prerequisite for the correct development and survival of all metazoans. Numerous experimental manipulations have demonstrated that disorganized cell cycles are deleterious to organism patterning (Follette and O'Farrell, 1997). Furthermore, aberrant cell cycles are hallmarks of lethal conditions such as cancer (Sherr, 1996). Several mechanisms arose for regulating CDK activity at the correct cell cycle stage early in eukaryotic evolution (Morgan, 1995). These include reversible covalent modification of CDKs, proteolytic destruction of cyclins and the activity of CKIs. CKIs associate with CDKs, cyclins or both (Peter and Herskowitz, 1994). CKIs inhibit CDK activity and prevent CDK activation. This report presents evidence that the *Drosophila* gene product Rux is a novel CKI. *rux* mutants have rough eyes and null mutants are male sterile (Gonczy et al., 1994; Thomas et al., 1994). Both phenotypes result from disturbances in the WT cell cycle and both are suppressed by removing a copy of *cycA* or *cdc25^{stg}*, as Rux is required to inhibit CycA activity during eye development and spermatogenesis. Here it is shown that Rux interacts physically with CycA and that this interaction has several consequences for CycA activity, most importantly inhibition of Cdk1/CycA complexes. Interestingly, Rux is the first CKI to be characterized in a multicellular organism which is specific for mitotic cyclins. This report also presents evidence that, in addition to its established role as a regulator of the G1 to S transition, Rux contributes to regulating the metaphase to anaphase transition. This is the first time such a function has been ascribed to a metazoan CKI.

Rux is a novel *Drosophila* CKI.

CKIs are defined as proteins that interact with CDKs, cyclins or both, inhibit CDK activity and prevent CDK activation without covalently modifying either CDKs or cyclins. This report presents evidence that Rux is a *Drosophila* CKI specific for mitotic cyclins.

1. Rux physically associates with CycA and CycB. Rux is a nuclear protein from *Drosophila* and its overexpression forces a nuclear accumulation of CycA and a pre-mitotic cell cycle arrest. Rux specifically precipitated CycA and CycB from extracts prepared from embryos expressing high amounts of Rux (*hs-rux*). RXL motifs were initially identified in CKIs of the KIP/CIP family of inhibitors as essential for interaction with cyclin proteins. The interactions between Rux and CycA are most likely mediated by two RXL motifs in the Rux protein. Mutating either the N-terminal or central RXL in Rux diminishes the ability of Rux to trigger a nuclear accumulation of

CycA and abolishes the ability of Rux to inhibit Cdk1/CycA. These RXL mutant forms are also impaired in their ability to prevent cell cycle progression. Furthermore, a mutant Rux construct where the central RGL has been mutated to KGK does not precipitate CycA from blastoderm embryos, while WT Rux does. The crystal structure of a human p27/CycA/Cdk2 complex has been resolved recently (Russo et al., 1996). p27 inserts into the cyclin box of CycA via an N-terminal RXL. p27 then inserts into the active sites of CDK and excludes ATP, thereby inactivating CDK. It is not clear whether Rux interacts with Cdk1. A minor amount of Cdk1 does co-precipitate with Rux from hs-rux extracts (data not shown), although it cannot be excluded whether this Cdk1 is associated with CycA or Rux. Nonetheless, Rux does inhibit Cdk1 kinase activity. Presumably the association of Rux and CycA is such that a part of the Rux protein prevents Cdk1 access to substrate molecules.

The three dimensional structure of a p27/CycA/Cdk2 complex showed that the RXL motif of p27 inserted into the cyclin box of CycA. Multiple hydrophobic and van der Waals interactions are made between p27 and the conserved MRAIL motif in the cyclin box of human CycA. The MRAIL motif is also found in all known Rux interacting proteins in *Drosophila*; CycA, CycB and CycE. It is therefore likely that the RXL motifs in Rux inserts into the cyclin box of its interacting partners. Attempts were made to confirm this by making a Rux-resistant CycA with point mutations in the cyclin box. Conversion of a conserved tryptophan (W242) in human CycA to an alanine does not reduce the ability of CycA to activate CDK but this CycA mutant is impervious to inhibition by p27 (Schulman et al., 1998). A W242A mutant was made with *Drosophila* CycA. However, this mutant form does not activate *Drosophila* Cdk1 (data not shown), making it impossible to determine whether Rux inhibits Cdk1/CycA via interactions with the MRAIL motif in CycA. In summary, Rux specifically interacts with the *Drosophila* mitotic cyclins A and B and this interaction is mediated by the N-terminal and central RXL motifs in the Rux protein.

2. Rux inhibits Cdk1 activity. Rux inhibited the kinase activity of Cdk1 in several experimental setups. The kinase activity of Cdk1 precipitated from hs-rux embryonic extracts was considerably lower than the kinase activity of Cdk1 precipitated from WT extracts of the same stage. Consistent with an inhibition of Cdk1 activity overexpression of Rux inhibits mitosis in embryos and various imaginal discs. An *in vitro* assay was developed to monitor Rux-mediated inhibition of Cdk1. Rux also inhibited the *in vitro* kinase activity of Cdk1/CycA and Cdk1/CycB. These effects were specific for Cdk1, as Rux did not inhibit Cdk2/CycE. This is consistent with previous reports that Rux does not prevent ectopic S phases induced by overexpression of

CycE whereas Rux does inhibit ectopic S phases induced by overexpression of CycA (Sprenger et al., 1997).

The H1 kinase activity of Cdk1/CycB decreased progressively upon addition of larger amounts of Rux. Inhibition was not achieved by disrupting Cdk1/CycB complexes, as equal amounts of CycB coprecipitated with Cdk1 regardless of the amount of Rux added. Large amounts of Rux reduced the extent of T161 phosphorylation on Cdk1. In contrast, Rux was a bimodal regulator of Cdk1/CycA activity. Large amounts of Rux inhibited Cdk1/CycA to almost background levels. Small amounts of Rux enhanced the activity of Cdk1/CycA by a factor of three. Activation was not achieved by increasing the total amount of Cdk1/CycA complexes formed. Irrespective of the amounts of Rux added in the assay Cdk1 precipitated an approximately equal amount of CycA, demonstrating that Rux does not modulate Cdk1/CycA activity by affecting the extent of Cdk1-CycA association. Enhancement of Cdk1/CycA activity was also not the result of increasing the extent of T161 phosphorylation on Cdk1. Cdk1 was phosphorylated to an equal extent on T161 in the presence of small amounts of Rux or of control reticulocyte lysate.

The ability of CKIs to enhance CDK/cyclin *in vitro* kinase activity has been described previously (Correa-Bordes and Nurse, 1995; Zhang et al., 1994). *rum1* enhances the activity of *S. pombe cdc2* and active Cdk2/CycA complexes contain the CKI p21 under some circumstances. In the case of p21 it was proposed that the stoichiometry of the different subunits determine Cdk2 activity. In this model one p21 molecule serves as a scaffold to assemble active Cdk2/CycA complexes and two p21 molecules are required for inhibition. However, more recent studies have demonstrated that a single p21 molecule completely inhibits Cdk2/cycA activity (Hengst et al., 1998).

The two cyclin-interacting, RXL motifs in Rux involved in Rux-CycA interactions are essential for inhibition of Cdk1/CycA. Removing either RXL abolishes the ability of rux to inhibit Cdk1/CycA. Deletion of either RXL motif does not abrogate the ability of Rux to enhance Cdk1/CycA activity. Thus, it seems unlikely that Rux enhances the kinase activity of CycA via a single RXL motif. It is conceivable that an additional region on the Rux molecule determines a mild CycA interaction and in some manner brings CycA into a more active conformation. Alternatively, removing a single RXL may not completely eliminate Rux-CycA interactions. It is possible that transitory associations still occur via the second RXL which results in an increase in CycA activity. As the increase in activity is not associated with an increase in T161 phosphorylation or Cdk1/CycA complex formation it is difficult to provide a mechanistic explanation for the effect. Furthermore, it is not clear whether activation

has an *in vivo* relevance, or whether it is an *in vitro* artifact. It is conceivable that the activation observed may have a minor role during the G1 to S phase transition or during S phase. At this stage Rux levels decline due to destruction and CycA levels rise due to increased transcription and a decrease in the rate of CycA proteolysis. At this point the relatively low levels of Rux may enhance CycA activity, thereby accelerating the G1-S transition.

It was previously reported that a purified GST-Rux fusion product did not inhibit Cdk1/CycA (Thomas et al., 1997). However, the GST tag is almost as large as the Rux protein itself and was attached to the N-terminus, i.e. proximal to the essential N-terminal RXL motif. This experiment was repeated in the *in vitro* kinase assays described in this report using *in vitro* translated GST-Rux. This fusion protein also failed to inhibit Cdk1/CycA (data not shown), confirming that this was an inappropriate choice of tag. In the *in vitro* assays performed above a relatively large amount of Rux is necessary to strongly inhibit Cdk1 kinase activity. In most experiments inhibition to background levels was only seen after using approximately twice as much Rux as CycA. However it is not possible to interpret these ratios in terms of efficiently folded and translated protein. Furthermore, analysis of the *rux* mutant phenotypes indicate that Rux functions in cooperation with other cellular activities at times when cyclin levels are low. Thus, in a cellular context the extent of inhibition is sufficient to downregulate CycA activity and establish a G1 state.

In several experiments a reduction of T161 phosphorylation on Cdk1 was observed after incubation of large amounts of Rux with Cdk1. However, Rux does not rely solely on preventing T161 phosphorylation as a means of inhibiting Cdk1. Rux inhibited T161-phosphorylated Cdk1 in two separate experiments. Cdk1/CycA complexes were pre-activated with a purified source of CAK, incubated with Rux and directly assayed for H1 kinase activity. In this experiment Rux greatly reduced the kinase activity of Cdk1, although the extent of T161 phosphorylation did not diminish. Removal of Rux from the reaction restored kinase activity to Cdk1/CycA entirely, confirming that the inhibition was mediated by Rux. In a second experiment, *in vitro* translated Rux was added to an embryonic extract and H1 kinase activity directly measured. Kinase levels fell to 14% of control levels although Cdk1 remained phosphorylated on T161.

In summary, Rux specifically inhibits the kinase activity of Cdk1 associated with CycA or CycB. Inhibition of CycB occurs in a relatively predictable manner; greater amounts of Rux inhibit Cdk1/CycB to greater extents. In the case of CycA the regulation is more complex; small amounts of Rux enhance Cdk1/CycA activity and large amounts of Rux inhibit Cdk1/CycA. There is no apparent explanation for the

observed enhancement either mechanistically or in terms of a potential *in vivo* significance. The inhibition does not rely on accessory *Drosophila* factors and does not depend on disruption Cdk1/cyclin complexes. Although a reduction in T161 phosphorylation of Cdk1 often accompanies inhibition this is not the only means by which Rux inhibits Cdk1, as Rux also inhibits T161 phosphorylated Cdk1 in complex with CycA.

3. Rux prevents Cdk1 activation. Cdk1 is activated by phosphorylation on T161 by CAK. T161 phosphorylation of Cdk1 was greatly reduced in the presence of Rux in several different experiments. This was seen by Western blot analysis of embryos expressing high levels of rux (hs-rux) and also in the *in vitro* kinase assays when *Drosophila* extract was used as a source of CAK. There are three possible explanations for the diminished phosphorylation of Cdk1 in the presence of Rux. Rux may be an inhibitor of CAK activity, Rux may promote a dephosphorylation of Cdk1 or Rux might block access of CAK to the T loop, thereby preventing Cdk1 activation. Rux inhibited Cdk1 when activated by GST-Civ1p or a 0-1 hr embryonic extract. An extract prepared from *cdk7^{ts}* embryos raised at the restrictive temperature did not phosphorylate Cdk1 on T161 or Cdk2 on T163 (data not shown), suggesting that Cdk7/CycH is the *Drosophila* CAK. Civ1p is a monomeric CAK with no structural similarity to the heterotrimeric Cdk7/CycH/Mat1 CAK. In addition, Civ1p and Cdk7/CycH/Mat1 differ in their substrate specificity (Kaldis et al., 1998). Thus, as Rux inhibited Cdk1 activated by two entirely different sources of CAK, it is unlikely that Rux is a CAK inhibitor. As mentioned above, it was shown that Rux inhibited pre-activated Cdk1/CycA complexes without any observable decrease in T161 phosphorylation of Cdk1 in an *in vitro* experiment and a kinase assay with an embryonic extract, ruling out that Rux recruits a phosphatase to T161. This suggests that through its association with CycA, Rux diminishes T161 phosphorylation of Cdk1 by preventing CAK access to the T-loop of CycA associated Cdk1.

In conclusion, Rux fulfills all the criteria required to define it as a CKI; it physically associates with CycA and CycB, it inhibits Cdk1 activity and prevents Cdk1 activation without covalently modifying Cdk1. Thus, Rux is a CKI specific for mitotic cyclins. Interestingly, Rux is the first CKI which specifically inhibits mitotic cyclins to be described in a multicellular organism.

Rux does not target CycA for degradation.

It has been proposed that Rux functions by targeting CycA for destruction, thereby downregulating Cdk1/CycA activity (Thomas et al., 1997). However, several lines of evidence presented here and elsewhere demonstrate that this is not the case.

Expression of an indestructible CycA, CycA Δ 170 induces ectopic S phases in the embryo (Sprenger et al., 1997). Co-expression of Rux suppresses these S phases. Suppression is not accompanied by a decline in CycA Δ 170 levels, demonstrating that Rux does not solely rely on destruction as a mechanism of inhibiting CycA *in vivo*. Furthermore, in the *in vitro* kinase assays presented here Rux inhibits Cdk1 partnered to CycA Δ 170 or CycB Δ 46. These N-terminally truncated cyclin molecules are stable in embryonic extracts. Thus, Rux inhibits Cdk1 activity, irrespective of whether Cdk1 is partnered to a destructible or indestructible cyclin. Finally, expression of Rux at three different levels in the embryo did not accelerate CycA protein turnover *in vivo*. Low level expression of Rux early in embryogenesis by crossing UAS-rux males to mat-GAL4 females did not accelerate CycA turnover. The level of Rux expression slightly delayed cell cycle progression and a corresponding delay in CycA turnover was observed. CycA was destroyed at the metaphase to anaphase transition in dividing cells of matGAL4 X UAS-rux embryos, as is observed in WT cell cycles. Therefore, CycA was destroyed at the expected time upon low level overexpression of Rux. A higher expression of Rux was observed in prdGAL4 X UAS-rux embryos. This level was sufficient to arrest cells in G2 of mitosis 15. However, despite the fact that the cell cycle was disturbed in these embryos, CycA turnover was no different in prd-expressing stripes to interstripes. Finally, high level expression of Rux from a heat-inducible promoter during embryogenesis arrested cell cycle progression for up to three hours (data not shown). This arrest was accompanied by a persistence of both CycA and Rux. Thus, no case was observed where Rux accelerated CycA destruction *in vivo* and Rux inhibited an indestructible CycA both *in vitro* and *in vivo*.

Rux functions during mitosis

RT-PCR revealed that *rux* is transcribed in 2-4hr embryos; a developmental stage where no G1 occurs, raising the possibility that Rux has functions extraneous to G1 maintenance. 2-4hr embryos are in the 14th and 15th cycles where cell cycle length is controlled primarily at the level of the G2 to M phase transition. To determine whether Rux functions during this stage of development entry into, passage through and exit from mitosis was compared for WT and *rux* mutant embryos. This was monitored by following the relative rates of appearance and disappearance of the various mitotic domains for mitosis 14. Mitosis 14 is the first zygotically controlled division and its spatiotemporal nature has been well described (Foe, 1989). *rux* mutants enter mitosis 14 at the same stage as WT embryos suggesting that G2 of mitosis 14 is equally long in both embryos. However, individual mitotic domains persist longer in

mutant embryos than in WT embryos, indicating that mutants progress through mitosis at a slower rate. This effect is not peculiar to an individual *rux* allele, as similar defects were observed in *rux*², *rux*³ and *rux*⁸ mutant embryos.

Progression through mitosis was followed in live embryos to analyze the mutant phenotype more closely. Mitosis was followed in individual cells from *rux* mutants where DNA was labeled with a GFP-histone transgene. At high magnification the individual stages of mitosis could be reliably distinguished and their relative lengths determined. Mitosis was considerably longer in *rux* mutants than in WT embryos. In particular, metaphase was almost doubled in *rux* mutants. The other stages of mitosis were not considerably longer in mutant embryos, indicating that Rux functions during the metaphase to anaphase transition.

The metaphase to anaphase transition is a tightly regulated event. A prerequisite for progression through mitosis in all eukaryotes studies is the correct alignment of DNA on the metaphase plate. Incorrectly oriented spindles induces a metaphase arrest (Waters et al., 1999). DNA damage induces a metaphase arrest in *S. cerevisiae* and a G2 arrest in other organisms (Su et al., 2000). A prolonged G2, misaligned chromosomes, abnormal spindles or lagging chromosomes were not detected in *rux* mutants (data not shown), suggesting that the metaphase delay is not related to activation of a DNA or spindle damage checkpoint. An additional requirement for the metaphase to anaphase transition is inactivation of Cdk1/CycA. In *Drosophila*, CycA function is required for metaphase execution (Lehner and O'Farrell, 1989). Mitotic cyclin activity must be downregulated to allow exit from mitosis in all eukaryotes. Downregulation of CycA activity is necessary for the metaphase to anaphase transition in *Drosophila* (Sigrist et al., 1995). It has been demonstrated previously that Rux interacts genetically with CycA (Sprenger et al., 1997; Thomas et al., 1994; Thomas et al., 1997). Here it was also shown that Rux interacts physically with CycA, inhibits the *in vitro* kinase activity of Cdk1/CycA and inhibits Cdk1 activity when overexpressed in embryos (Su et al., 2000). Therefore, the most likely explanation of the mitotic phenotype described is that Rux contributes to the inactivation of CycA/Cdk1 during metaphase. In the absence of Rux, CycA is only downregulated by proteolytic destruction. Accordingly, CycA is down-regulated at a slower rate in *rux* mutants, leading to an extension of metaphase.

The heat shock response in *Drosophila* embryos affects mitosis.

To confirm that Rux can function during the metaphase to anaphase transition, cells were arrested in metaphase in stripes of the embryonic epidermis by crossing UAS-CycA Δ 170; hs-*rux* flies to prd-GAL4 flies. Rux expression was induced from a heat-

inducible promoter after cells had arrested in metaphase and progression through the cell cycle was then monitored as a function of time. Induction of *rux* expression during metaphase is not a trivial issue for two reasons. Firstly, the highly compact nature of DNA in metaphase is a large physical barrier for access of transcription factors to promoter regions. For this reason metaphase DNA is considered transcriptionally inert, although recent gene expression studies have demonstrated that approximately 300 genes are specifically transcribed during mitosis in *S. cerevisiae* (Krebs et al., 2000; Spellman et al., 1998). Secondly, nascent transcripts are aborted during mitosis (Shermoen and O'Farrell, 1991).

Nonetheless, it was shown here that a mild heat pulse is sufficient to induce *rux* expression in metaphase-arrested cells. *rux* mRNA was detected by *in situ* hybridization in metaphase arrested cells 10min after a 5min heat pulse. Rux protein was detected several minutes later, demonstrating that a mild heat pulse is sufficient to induce gene expression from mitotic cells and that the transcripts are stable enough to allow translation. This is possible because of several effects heat pulses have on mitotic cells. Analysis of live embryos showed that a heat pulse induces decondensation of metaphase DNA, allowing access of transcription factors to the correct promoters. Furthermore, tubulin staining and nuclear envelope structure reveal that all cells adopt an interphase or early prophase structure in which transcription and translation is possible. These effects do not completely disturb the cell cycle program of an organism and are transitory. PH3 staining persists throughout the recovery period of a heat pulse regime and the mitotic program is completely restored within 10min.

A heat pulse is not sufficient to abrogate a *CycA Δ 170*-mediated metaphase arrest in control *prdGAL4*; *UAS-CycA Δ 170* embryos. However, induction of Rux does overcome this arrest. The number of metaphase cells drops 5min after appearance of Rux protein and is greatly reduced 40min later. Rux induction forces completion of mitosis, as anaphase and telophase figures are distinguishable 20min after induction. Therefore expression of Rux is sufficient to induce a metaphase to anaphase transition in *CycA Δ 170* expressing cells.

The *prd-GAL4* driver line used in the experiment described above induces a sufficiently high expression of *CycA Δ 170* to induce a metaphase arrest during mitosis 15 in late stage 10 embryos. Examination of DNA morphology of expressing cells in stage 12 *prdGAL4* X *UAS-CycA Δ 170* embryos approximately two hours later revealed that most cells had exited metaphase and had decondensed interphase DNA. Therefore, other mechanisms of *CycA* downregulation exist, which are

independent of proteolysis. As Rux appears to have a role in the metaphase to anaphase transition it was reasoned that Rux may be one of the activities contributing to CycA inhibition in *prdGAL4; UAS-CycA Δ 170* embryos. Stage 12 *rux*³; *prdGAL4; UAS-CycA Δ 170* embryos were examined to address this issue. DNA morphology revealed that almost half of all CycA Δ 170 expressing cell were still in metaphase. Therefore, *rux*³ mutants were greatly impaired in their ability to overcome a metaphase arrest induced by CycA Δ 170, confirming that Rux contributes to down-regulating CycA during mitosis. These results are very similar to what has been described previously for the budding yeast. In *S. cerevisiae* the metaphase arrest induced by low level expression of a stable CLB in yeast is only transitory (Amon et al., 1994). Eventually, CDC28 is down-regulated by rising Sic1p activity.

Understanding of exit from mitosis in budding yeast has advanced rapidly in the last decade and a picture of multiple intrinsic cellular activities overseeing the process has emerged (Bachant and Elledge, 1999). APC/C mediated destruction of mitotic cyclins and Sic1p dependent inhibition of Cdc28p downregulate Cdc28p in mitosis. In contrast, the only function known to be conserved in multicellular organisms is APC/C dependent destruction of cyclins. It is likely that the more complex nature of metazoans necessitates an equal if not more rigorous regulation of exit from mitosis than in budding yeast. The data described above indicate that Rux performs functions very similar to SIC1 and that Rux cooperates with other mechanisms to trigger exit from mitosis. Removal of Rux function does not abrogate the ability of a cell to leave mitosis, however the process is delayed. This delay is specific to metaphase as Rux is a negative regulator of CycA and CycA must be downregulated to exit metaphase. It was demonstrated in this report that Rux interacts with CycB and that Rux inhibits the *in vitro* kinase activity of Cdk1/CycB. However, Rux does not appear to downregulate CycB during mitosis, as *rux* mutants progress through anaphase and telophase almost as quickly as WT embryos. It is possible that Rux function is only required during the metaphase to anaphase, transition as this is a key step in mitosis. Prolonged metaphases are potentially deleterious to a cell, as they increase the possibility of incorrect segregation of sister chromatids. In a cell where no spindle or DNA damage has occurred a prompt metaphase to anaphase transition is expedient, as it lowers the likelihood of an incorrect segregation.

Rux is downregulated prior to S phase.

Many CKIs are downregulated at distinct stages to permit cell cycle progression. Sic1p is destroyed at the G1/S transition and the mammalian CKI p27 is degraded prior to S phase (Montagnoli et al., 1999; Swanson et al., 2000; Vlach et al., 1997).

Down-regulation is often initiated by CDK dependent phosphorylation of the target CKIs. Phosphorylated CKIs are recognized by specific E3s such as the APC or SCF complexes, ubiquitinated and degraded by the proteasome. SIC1 was originally purified as a substrate of CDC28 (Mendenhall, 1993). Sic1p is phosphorylated by rising CLN levels in late G1 and targeted for destruction by the SCF^{Cdc4} complex (Feldman et al., 1997).

It has been demonstrated previously that Rux protein levels are also regulated at specific cell cycle stages (Thomas et al., 1997). Rux is stable in G1 cells and destroyed in S phase cells of the developing eye imaginal disc. In agreement with this result Rux was also shown here to be stable in G1 cells of cycle 17. In this report the course of Rux protein turnover was also monitored in embryonic cell cycles that lack a G1. Rux expression was induced from a UAS transgene early in embryogenesis with a maternal-GAL4 driver line and the Rux protein was followed in the 14th and 15th division cycles. Rux protein was stable in G2 cells and in early mitotic cells. The protein disappeared in telophase or early interphase. This pattern of Rux destruction matches the proposed cell cycle stages of Rux function. Rux is stable during metaphase, where it contributes to downregulation of Cdk1/CycA kinase activity. Rux is rapidly turned over prior to S phase, allowing CycA to contribute to S phase. Rux is stable during G1, thus allowing G1 maintenance in cooperation with cyclin destruction and inhibitory phosphorylation of Cdk1 (Sprenger et al., 1997).

It was proposed that Rux is targeted for destruction by Cdk2-dependent phosphorylation (Thomas et al., 1997). Rux is phosphorylated by Cdk2/CycE precipitated from embryos and overexpression of CycE in the eye imaginal disc accelerates the rate of Rux disappearance. However, several results presented here show that Rux destruction does not require CycE activity. Overexpressing CycE in segmental stripes does not accelerate the rate of Rux turnover in the embryo. Furthermore, a Rux mutant construct lacking all potential CDK phosphorylation sites is turned over in an *in vitro* degradation assay as rapidly as WT Rux. More importantly, Rux is rapidly degraded in *cycE* mutant embryos. It is unlikely that Rux is phosphorylated by Cdk1 in this experiment, as Cdk1 is efficiently inhibited by Rux in the embryo. Therefore, CycE activity is not essential for Rux destruction. It is more likely that the increased rate of Rux turnover in imaginal discs overexpressing CycE is a secondary cause of an increased rate of S phase entry caused by CycE overexpression.

An *in vitro* assay was established to monitor the turnover of radiolabeled Rux in a cell free system. Rux was rapidly turned over in this assay, and the protein was stabilized

by the addition of proteasome inhibitors. Therefore, it is likely that Rux is degraded in a proteasome dependent manner. Interestingly, no Rux-Ubiquitin conjugates were detected (data not shown) and ubiquitination inhibitors such as methylated-Ubiquitin or Ubiquitin-Aldehyde did not prevent destruction (data not shown). There are at least two other cases known where proteins are turned over by the proteasome in a ubiquitin-independent manner. One of these proteins is the mammalian CKI, p21 (Sheaff et al., 2000).

A sequence element known to target several proteins to the proteasome for destruction is the PEST motif (Rechsteiner and Rogers, 1996). PEST sequences are defined as hydrophilic stretches of amino acids greater than or equal to 12 residues in length. Such regions contain at least one proline, one aspartate or glutamate and one serine or threonine. They are flanked by lysine, arginine or histidine residues. Positively charged residues are disallowed within the PEST sequence. A potential PEST sequence of 21 amino acids was identified in Rux, starting at residue 222. An algorithm designed to predict secondary structure predicts that the potential PEST sequence forms a loop which is flanked N-terminally by an alpha helix and C-terminally by a β -pleated sheet (Rost and Sander, 1993). Rux Δ PEST also migrates as a protein of its predicted molecular weight under SDS-PAGE, whereas WT Rux displays decreased electrophoretic mobility (data not shown). Thus, removing the PEST from Rux removes a secondary structure which is not resolved under denaturing conditions. A C-terminal truncation removing the PEST motif confers stability on the protein *in vitro*. The C-terminally deleted protein still functions as a Cdk1/CycA inhibitor in *in vitro* kinase assays. Rux Δ PEST is also stable *in vivo*, as it is not degraded in telophase/interphase cells.

Similarities between Rux and other CKIs

The data presented above highlight similarities between Rux and other CKIs. The similarities between Rux and SIC1 are particularly strong. Both have roles in maintenance of G1 by inhibiting the kinase activity of mitotic CDK/cyclins. Both interact with target cyclins via RXL motifs. Neither gene product is essential, as they functionally overlap with other mechanisms, such as APC/C mediated proteolysis. Overexpression of either inhibits mitosis and induces endocycles. Both proteins are downregulated at the G1/S transition by the proteasome. This report also demonstrates that Rux functions in mitosis, as has been described for SIC1. Despite the numerous similarities there is no homology between both sequences. Thus, it is likely that both genes evolved separately, or diverged at an extremely rapid pace. In this case it appears there is an evolutionary advantage to having such a gene

function, raising the possibility that functional homologues may exist in other organisms. In support of this idea it has been demonstrated that SIC1 from *S. cerevisiae* and *rum1* from *S. pombe* can complement each other although the sequence homology between both proteins is extremely tenuous (Sanchez-Diaz et al., 1998). Thus, it appears that there are very few sequence constraints on CKIs with specificity for mitotic cyclins.

Despite the lack of a sequence homology between SIC1 and Rux it was demonstrated here that Sic1p has similar effects to Rux on the *Drosophila* cell cycle. Overexpressing either protein in embryos during the cellular blastoderm cell cycle induced a G2 cell cycle arrest. Sic1p also efficiently inhibited the *in vitro* kinase activity of *Drosophila* Cdk1/CycA and *Drosophila* Cdk1/CycB, whereas it did not inhibit Cdk2/CycE complexes. Thus, Sic1p recognized the same target proteins as Rux and Sic1p elicits the same cell cycle arrest as Rux.

There are several differences between the behavior of Sic1p and Rux under these experimental conditions. Whereas Rux is an exclusively nuclear protein Sic1p is present throughout the cell. Furthermore, nuclear Rux leads to a nuclear accumulation of CycA, whereas nuclear Sic1p does not. Sic1p does not have any obvious NLS. The nuclear fraction of Sic1p observed is likely the result of free diffusion of the protein through the cell as it has a relatively small molecular weight (40kDa). It is possible that *Drosophila* CycA is retained in the cytoplasm by an active cytoplasmic retention signal (CRS) and that the CRS is overcome by an NLS on CycA-interacting proteins, such as Rux. In this model, Sic1p is unable to direct a nuclear accumulation of CycA, as it lacks the sequence determinant necessary to overcome the CRS on CycA. Another difference between Rux and Sic1p is that Sic1p enhances the *in vitro* kinase activity of Cdk2/CycE, whereas Cdk2/CycE is refractory to Rux activity. However, it is noteworthy that low levels of Rux enhance Cdk1/CycA activity and that both CycE and CycA have S phase functions in *Drosophila*. Thus, in the *in vitro* kinase assays described here both Rux and Sic1p specifically enhance the activity of S phase cyclins, whereas Rux and Sic1p specifically inhibit the activity of M phase cyclins. Despite the minor differences between both proteins the data presented above further emphasize the functional similarity between both proteins. Identical to what has been described for Rux, Sic1p inhibits the kinase activity of *Drosophila* mitotic CDK/cyclin complexes and arrests cells in G2 of the cell cycle when overexpressed.

A model for Rux function

Based on the results described above and published elsewhere the following model of Rux function is presented (Fig. 3.1). Rux is a nuclear protein that interacts physically with the mitotic cyclins A and B via two cyclin-binding RXL motifs in the protein. Overexpression of Rux induces a nuclear import of the two mitotic cyclins in a manner that relies on two critical RXL motifs, indicating that the nuclear accumulation observed for CycA and CycB is a direct result of their interaction with Rux. Rux specifically inhibits the kinase activity of Cdk1/CycA and Cdk1/CycB complexes *in vitro* and overexpressing Rux prevents execution of mitosis in embryos and imaginal disc cells. Rux also prevents CAK dependent activation of Cdk1, demonstrating that Rux is a CKI specific for mitotic cyclins. This is the first such CKI to be described in a multicellular organism and Rux does not have any obvious homologues in the sequence databases. However, genes with similar activities have been described in budding and fission yeast and it was shown here that the budding yeast gene product, SIC1 mimics Rux in *Drosophila*. Thus, it is probable that the requirement for a CKI activity which specifically inhibits mitotic cyclins has been conserved during evolution.

Rux is an integral element of the *Drosophila* cell cycle which establishes and maintains a G1 by inhibiting the kinase activity of Cdk1/CycA complexes from metaphase until S phase. This is necessary for correct patterning of the developing eye epithelium and spermatogenesis. Cdk1/CycA activity is elevated in *rux* mutants resulting in precocious S phase in the morphogenetic furrow of the eye disc, as well as an extra meiotic division during spermatogenesis. As *rux* mutants display a reduced viability the protein must also function during other stages of development. Rux protein and mRNA levels are low at all stages of development. However, the expression levels are sufficient to make a significant contribution to cell cycle control as Rux cooperates with other CDK inhibiting activities such as cyclin proteolysis and inhibitory phosphorylation of Cdk1. *rux* transcript is not detected in 0-2hr old embryos which corresponds to the first 13 cell cycles. These cycles are extremely rapid in *Drosophila* embryos and occur in a common syncytium without any G1. Any aberrant mitoses at this stage are dealt with by internalizing resulting nuclei and subsequently destroying them. Therefore, Rux function is not required during these cycles, explaining the lack of a maternally provided transcript.

After completion of mitosis 13 cell cycle control shifts from maternally provided products to zygotically transcribed genes. Cycles 14 to 16 are much longer and occur in a cellular blastoderm. Incorrect cell cycles at this stage of development are

potentially deleterious to the entire organism. The embryo responds to this challenge by introducing numerous controls to cell cycle progression, such as inhibitory phosphorylation of Cdk1, responsiveness to checkpoints and Rux. The Cdc25^{Stg} phosphatase controls entry into mitosis by removing inhibitory phosphates from Cdk1. Cdk1 activity must be downregulated to allow a subsequent exit from mitosis. this is achieved mainly by APC/C mediated proteolysis of mitotic cyclins. In addition to irreversible destruction of mitotic cyclins, Rux also contributes to exit from mitosis in these cycles by inhibiting the kinase activity of Cdk1/CycA. This activity is not absolutely necessary for exit from mitosis, however in its absence metaphase is almost twice as long. The 14th, 15th and 16th cell cycles occur without any G1 and Rux is destroyed almost immediately after completion of mitosis, allowing CycA to contribute to S phase. Rux is stable during G1, which is introduced during later cell cycles. In G1 rux cooperates with other cellular activities such as APC/C dependent proteolysis of CycA and inhibitory phosphorylation of Cdk1 to maintain Cdk1/CycA activity in a low state. Prior to entry into S phase Rux is turned over in embryonic and imaginal disc cells. Rux destruction does not depend on Cdk2/CycE activity or on CDK mediated phosphorylation of Rux, rather it depends on a PEST motif towards the C-terminus of the protein. The decline in Rux protein levels, as well as a concomitant increase in CycA levels allows CycA to contribute to execution of, or passage through S phase.

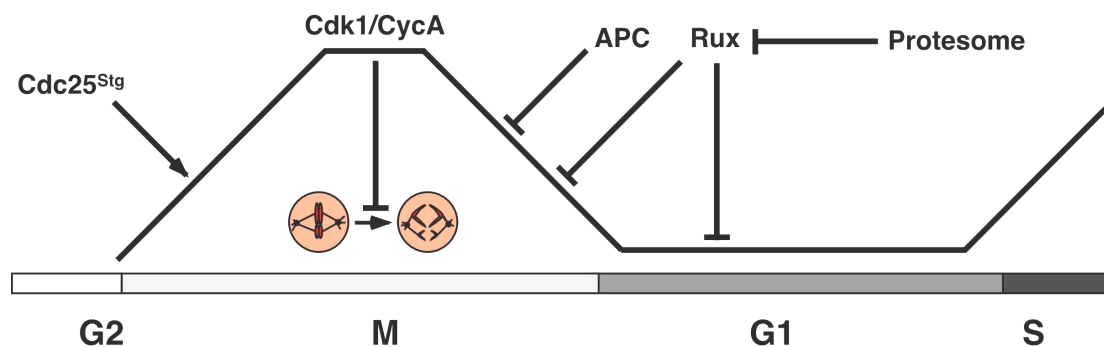


Fig. 3.1: A model of Rux function during the *Drosophila* cell cycle.

Cdk1/CycA is activated during G2 by the phosphatase Cdc25^{Stg}, which removes inhibitory phosphates from T14 and Y15 on cdk1. Rising levels of Cdk1 activity induce entry into mitosis. It is then necessary to downregulate Cdk1, as high levels of Cdk1 activity prevent transition through mitosis. CycA is destroyed by APC/C dependent proteolysis during metaphase and Cdk1/CycA is also inhibited by Rux. The resulting drop in Cdk1/CycA activity allows a transition from metaphase to anaphase. APC/C dependent proteolysis of the B-type cyclins completes mitosis. Cdk1/CycA activity is maintained in a low state through proteolysis and inhibition by Rux during G1. Rux is degraded by the proteasome before S phase in a manner that depends on a C-terminal PEST sequence in the Rux protein. The continuous black line represents Cdk1/CycA activity levels during the various cell cycle stages. Arrows indicate activation and bars indicate inhibition.

MATERIALS AND METHODS

MATERIALS

Computers and software

This thesis was prepared on an Apple Macintosh using Adobe PhotoShop (Adobe Systems), Canvas (Deneba Systems), IPLab Spectrum (Signal Analytics) Microsoft Word and Excel (Microsoft Corp.).

Drosophila melanogaster

Oregon R flies were used for the preparation of embryo extracts and as WT embryos for immunohistological staining. The *prd*-GAL4 flies have been described in (Leismann et al., 2000). *mat*-GAL4 flies were a gift of Maythrei Narashima. *hs-rux*, *hs-cycA*, *hs-Cdc2^{AF}* and *hs-stg* flies have been described in (Foley et al., 1999) respectively. The *rux⁸* and *rux³* strains have been described previously (Thomas et al., 1994; Thomas et al., 1997). *rux2* was a gift from the Bloomington stock collection. The GFP-His2AvD flies have been described in (Clarkson and Saint, 1999). UAS-*rux* flies were a gift of Dr. Barbara Thomas. *hs-rux* ; *cycE/CyO* were a gift of Nikita Yakubovitch. UAS-*CycE* flies were provided by Ruth Grosskortenhaus. UAS-*stg* flies were provided by Dr. Bruce Edgar.

Antibodies

The Rux antibody was made by immunizing rats with a purified GST-Rux gel slice (Eurogentec). Antibodies against *CycA*, *CycB* and *Cdk1* have been previously described (Knoblich and Lehner, 1993). The antibodies against β -tubulin, HA, PH3 and PSTAIR were obtained from Amersham, Boehringer Mannheim, Upstate Biotechnology and Sigma respectively. Secondary antibodies were purchased from Dianova.

Escherichia coli

Transformations were performed in *E. coli* strain DH10B (gift of Robert Wilson, genotype; F', *mcrAD*⁻ (*mrr hsdRMS*⁻*mcrBX*), *j80dlacZDM15*, *DlacX74*, *deoR*, *recA1*, *araD139*, *D(ara, leu)7694*, *galU*, *galK*, λ ⁻, *rspL*, *endA1*, *nupG*). GST fusion proteins were produced in *E. coli* strain C43 (Miroux and Walker 1996). GST-CIV was

produced using *E. coli* strain B834 (Genotype; F^- ompT hsdS_B (r_B⁻m_B⁻) gal dcm met (DE3)pLysS (cam^R). The *E. coli* strains ES1301 and JM109 were used for site directed mutagenesis.

DNA Molecular weight markers.

A 1kb molecular weight marker from GibcoBRL was used to mark molecular lengths of DNA fragments.

Oligonucleotides

The following oligonucleotides were used for making the various point mutations

CycA W242A	CACAATGCGCGCTCCATCGCTATTGATGCGCTGGTT
Rux T10A	CTCCAAAGGGGCCTCCTTATG
Rux T128A	ACGGGGCGGGGCGATCAGGGT
Rux T238A	TGTTGGCGGGGCTGAATCCTC
Rux T309A	TTTCCTCGGGGCACAGCTGCT
Rux R29KL31K	GCAGTCCTCCCCTTTGTCTTTGCGTATGGTCCCC
Rux R196KL198K	TTTGAGGCTTGTTTTACCTTTATCGTAGACAGC
Rux R248KL250K	CTCCTCTGTAAATTTAGTTTTACGCACGCAGCG

SIC1 DNA was amplified with the following two oligonucleotides

SIC1.1	ATATCCATGGCTCCTTCCACCCACCAA
SIC1.2	TATATCTAGAGCTCTTGATCCCTAGATT

The following oligonucleotides were used for the RT-PCR reactions

rp49.1	CGACCAGGTTACAAGAAC
rp49.2	CCGCCCAGCATAACAGGCC
rux.1	GAAACGCATCCGCCT
rux.2	AACGCATCCGCCTTGGTC

The rux promoter was amplified in the rux² mutant using the primers

rux2.1	GCTGCTGAATGCTGGAAA
rux2.2	GGAGATAAAAGTGATAA
rux2.3	CCACTTCTATGTTCTTC

The Rux Δ PEST construct was made with the following oligo

Rux Δ PEST	TATATCTAGATATTACATCGGGCGCTGGC
-------------------	-------------------------------

Restriction endonucleases.

Restriction enzymes and the corresponding reaction buffers from Boehringer Mannheim and New England Biolabs were used for DNA digestion.

DNA constructs

GST-Rux was produced by cloning the 1700bp fragment of an Nco I/Sac I digest of pSF821 (Frank Sprenger) into the 3000bp vector arising from digesting pSF470 with Nco I/Sac I (Frank Sprenger). HA-Rux (EF018) was produced by cloning the 1360bp fragment arising from a Bam HI/Sac I digest of pSF821 into the 3000bp vector arising from a Bam HI/Sac I digest pSF398 (gift of F. Sprenger). Other DNA constructs. e.g. pSF 191 (HA-Cdk1), pSF63 (Cdk1), pSF281 (CycA Δ 170), pSF421 (CycA) and pSF821 (Rux) were provided by F. Sprenger. SIC1 genomic DNA was a kind gift of Sue Jaspersen. SIC1 was amplified as a PCR fragment using the oligos SIC1.1 and SIC1.2 and cloned into EF018 as a Nco I/Xba I fragment to make SP6-SIC1 or into TS002 as a Nco I/Xba I to make HA-SIC1 under the control of an SP6 promoter.

Protein molecular weight markers.

Medium range molecular weight markers from Amersham and BioRad were used to determine apparent molecular weights after SDS-PAGE of proteins.

GST-fusion proteins

Proteins were produced as described in Methods section, except GST-CycB which was provided by F. Sprenger. Cells stably transformed with a GST-CIV expression vector were a gift of Carl Mann. All GST-fusion proteins were prepared by Hayati Özden.

Films

Amersham hyperfilm ECL films were used for Western blotting and Kodak Biomax MR films for autoradiography.

Media, solutions and buffers**Agarose gel loading buffer**

0.25% BPB

0.25% Xylene cyanol

30% Glycerol

Coomassie staining solution

0.25% Coomassie brilliant blue, R250

50% Methanol

10% Glacial acetic acid

Destaining solution

10% Glacial acetic acid

30% Ethanol

First strand buffer (FSB)

250mM Tris/Cl (pH 7.6)

300mM KCl

50mM MgCl₂

GST-wash buffer

100mM NaCl

10mM Tris pH 8

1mM EDTA

500µl 0.5M PMSF

2µg/ml Leupeptin

2µg/ml Pepstatin A

2µg/ml Chymostatin

2µg/ml Aprotinin

GST-Suspension buffer

500µl 0.5M PMSF

2µg/ml Leupeptin

2µg/ml Pepstatin A

2µg/ml Chymostatin

2µg/ml Aprotinin

1X PBS

GST-binding buffer

500µl of 50% Glutathione Sepharose 4B (Pharmacia) slurry per 25ml
15mM DTT
0.1% Tween-20

GST-elution buffer

50mM Tris pH 8.0
250mM KCl
2mM DTT

Homogenization buffer

10mM Tris pH 7.5
80mM K-β-Glycerophosphate pH 7.3
20mM EGTA
15mM MgCl₂
10% Glycerol

Shortly before use add:

1mM benzamidine
2mM Na₃VO₄
1mM DTT

Directly before use add

25µg/ml aprotinin
25µg/ml leupeptin
0.5mM PMSF

Immunoprecipitation buffer

10mM Tris pH 7.5
80mM K-β-Glycerophosphate pH 7.3
20mM EGTA pH 8.0
15mM MgCl₂
10% Glycerol
0.02% NP40

Before use add

0.5mM DTT

2mM Na₃VO₄

Pre-kinase wash buffer

25mM HEPES pH 7.4

10mM MgCl₂

1mM DTT

5μM ATP

Kinase assay buffer

25mM HEPES pH 7.4

10mM MgCl₂

1mM DTT

125μM ATP

250μg/ml Histone H1

0.3mCi/ml γ-ATP

Laemmli sample buffer (4X)

8% SDS

400mM DTT

240mM Tris pH 6.8

0.004% BPB

40% Glycerol

DNA Mini-prep buffers and solutions

Resuspension buffer P1

100μg RNase A

50mM Tris/HCl

10mM EDTA pH 8.0

Lysis buffer P2

200mM NaOH

1% SDS

Neutralization buffer P3

3.0M Kac pH 5.5

Na-acetate buffer

50mM Na-acetate pH5.1

10mM EDTA

2I 10XPBS

160g NaCl (1.37M)

4g KCl (26.8mM)

28.8g Na₂HPO₄ (80mM)4.8g KH₂PO₄ (17.6mM)

Adjust pH to 7.4 with HCl

2I 10XPBT

0.1% TWEEN 20 IN PBS

10XPonceau S

2g Ponceau S

30g Trichloroacetic acid

30g Sulfosalicylic acid

SDS-Polyacrylamide minigels

	8.5%	10%	12.5%	15%	17.5%
H ₂ O (ml)	3.5	3.1	2.5	1.8	1.2
30% Acrylamide (ml)	2.0	2.4	3.0	3.7	4.3
4X Resolving gel buffer (ml)	1.9	1.9	1.9	1.9	1.9
10% APS (μl)	112	112	112	112	112
TEMED (μl)	5	5	5	5	5

10I 10X running buffer for SDS-PAGE

300g Tris-base (0.25M)

1440g Glycine (1.9M)

1l 10% SDS

1l 4X Resolving gel buffer

181.7g Tris base (1.5M)

4ml 10% SDS

Adjust pH to 8.8 with HCl

500ml 4X Stacking gel buffer

30.3g Tris base (0.5M)

20ml 10% SDS

Adjust pH to 6.8 with HCl

Stripping buffer

100mM β -mercaptoethanol

2% SDS

62.5mM Tris pH6.7

Squashing buffer

10mM Tris/Cl pH8.2

1mM EDTA pH8.0

25mM NaCl

200 μ g/ml Proteinase K

1l Transfer buffer for western blots

5.82g Tris (48mM)

2.93g Glycine (39mM)

3.75ml 10% SDS

200ml Methanol

TE

10mM Tris/Cl pH 8.0

1mM EDTA pH 8.0

1l 50X TAE

242g Tris base (2M)

57.1ml glacial acetic acid

500mM EDTA pH 8.0

Terrific broth

A 12g Bactotrypton

24g Bacto-yeast-extract

4ml Glycerol

Adjust to 900ml with ddH₂O

B 2.31g KH₂PO₄

12.54g K₂HPO₄

Adjust to 90ml with ddH₂O

Mix A and B when less than 60°C

METHODS

DNA Methods

Restriction digests of DNA.

Restriction digests were performed in buffers and at temperatures recommended by enzyme manufacturers for a minimum of 1.5hrs and maximum of 16hrs.

Dephosphorylation of DNA ends.

Vectors to be dephosphorylated were brought to a total end volume of 50 μ l by the addition of H₂O, 5 μ l dephosphorylation buffer and 0.3 μ l CIP (Calf Intestinal Phosphatase, 56U/ μ l). This was then incubated at 37°C for 15 min. The reaction was stopped by incubating at 75°C for 10 min in 5mM EDTA.

Klenow fill in of DNA ends.

The substrate DNA was incubated with 40 μ M of each dNTP and 1U Klenow/ μ g DNA for 15 min at 25°C. Reaction was stopped by adding EDTA to 10mM and heating at 75°C for 10 min.

Eluting DNA.

DNA fragments to be isolated from agarose gels were first separated by electrophoresis. The required fragment was then visualized on a UV lamp and excised using a sterile scalpel. DNA was then purified from these fragments using the Qiaex II kit from Qiagen or the DNA Purification Kit from Biozym.

Agarose gel electrophoresis.

Agarose gel electrophoresis was performed as described (Sambrook et al., 1989). DNA fragments were separated on a 1 % agarose gel, with 10 μ l 10mg/ml EtBr in 100ml TAE buffer.

DNA ligation.

Ligation reactions were carried out with an approximate molar ratio of insert : vector of 3:1. Finally 0.5 μ l T4 DNA Ligase was added and the ligation reactions were either

incubated overnight at 16°C or for 3 hours at RT. DNA was then used to transform competent cells.

Preparation of electrocompetent cells.

The method used to prepare electrocompetent cells is based on the protocols from Dower et al. (Dower et al., 1992). DH10B cells were plated out from a DH10B glycerol stock onto LB plates and grown overnight at 37°C. A colony was picked from this plate and grown overnight in 50ml LB. The following day these cells were diluted 1 in 100 with TB and grown until the OD₆₀₀ was 0.5. The cells were cooled on ice for 30 min. and then centrifuged at 4000rpm in a Sorvall GS3 rotor for 10min at 4°C. The cells were resuspended on ice over about 30 min in 500ml filtered Millipore water and then spun at 8000rpm in a Sorvall GS3 rotor for 20 min at 4°C. Cell were resuspended in ice cold 10% (w/v) glycerol and spun out in a Heraeus bench top centrifuge at 4000rpm for 7min at 4°C. The cells were resuspended in 1ml ice cold 10% glycerol. They were then divided into 40µl aliquots, frozen in liquid nitrogen and stored at -70°C.

Transformation.

coli cells were transformed by electrotransformation. 0.5-1µl of the plasmid DNA to be transformed was mixed with a 40µl aliquot of electrocompetent cells. Immediately after transformation cells were resuspended in 1ml LB. 100µl were then plated on LB-Agar plates containing the appropriate antibiotic for selection. Plates were incubated overnight at 37°C and individual colonies were then picked.

Isolation of Plasmid DNA

The following protocol was used to isolate plasmid DNA for sequencing. 1.5ml of an overnight culture was centrifuged for 10min at 4000 rpm. The pellet was resuspended in TE with 100µg/ml RNase. 200µl lysis buffer was added to the resuspended bacteria, shaken and incubated for 5min at RT. Afterwards 150µl neutralization buffer was added, shaken and incubated for a further 5min at RT. The mix was spun for 30min at 14000rpm in a bench top centrifuge. 1ml of 100% ethanol was added to the supernatant and centrifuged for 20min at 14000rpm. 1ml of 70% ethanol was added to the pellet and centrifuged for 5min at 14000rpm. The pellet was dried and resuspended in 20µl TE.

The following protocol was used to isolate plasmid DNA for all other applications. 1.5ml of an overnight culture was centrifuged briefly at 14000rpm in a bench top

centrifuge. The pellet was resuspended in 100µl TE and mixed with 100µl lysis buffer. Lysis was stopped after 5min by addition of 100µl neutralization buffer and mixing. The mixture was centrifuged for 1min at 14000rpm. 250µl TE-saturated phenol was added to the supernatant, vortexed and centrifuged for 1min at full speed. The upper aqueous phase was removed, mixed with 500µl 100% ethanol and centrifuged for 5min at full speed. The pellet was washed with 100µl 80% ethanol and centrifuged for 1min at full speed. The pellet was dried and resuspended in 20µl TE with 25µg/ml RNase.

Precipitation of DNA.

1/10 Vol. NH₄Oac, 3 Vol. 96% Ethanol and 0.5µl glycogen were added To the DNA to be precipitated. This mixture was incubated at -70°C for 20 min and centrifuged at 14,000 rpm for 15 min in a bench top centrifuge at 4°C. The supernatant was removed and the pellet washed in 1 ml 80% ethanol. This was centrifuged for a further 15 min at 14,000 rpm an 4°C in a bench top centrifuge, the supernatant was removed and the pellet dried at 37°C for 10 min. Finally the DNA was resuspended in TE.

Site directed mutagenesis

Site directed mutagenesis was performed according to the Altered Sites II manual from Promega.

DNA sequencing

DNA sequencing was done using an ABI-Sequencer (Models 373 and 377) with the Dye-Terminator Kit (Perkin-Elmer).

Single fly PCR

One fly was placed in a 0.5ml tube and mashed for 10 seconds with a pipette tip containing 50µl squashing buffer. After mashing the remaining buffer was expelled. The mixture was incubated for 30min at 37°C and then 95°C for 2min. The preparation was stored at 4°C and typically 2.5µl used in a 25µl PCR reaction.

Isolation of mRNA from flies.

Total RNA was isolated from 100 adult flies or the equivalent number of embryos, larvae or pupae using phenol as a grinding material. Phenol was saturated with Na

acetate buffer, frozen in a mortar filled with liquid nitrogen and ground to a fine powder using a heavy pestle. The samples were then submerged in liquid nitrogen and ground with the phenol for 6min. The samples were thawed by addition of 1%SDS and heated to 60°C for 10min. Samples were then cooled on ice and centrifuged to separate the phases. The aqueous phase was removed, extracted once with phenol/chloroform/iso-amylalcohol (25:24:1) and once with chloroform/iso-amylalcohol (24:1). RNA was precipitated with 0.1vol 3M Na-acetate (pH 5.8) and 2.5vols ethanol, centrifuged at 12000Xg for 10min and washed with 70% ethanol. The pellet was resuspended in 20µl TE and stored at -70°C. Poly-adenylated mRNA was isolated with the QuickPrep micro mRNA Purification Kit (Pharmacia).

RT-PCR

The following reaction was incubated for 2hr at 42°C. for the synthesis of cDNA

H ₂ O	25µl
dNTPs (10mM)	2.5µl
5XFSB	10µl
DTT (100mM)	5µl
Primer (10pmol/µl)	0.5µl
RNasin (40U/µl)	1µl
SuperscriptII (200U/µl)	0.5µl
PolyA ⁺ -RNA (100µg/µl)	5µl

Database searches.

Homology searches were performed using the Basic Local Alignment Search Tool (BLAST); <http://www.ncbi.nlm.nih.gov/cgi-bin/BLAST/nph-blast> (Altschul et al., 1997). PEST motifs were identified using a PESTfind algorithm (Rechsteiner and Rogers, 1996).

BIOCHEMICAL METHODS

Production of GST fusion proteins.

GST-fusion proteins (GST-Rux and GST-CIV) were produced according to the following protocol. A 50ml overnight culture was prepared in LB/Amp (50µg/ml Amp). The following morning 10ml of the overnight culture was inoculated in 500ml

LB/Amp, grown at RT and induced with 0.1mM IPTG upon reaching an OD of 0.4 at 600nm. Culture was then allowed grow overnight. The following day the culture was centrifuged for 10min at 5,000 rpm and 4°C. The supernatant was decanted and the pellet resuspended in 25ml GST-wash buffer. Cells were centrifuged for 10min at 10,000 rpm and the supernatant removed. The pellet was suspended in 25ml ice-cold GST-suspension buffer.

Pellet was sonicated at a duty cycle of 40 and Output Control of 4 for 3 periods of 2min on ice. KCl (final conc. 250mM), DTT (final conc. 15mM) and Triton X-100 (final conc. 1%) were added to the pellet. This was then incubated under gentle shaking for 30min. at 4°C and centrifuged at 10,000 rpm for 10min. at 4°C. The supernatant was decanted into new containers. GST-binding buffer was added to the supernatant and incubated for 30min under gentle agitation at 4°C. Suspension was centrifuged at 2500 rpm and 4°C for 5min. The supernatant was decanted and the beads were washed 3 times in 25ml PBS and 15mM DTT. Finally, GST-fusion proteins were eluted by incubating the beads in GST-elution buffer three times at 4°C under gentle agitation followed by centrifugation for 2min at 2500 rpm and 4°C

Determining protein concentration

Protein concentration was determined using the Bio-Rad Protein Micro Assay Kit.

Gel electrophoresis of proteins.

Proteins were analyzed on a 0.75mm thick polyacrylamide gel using the SDS-discontinuous buffer system (Laemmli 1970). Analysis was done using a Mini Protean 2 System (Biolabs). Samples were suspended in loading buffer and heated for 5 min at 95°C before loading. Gels were run at a constant current that gave a starting voltage of approx. 100V. For large gels analyzing phosphoisoforms of Cdk1 the default voltage was set to 600V and the gel was run at 55mA and 4°C to prevent overheating. Kinase assay products were primarily run on large gels with a default voltage of 300V.

Coomassie blue staining.

Gels were incubate in approx. 5 vol. staining solution for 4hr to overnight at RT with shaking. They were then fixed in destaining solution and dried on Whatman 3MM paper.

Ponceau S staining.

Filter was incubated for 5-10 min in 1X Ponceau S with gentle agitation. It was then washed in several changes of deionized H₂O with agitation at RT, until individual protein bands became apparent.

Western blotting.

Gels to be analyzed by Western blotting were blotted onto Amersham Hybond Nitrocellulose filters for ECL analysis using a dry blotting system (Biorad). The current limit was set to 5.5mA/cm² for minigels and blotting was performed for 30 min. The filter was then blocked by washing it in 5% low fat milk in PBT with gentle agitation for 1hr at 4°C. The filter was washed 3 times in PBT and incubated with the corresponding primary antibody (preabsorbed for 1hr at 4°C in 5% low fat milk in PBT) and shaken overnight at 4°C. After washing 3 times in PBT the secondary antibody (also preabsorbed for 2hr in 5% low fat milk in PBT at 4°C) was added to the filter and this was shaken for 2 hr at RT. The filter was washed three times in PBT and proteins were visualized using the Amersham ECL protocol.

SP6 in vitro transcription.

The following reaction protocol is for the transcription of 2µl RNA

10X Transcription buffer (Boehringer)	2µl
10X NTPs (10X=5mM)	2µl
Template DNA (approx. 1µg/ml)	2µl
RNasin (40U/µl)	1µl
SP6 RNA Polymerase (Boehringer)	2µl
ddH ₂ O	11µl

Transcription was performed for 2hr at 40°C and RNA was stored at -70°C. Capped mRNA was produced using the MEGAscript transcription kit from Ambion.

Rabbit reticulocyte in vitro translation.

The following reaction protocol is for a translation volume of 50µl

Rabbit reticulocyte lysate	35µl
1mM Amino acids minus Met	1µl

³⁵ S-Met (11mCi/ml)	4μl
RNasin (40U/μl)	0.5μl
Template RNA(100-200μg/ml)	2μl
ddH ₂ O	7.5μl

The relative proportions of each of the individual components was maintained for every *in vitro* translation reaction. Reactions were performed for 1.5 hr at 30°C.

Kinase assays.

Aliquots of Cyclin A and Cdk1 were *in vitro* translated using the protocol outlined above. These aliquots were then mixed together with either a 0-1hr embryonic extract or an aliquot of GST-CIV with 10mM MgCl₂ and 2mM ATP. Mixtures were incubated for 30 min at 30°C to allow sufficient T161 phosphorylation of Cdk1. Fractions were immunoprecipitated through the addition of 1.5μl monoclonal mouse anti-HA antibody (1mg/ml, Boehringer clone 12CA5) and 10μl Protein G-agarose beads (Pharmacia). This was then gently shaken in 300μl immunoprecipitation buffer for 2hr at 4°C. Beads were pelleted by centrifuging for 2min at 2000rpm in a bench-top centrifuge at 4°C, washed twice in immunoprecipitation buffer and either directly analyzed on a polyacrylamide gel or processed further for a kinase assay. Immunoprecipitation fractions were washed a further two times in 300μl pre-kinase wash buffer. Beads were then pelleted by centrifuging at 4°C for 2min with 2000rpm in a bench-top centrifuge and the buffer was completely removed. Each fraction was completely resuspended in 15μl kinase buffer and incubated for 20min at 30°C. Reactions were stopped by the addition of 15μl sample loading buffer. For the analysis of kinase assay reaction products on small gels 7.5μl aliquots of each sample was loaded on a 5%-12% gel. For the analysis of reaction products on larger gels 15μl samples were loaded. Electrophoretic conditions were as described above. ³²P-H1 was visualized by autoradiography and phosphorimaging.

Phosphorimaging.

phosphorimaging was performed using a Fuji phosphorimager screen and phosphorimager. Large gels were exposed for 3hr and minigels were exposed for a maximum of 2hr. To determine the intensity of each signal an area corresponding to what could be clearly identified as the ³²P-H1 signal was marked and analyzed. An equal area was then marked in the lane in which the molecular weight markers ran,

and used to determine the background value. This value was subtracted from the ^{32}P -H1 signal to determine the actual level of H1 phosphorylation.

***DROSOPHILA* METHODS**

Maintenance of flies.

Flies were maintained under standard conditions (Ashburner, 1989, Wieschaus and Nüsslein Volhard, 1986) in large (4.5cm diameter, 9.5cm length) or small (2.1cm diameter, 6.3cm length) cylindrical plastic containers filled to one third food and plugged with a foam top. They were kept at 18°C. Food was prepared by boiling 240g Agar in 10l water for 2.5hr. 2.4kg corn flour, 430g yeast, 300g Soya flour, 2.4kg malt extract and 640g molasses in 15l water were added and this mixture was boiled for a further 2.5 hours. Once the mixture cooled to below 60°C 190ml Propionic Acid was added and the food was poured into the plastic containers.

Collecting embryos.

Embryos were collected under standard conditions (Ashburner, 1989, Wieschaus and Nüsslein Volhard, 1986), using laying cages. Apple juice agar plates were made by dissolving 90g Select Agar (GibcoBRL) in 3l water by bringing to the boil. Meanwhile 1l apple juice, 6g p-hydroxy-benzoic acid methyl ester (Nipagen, Sigma) and 100g sugar were heated until the nipagen was dissolved. The two solutions were mixed after cooling to below 60°C. The mixture was then poured onto 100mm diameter plates. Embryos were collected from apple-juice agar plates and snap frozen in liquid nitrogen (see Embryo Homogenization) for preparation of extracts. Embryos were fixed in formaldehyde/heptane, dehydrated in methanol and stored in methanol at -20°C for immunohistology.

Production of embryo extracts.

Wild type eggs were collected on apple juice agar plates, as described above. The eggs were gathered hourly and snap frozen immediately in liquid nitrogen. 0.75ml samples were homogenized on ice in 1ml homogenization buffer with six strokes a glass homogenizer. These samples were then centrifuged for 20min at 4°C and 14,000rpm in a bench-top centrifuge. The interphase was then removed, divided into 40µl aliquots, snap frozen immediately and stored at -70°C.

Precipitation of proteins from *Drosophila* embryos.

Embryos of the correct stage and genotype were collected from apple juice agar plates, snap frozen in liquid nitrogen and stored at -70°C . 0.75ml embryos were homogenized in 1ml homogenization buffer on ice with six strokes of a glass homogenizer. 10 μl Protein G beads and the correct amount of antibody were added to the extract. The extract was shaken overnight at 4°C . Beads were collected at the bottom of the tube by centrifuging for 2min at 2000rpm and 4°C in a bench top centrifuge. The supernatant was discarded and the beads washed three times in IP buffer. Precipitated proteins were either retained for a kinase assay or analyzed by SDS-PAGE and Western Blotting.

Fixation of embryos

Embryos were dechorionated in a 1:1 mixture of water and bleach for 2min on an apple juice agar plate. Embryos were poured through a sieve and washed with water. The embryos were then transferred to a 1.5ml sample tube containing 700 μl heptane and 700 μl 4% formaldehyde in PBS and shaken for 20min at 37°C . Afterwards the aqueous (lower) phase was removed and the embryos devitellinized by shaking vigorously for 30s after addition of 700 μl methanol. Embryos were washed three times with methanol and either stored at -20°C or rehydrated by washing five times in PBT.

In situ hybridization

mRNA was visualized in *Drosophila* embryos by *in situ* hybridization (Tautz and Pfeifle, 1989). mRNA probes were prepared using the DIG-DNA labeling kit (Boehringer Mannheim).

Immunohistology

Rehydrated embryos were blocked by rotating for 1hr at RT in blocking mix (1%NGS and 5%BSA in PBT). Embryos were incubated by rotation in the primary antibody in blocking mix overnight at 4°C . The primary antibody was removed and the embryos washed five times quickly in PBT. Embryos were then washed for 3 X 15min in 300mM NaCl in PBT and then washed five times quickly in PBT. The secondary antibody was incubated with the embryos in blocking mix for 2hr at RT. Secondary antibodies were coupled with a fluorescent dye (FITC, Texas Red, Alexa 488). Nuclear envelopes were visualized by incubating the embryos with Texas Red

labeled Wheat Germ Agglutinin for 2hr at RT. Embryos were washed five times quickly and 3 X 10min in PBT. Stained embryos were imbedded in Vectashield and stored at 4°C.

RNA injection into *Drosophila* embryos

RNA was injected into *Drosophila* embryos according to the technique in (Sprenger and Nüsslein Vollhard, 1992). 0-1hr embryos were dechorionated on apple juice agar plates, collected in a sieve and washed in water. Approx. 300 embryos were lined up on a cold slice of apple juice agar and stuck to a coverslip with heptane. The embryos were dried for 9-12 minutes in a dessicator and covered with 10S Voltalef oil. RNA was injected into one pole of the embryos prior to cellularization and embryos were aged for a further 2hr to allow translation of the injected mRNA.

Microscopy

Immunofluorescent pictures were taken using a Leica Confocal microscope and a Zeiss Axiovert 10. For high magnification pictures, z-stacks were obtained using a piezoelectric mover and deconvolved using the AutoDeBlur program (Autoquant). For time-lapse video microscopy, images were taken every 20 sec on the Zeiss Axiovert 10 microscope using a Quantix CCD-camera (Photometrics).

- Adams, P. D., Sellers, W. R., Sharma, S. K., Wu, A. D., Nalin, C. M., and Kaelin, W. G., Jr. (1996). Identification of a cyclin-cdk2 recognition motif present in substrates and p21-like cyclin-dependent kinase inhibitors. *Mol Cell Biol* **16**, 6623-33.
- Altschul, S. F., Madden, T. L., Schaffer, A. A., Zhang, J., Zhang, Z., Miller, W., and Lipman, D. J. (1997). Gapped BLAST and PSI-BLAST: a new generation of protein database search programs. *Nucleic Acids Res* **25**, 3389-402.
- Amon, A., Irniger, S., and Nasmyth, K. (1994). Closing the cell cycle circle in yeast: G2 cyclin proteolysis initiated at mitosis persists until the activation of G1 cyclins in the next cycle. *Cell* **77**, 1037-50.
- Ashburner, M. (1989). *Drosophila - A laboratory handbook*. Cold Spring Harbor Laboratory Press.
- Bai, C., Sen, P., Hofmann, K., Ma, L., Goebel, M., Harper, J. W., and Elledge, S. J. (1996). SKP1 connects cell cycle regulators to the ubiquitin proteolysis machinery through a novel motif, the F-box. *Cell* **86**, 263-74.
- Chang, F., and Herskowitz, I. (1990). Identification of a gene necessary for cell cycle arrest by a negative growth factor of yeast: FAR1 is an inhibitor of a G1 cyclin, CLN2. *Cell* **63**, 999-1011.
- Chen, J., Saha, P., Kornbluth, S., Dynlacht, B. D., and Dutta, A. (1996). Cyclin-binding motifs are essential for the function of p21CIP1. *Mol Cell Biol* **16**, 4673-82.
- Cheng, M., Olivier, P., Diehl, J. A., Fero, M., Roussel, M. F., Roberts, J. M., and Sherr, C. J. (1999). The p21(Cip1) and p27(Kip1) CDK 'inhibitors' are essential activators of cyclin D-dependent kinases in murine fibroblasts. *Embo J* **18**, 1571-83.
- Ciosk, R., Zachariae, W., Michaelis, C., Shevchenko, A., Mann, M., and Nasmyth, K. (1998). An ESP1/PDS1 complex regulates loss of sister chromatid cohesion at the metaphase to anaphase transition in yeast. *Cell* **93**, 1067-76.
- Clarkson, M., and Saint, R. (1999). A His2AvDGFP fusion gene complements a lethal His2AvD mutant allele and provides an in vivo marker for Drosophila chromosome behavior. *DNA Cell Biol* **18**, 457-62.
- Cohen-Fix, O., Peters, J. M., Kirschner, M. W., and Koshland, D. (1996). Anaphase initiation in *Saccharomyces cerevisiae* is controlled by the APC-dependent degradation of the anaphase inhibitor Pds1p. *Genes Dev* **10**, 3081-93.
- Correa-Bordes, J., and Nurse, P. (1995). p25rum1 orders S phase and mitosis by acting as an inhibitor of the p34cdc2 mitotic kinase. *Cell* **83**, 1001-9.
- D'Andrea, R. J., Stratmann, R., Lehner, C. F., John, U. P., and Saint, R. (1993). The three rows gene of *Drosophila melanogaster* encodes a novel protein that is required for chromosome disjunction during mitosis. *Mol Biol Cell* **4**, 1161-74.
- Datar, S. A., Jacobs, H. W., de La Cruz, A. F., Lehner, C. F., and Edgar, B. A. (2000). The *Drosophila* Cyclin D-Cdk4 complex promotes cellular growth. *Embo J* **19**, 4543-4554.
- Dawson, I. A., Roth, S., Akam, M., and Artavanis-Tsakonas, S. (1993). Mutations of the fizzy locus cause metaphase arrest in *Drosophila melanogaster* embryos. *Development* **117**, 359-76.
- Dawson, I. A., Roth, S., and Artavanis-Tsakonas, S. (1995). The *Drosophila* cell cycle gene fizzy is required for normal degradation of cyclins A and B during mitosis and has homology to the CDC20 gene of *Saccharomyces cerevisiae*. *J Cell Biol* **129**, 725-37.
- de Nooij, J. C., Letendre, M. A., and Hariharan, I. K. (1996). A cyclin-dependent kinase inhibitor, Dacapo, is necessary for timely exit from the cell cycle during *Drosophila* embryogenesis. *Cell* **87**, 1237-47.
- Devault, A., Martinez, A. M., Fesquet, D., Labbe, J. C., Morin, N., Tassan, J. P., Nigg, E. A., Cavadore, J. C., and Doree, M. (1995). MAT1 ('menage a trois') a new RING finger protein subunit stabilizing cyclin H-cdk7 complexes in starfish and *Xenopus* CAK. *Embo J* **14**, 5027-36.

- Dingwall, C., and Laskey, R. A. (1991). Nuclear targeting sequences--a consensus? *Trends Biochem Sci* *16*, 478-81.
- Dirick, L., Bohm, T., and Nasmyth, K. (1995). Roles and regulation of Cln-Cdc28 kinases at the start of the cell cycle of *Saccharomyces cerevisiae*. *Embo J* *14*, 4803-13.
- Donovan, J. D., Toyn, J. H., Johnson, A. L., and Johnston, L. H. (1994). P40SDB25, a putative CDK inhibitor, has a role in the M/G1 transition in *Saccharomyces cerevisiae*. *Genes Dev* *8*, 1640-53.
- Dower, W.J., Chassy, B.M., Trevors, J.T. and Blaschek, H.P. (1992). Protocols for the Transformation of Bacteria by Electroporation. In *Guide to Electroporation and Electrofusion*, Edited by Chang, Chassy, Saunders and Sowers. Academic Press Inc., 485-499
- Dyson, N. (1998). The regulation of E2F by pRB-family proteins. *Genes Dev* *12*, 2245-62.
- Edgar, B. A., and Lehner, C. F. (1996). Developmental control of cell cycle regulators: a fly's perspective. *Science* *274*, 1646-52.
- Edgar, B. A., and O'Farrell, P. H. (1989). Genetic control of cell division patterns in the *Drosophila* embryo. *Cell* *57*, 177-87.
- Edgar, B. A., and O'Farrell, P. H. (1990). The three postblastoderm cell cycles of *Drosophila* embryogenesis are regulated in G2 by string. *Cell* *62*, 469-80.
- Edgar, B. A., Sprenger, F., Duronio, R. J., Leopold, P., and O'Farrell, P. H. (1994). Distinct molecular mechanisms regulate cell cycle timing at successive stages of *Drosophila* embryogenesis. *Genes Dev* *8*, 440-52.
- Fang, G., Yu, H., and Kirschner, M. W. (1998). Direct binding of CDC20 protein family members activates the anaphase-promoting complex in mitosis and G1. *Mol Cell* *2*, 163-71.
- Fantl, V., Stamp, G., Andrews, A., Rosewell, I., and Dickson, C. (1995). Mice lacking cyclin D1 are small and show defects in eye and mammary gland development. *Genes Dev* *9*, 2364-72.
- Feldman, R. M., Correll, C. C., Kaplan, K. B., and Deshaies, R. J. (1997). A complex of Cdc4p, Skp1p, and Cdc53p/cullin catalyzes ubiquitination of the phosphorylated CDK inhibitor Sic1p. *Cell* *91*, 221-30.
- Fisher, R. P. (1997). CDKs and cyclins in transition(s). *Curr Opin Genet Dev* *7*, 32-8.
- Fisher, R. P., and Morgan, D. O. (1994). A novel cyclin associates with MO15/CDK7 to form the CDK-activating kinase. *Cell* *78*, 713-24.
- Foe, V. E. (1989). Mitotic domains reveal early commitment of cells in *Drosophila* embryos. *Development* *107*, 1-22.
- Foley, E., O'Farrell, P. H., and Sprenger, F. (1999). Rux is a cyclin-dependent kinase inhibitor (CKI) specific for mitotic cyclin-Cdk complexes. *Curr Biol* *9*, 1392-402.
- Glotzer, M., Murray, A. W., and Kirschner, M. W. (1991). Cyclin is degraded by the ubiquitin pathway. *Nature* *349*, 132-8.
- Gonczy, P., Thomas, B. J., and DiNardo, S. (1994). roughex is a dose-dependent regulator of the second meiotic division during *Drosophila* spermatogenesis. *Cell* *77*, 1015-25.
- Guacci, V., Koshland, D., and Strunnikov, A. (1997). A direct link between sister chromatid cohesion and chromosome condensation revealed through the analysis of MCD1 in *S. cerevisiae* [see comments]. *Cell* *91*, 47-57.
- Guan, K. L., Jenkins, C. W., Li, Y., Nichols, M. A., Wu, X., O'Keefe, C. L., Matera, A. G., and Xiong, Y. (1994). Growth suppression by p18, a p16INK4/MTS1- and p14INK4B/MTS2-related CDK6 inhibitor, correlates with wild-type pRb function. *Genes Dev* *8*, 2939-52.

- Hochstrasser, M. (1996). Ubiquitin-dependent protein degradation. *Annu Rev Genet* 30, 405-39.
- Hunt, T., Luca, F. C., and Ruderman, J. V. (1992). The requirements for protein synthesis and degradation, and the control of destruction of cyclins A and B in the meiotic and mitotic cell cycles of the clam embryo. *J Cell Biol* 116, 707-24.
- Jacobs, H. W., Knoblich, J. A., and Lehner, C. F. (1998). Drosophila Cyclin B3 is required for female fertility and is dispensable for mitosis like Cyclin B. *Genes Dev* 12, 3741-51.
- Jaspersen, S. L., Charles, J. F., Tinker-Kulberg, R. L., and Morgan, D. O. (1998). A late mitotic regulatory network controlling cyclin destruction in *Saccharomyces cerevisiae*. *Mol Biol Cell* 9, 2803-17.
- Kaldis, P., Russo, A. A., Chou, H. S., Pavletich, N. P., and Solomon, M. J. (1998). Human and Yeast Cdk-activating Kinases (CAKs) Display Distinct Substrate Specificities. *Mol Biol Cell* 9, 2545-60.
- Kaldis, P., Sutton, A., and Solomon, M. J. (1996). The Cdk-activating kinase (CAK) from budding yeast. *Cell* 86, 553-64.
- Kato, J., Matsushime, H., Hiebert, S. W., Ewen, M. E., and Sherr, C. J. (1993). Direct binding of cyclin D to the retinoblastoma gene product (pRb) and pRb phosphorylation by the cyclin D-dependent kinase CDK4. *Genes Dev* 7, 331-42.
- Knoblich, J. A., Sauer, K., Jones, L., Richardson, H., Saint, R., and Lehner, C. F. (1994). Cyclin E controls S phase progression and its down-regulation during *Drosophila* embryogenesis is required for the arrest of cell proliferation. *Cell* 77, 107-20.
- Koegl, M., Hoppe, T., Schlenker, S., Ulrich, H. D., Mayer, T. U., and Jentsch, S. (1999). A novel ubiquitination factor, E4, is involved in multiubiquitin chain assembly. *Cell* 96, 635-44.
- Koepp, D. M., Harper, J. W., and Elledge, S. J. (1999). How the cyclin became a cyclin: regulated proteolysis in the cell cycle. *Cell* 97, 431-4.
- Kramer, E. R., Gieffers, C., Holz, G., Hengstschlager, M., and Peters, J. M. (1998). Activation of the human anaphase-promoting complex by proteins of the CDC20/Fizzy family. *Curr Biol* 8, 1207-10.
- Krebs, J. E., Fry, C. J., Samuels, M. L., and Peterson, C. L. (2000). Global role for chromatin remodeling enzymes in mitotic gene expression. *Cell* 102, 587-98.
- Knoblich, J.A., and Lehner, C.F. (1993). Synergistic action of *Drosophila* cyclins A and B during the G2-M transition. *Embo J* 12, 65-74.
- Laemmli, U.K. (1970). Cleavage of structural proteins during the assembly of the head of bacteriophage T4. *Nature* 227, 680-5.
- Lane, M. E., Sauer, K., Wallace, K., Jan, Y. N., Lehner, C. F., and Vaessin, H. (1996). Dacapo, a cyclin-dependent kinase inhibitor, stops cell proliferation during *Drosophila* development. *Cell* 87, 1225-35.
- Larochelle, S., Pandur, J., Fisher, R. P., Salz, H. K., and Suter, B. (1998). Cdk7 is essential for mitosis and for in vivo Cdk-activating kinase activity. *Genes Dev* 12, 370-81.
- Lehner, C. F., and O'Farrell, P. H. (1989). Expression and function of *Drosophila* cyclin A during embryonic cell cycle progression. *Cell* 56, 957-68.
- Leismann, O., Herzig, A., Heidmann, S., and Lehner, C. F. (2000). Degradation of *Drosophila* PIM regulates sister chromatid separation during mitosis. *Genes Dev* 14, 2192-205.
- Losada, A., Hirano, M., and Hirano, T. (1998). Identification of *Xenopus* SMC protein complexes required for sister chromatid cohesion. *Genes Dev* 12, 1986-97.
- Matsushime, H., Quelle, D. E., Shurtleff, S. A., Shibuya, M., Sherr, C. J., and Kato, J. Y. (1994). D-type cyclin-dependent kinase activity in mammalian cells. *Mol Cell Biol* 14, 2066-76.

- Mendenhall, M. D. (1993). An inhibitor of p34CDC28 protein kinase activity from *Saccharomyces cerevisiae*. *Science* 259, 216-9.
- Meyer, C. A., Jacobs, H. W., Datar, S. A., Du, W., Edgar, B. A., and Lehner, C. F. (2000). *Drosophila* cdk4 is required for normal growth and is dispensable for cell cycle progression. *Embo J* 19, 4533-42.
- Michaelis, C., Ciosk, R., and Nasmyth, K. (1997). Cohesins: chromosomal proteins that prevent premature separation of sister chromatids. *Cell* 91, 35-45.
- Moll, T., Tebb, G., Surana, U., Robitsch, H., and Nasmyth, K. (1991). The role of phosphorylation and the CDC28 protein kinase in cell cycle- regulated nuclear import of the *S. cerevisiae* transcription factor SWI5. *Cell* 66, 743-58.
- Morgan, D. O. (1995). Principles of CDK regulation. *Nature* 374, 131-4.
- Nasmyth, K., Peters, J. M., and Uhlmann, F. (2000). Splitting the chromosome: cutting the ties that bind sister chromatids. *Science* 288, 1379-85.
- Nishizawa, M., Kawasumi, M., Fujino, M., and Toh-e, A. (1998). Phosphorylation of sic1, a cyclin-dependent kinase (Cdk) inhibitor, by Cdk including Pho85 kinase is required for its prompt degradation. *Mol Biol Cell* 9, 2393-405.
- Nurse, P. (1990). Universal control mechanism regulating onset of M-phase. *nature* 344, 503-8.
- Pagano, M., Pepperkok, R., Verde, F., Ansorge, W., and Draetta, G. (1992). Cyclin A is required at two points in the human cell cycle. *Embo J* 11, 961-71.
- Peter, M., Gartner, A., Horecka, J., Ammerer, G., and Herskowitz, I. (1993). FAR1 links the signal transduction pathway to the cell cycle machinery in yeast. *Cell* 73, 747-60.
- Peter, M., and Herskowitz, I. (1994). Joining the complex: cyclin-dependent kinase inhibitory proteins and the cell cycle. *Cell* 79, 181-4.
- Ready, D. F., Hanson, T. E., and Benzer, S. (1976). Development of the *Drosophila* retina, a neurocrystalline lattice. *Dev Biol* 53, 217-40.
- Rechsteiner, M., and Rogers, S. W. (1996). PEST sequences and regulation by proteolysis. *Trends Biochem Sci* 21, 267-71.
- Richardson, H. E., Wittenberg, C., Cross, F., and Reed, S. I. (1989). An essential G1 function for cyclin-like proteins in yeast. *Cell* 59, 1127-33.
- Roy, R., Adamczewski, J. P., Seroz, T., Vermeulen, W., Tassan, J. P., Schaeffer, L., Nigg, E. A., Hoeijmakers, J. H., and Egly, J. M. (1994). The MO15 cell cycle kinase is associated with the TFIIH transcription- DNA repair factor. *Cell* 79, 1093-101.
- Russell, P., and Nurse, P. (1986). cdc25+ functions as an inducer in the mitotic control of fission yeast. *Cell* 45, 145-53.
- Russo, A. A., Jeffrey, P. D., Patten, A. K., Massague, J., and Pavletich, N. P. (1996). Crystal structure of the p27Kip1 cyclin-dependent-kinase inhibitor bound to the cyclin A-Cdk2 complex. *Nature* 382, 325-31.
- Sambrook, J., Fritsch, E.F., and Maniatis, T. (1989). *Molecular cloning: a laboratory manual*. Cold Spring Harbor Laboratory Press.
- Schulman, B. A., Lindstrom, D. L., and Harlow, E. (1998). Substrate recruitment to cyclin-dependent kinase 2 by a multipurpose docking site on cyclin A. *Proc Natl Acad Sci U S A* 95, 10453-8.
- Schwab, M., Lutum, A. S., and Seufert, W. (1997). Yeast Hct1 is a regulator of Clb2 cyclin proteolysis. *Cell* 90, 683-93.

- Schwob, E., Bohm, T., Mendenhall, M. D., and Nasmyth, K. (1994). The B-type cyclin kinase inhibitor p40SIC1 controls the G1 to S transition in *S. cerevisiae*. *Cell* **79**, 233-44.
- Serizawa, H., Makela, T. P., Conaway, J. W., Conaway, R. C., Weinberg, R. A., and Young, R. A. (1995). Association of Cdk-activating kinase subunits with transcription factor TFIIH. *Nature* **374**, 280-2.
- Serrano, M., Hannon, G. J., and Beach, D. (1993). A new regulatory motif in cell-cycle control causing specific inhibition of cyclin D/CDK4 [see comments]. *Nature* **366**, 704-7.
- Sherr, C. J., and Roberts, J. M. (1999). CDK inhibitors: positive and negative regulators of G1-phase progression. *Genes Dev* **13**, 1501-12.
- Sherr, C. J., and Roberts, J. M. (1995). Inhibitors of mammalian G1 cyclin-dependent kinases. *Genes Dev* **9**, 1149-63.
- Shou, W., Seol, J. H., Shevchenko, A., Baskerville, C., Moazed, D., Chen, Z. W., Jang, J., Charbonneau, H., and Deshaies, R. J. (1999). Exit from mitosis is triggered by Tem1-dependent release of the protein phosphatase Cdc14 from nucleolar RENT complex. *Cell* **97**, 233-44.
- Sigrist, S., Jacobs, H., Stratmann, R., and Lehner, C. F. (1995). Exit from mitosis is regulated by *Drosophila* fizzy and the sequential destruction of cyclins A, B and B3. *Embo J* **14**, 4827-38.
- Sigrist, S. J., and Lehner, C. F. (1997). *Drosophila* fizzy-related down-regulates mitotic cyclins and is required for cell proliferation arrest and entry into endocycles. *Cell* **90**, 671-81.
- Skowyra, D., Craig, K. L., Tyers, M., Elledge, S. J., and Harper, J. W. (1997). F-box proteins are receptors that recruit phosphorylated substrates to the SCF ubiquitin-ligase complex. *Cell* **91**, 209-19.
- Skowyra, D., Koepf, D. M., Kamura, T., Conrad, M. N., Conaway, R. C., Conaway, J. W., Elledge, S. J., and Harper, J. W. (1999). Reconstitution of G1 cyclin ubiquitination with complexes containing SCFGrr1 and Rbx1 [see comments]. *Science* **284**, 662-5.
- Solomon, M. J., Lee, T., and Kirschner, M. W. (1992). Role of phosphorylation in p34cdc2 activation: identification of an activating kinase. *Mol Biol Cell* **3**, 13-27.
- Spellman, P. T., Sherlock, G., Zhang, M. Q., Iyer, V. R., Anders, K., Eisen, M. B., Brown, P. O., Botstein, D., and Futcher, B. (1998). Comprehensive identification of cell cycle-regulated genes of the yeast *Saccharomyces cerevisiae* by microarray hybridization. *Mol Biol Cell* **9**, 3273-97.
- Sprenger, F., Yakubovich, N., and O'Farrell, P. H. (1997). S-phase function of *Drosophila* cyclin A and its downregulation in G1 phase. *Curr Biol* **7**, 488-99.
- Sprenger, F., and Nüsslein Volhard, C. (1992). Torso receptor activity is regulated by a diffusible ligand produced at the extracellular terminal regions of the *Drosophila* egg. *Cell* **71**, 987-1001.
- Su, T. T., Walker, J., and Stumpff, J. (2000). Activating the DNA damage checkpoint in a developmental context. *Curr Biol* **10**, 119-26.
- Tautz, D., and Pfeifer, C. (1989). A non-radioactive in situ hybridization method for the localization of specific RNAs in *Drosophila* embryos reveals translational control of the segmentation gene hunchback. *Chromosoma* **98**, 81-5.
- Thomas, B. J., Gunning, D. A., Cho, J., and Zipursky, L. (1994). Cell cycle progression in the developing *Drosophila* eye: roughex encodes a novel protein required for the establishment of G1. *Cell* **77**, 1003-14.
- Thomas, B. J., Zavitz, K. H., Dong, X., Lane, M. E., Weigmann, K., Finley, R. L., Jr., Brent, R., Lehner, C. F., and Zipursky, S. L. (1997). roughex down-regulates G2 cyclins in G1. *Genes Dev* **11**, 1289-98.
- Thuret, J. Y., Valay, J. G., Faye, G., and Mann, C. (1996). Civ1 (CAK in vivo), a novel Cdk-activating kinase. *Cell* **86**, 565-76.

- Toyn, J. H., Johnson, A. L., Donovan, J. D., Toone, W. M., and Johnston, L. H. (1997). The Swi5 transcription factor of *Saccharomyces cerevisiae* has a role in exit from mitosis through induction of the cdk-inhibitor Sic1 in telophase. *Genetics* *145*, 85-96.
- Toyoshima, H., and Hunter, T. (1994). p27, a novel inhibitor of G1 cyclin-Cdk protein kinase activity, is related to p21. *Cell* *78*, 67-74.
- Uhlmann, F., Lottspeich, F., and Nasmyth, K. (1999). Sister-chromatid separation at anaphase onset is promoted by cleavage of the cohesin subunit Scc1. *Nature* *400*, 37-42.
- Valtz, N., Peter, M., and Herskowitz, I. (1995). FAR1 is required for oriented polarization of yeast cells in response to mating pheromones. *J Cell Biol* *131*, 863-73.
- Visintin, R., Craig, K., Hwang, E. S., Prinz, S., Tyers, M., and Amon, A. (1998). The phosphatase Cdc14 triggers mitotic exit by reversal of Cdk- dependent phosphorylation. *Mol Cell* *2*, 709-18.
- Visintin, R., Hwang, E. S., and Amon, A. (1999). Cfi1 prevents premature exit from mitosis by anchoring Cdc14 phosphatase in the nucleolus. *Nature* *398*, 818-23.
- Waters, J. C., Chen, R. H., Murray, A. W., Gorbsky, G. J., Salmon, E. D., and Nicklas, R. B. (1999). Mad2 binding by phosphorylated kinetochores links error detection and checkpoint action in mitosis. *Curr Biol* *9*, 649-52.
- Wieschaus, E. and Nüsslein-Volhard, C. (1986). Looking at embryos in *Drosophila*. A practical approach. D.B. Roberts, Editor. IRL Press, Oxford, Washington D.C. 199-227
- Zachariae, W., and Nasmyth, K. (1999). Whose end is destruction: cell division and the anaphase-promoting complex. *Genes Dev* *13*, 2039-58.
- Zachariae, W., Schwab, M., Nasmyth, K., and Seufert, W. (1998). Control of cyclin ubiquitination by CDK-regulated binding of Hct1 to the anaphase promoting complex. *Science* *282*, 1721-4.
- Zhang, H., Hannon, G. J., and Beach, D. (1994). p21-containing cyclin kinases exist in both active and inactive states. *Genes Dev* *8*, 1750-8.

ZUSAMMENFASSUNG

Ein normaler Ablauf des Zellzyklus ist essentiell für die korrekte Musterbildung und das Überleben eines Eukaryontens. Zwei Schlüsselereignisse im Zellzyklus, die DNA Replikation während S phase und die Chromatidsegregation während der Mitose, werden von einer konservierten Kinasefamilie, den Cyclin Dependent Kinases (CDKs), katalysiert. Während der Evolution sind mehrere Mechanismen entstanden, die die CDK Aktivität kontrollieren; kovalente Modifikation von CDKs, Cyclinproteolyse und CDK/Cyclin Inhibition durch die sogenannten CDK Inhibitors (CKIs).

Das Produkt des Drosophilagens Rux inhibiert CycA abhängige Aktivität und verhindert dadurch einen frühzeitigen Eintritt in die S Phase während der Augenentwicklung. In dieser Arbeit wird gezeigt, dass Rux ein *Drosophila* CKI ist. Rux assoziiert mit den mitotischen Cyclinen A und B und seine Überexpression im Embryo verhindert die Mitose. Die in dieser Arbeit beschriebenen *in vitro* Experimente zeigen, dass Rux die Aktivität von Cdk1/CycA und Cdk1/CycB Komplexen inhibieren, aber auch die eigentliche Aktivierung von Cdk1 verhindern kann. Die Aktivität des Cdk2/CycE Komplexes wird in diesen Experimenten nicht inhibiert und die Überexpression von Rux in Embryonen stört die CycE abhängigen S-Phasen nicht. Interessanterweise ist Rux die erste CKI spezifisch für mitotische Cycline, die in einem multizellulärem Organismus charakterisiert worden ist.

In dieser Arbeit wird auch gezeigt, dass das Rux Genprodukt eine Rolle in der Mitose spielt. Die Metaphase in *rux* Mutantendauert länger. Rux Überexpression kann einen Metaphase-Arrest aufheben, der durch Expression von stabilem CycA hervorgerufen wird und *rux* Mutanten zeigen eine verringerte Fähigkeit die Metaphase nach Überexpression von stabilem CycA zu verlassen. Rux trägt also zur Metaphase zu Anaphase Transition durch die Inhibition von Cdk1/CycA Aktivität bei, das heißt in einer Weise, die nicht von der CycA Proteolyse abhängt. Eine ähnliche Funktion ist schon für den *S. cerevisiae* CKI, SIC1 gezeigt worden. Diese Arbeit zeigt, dass SIC1 überexpression in *Drosophila* Mitose und die Cdk1/CycA und Cdk1/CycB Komplexe inhibieren kann. Dies deutet auf eine funktionelle Ähnlichkeit zwischen Sic1p und Rux deutet.

In dieser Arbeit wird zusätzlich gezeigt, dass Rux in G1 Zellen stabil ist und vom Proteasom vor der S Phase abgebaut wird. Rux Abbau ist durch ein PEST Sequenz im C-terminus des Proteins bestimmt. Aufgrund der vorliegenden Ergebnisse wird folgendes Modell für die Funktion von Rux vorgeschlagen; Rux ist ein *Drosophila* CDK Inhibitor mit einer Spezifität für mitotischen Cycline, der die Cdk1/CycA

Aktivität während der Metaphase inhibiert und diese Aktivität auch in der G1 phase auf einem niedrigen Niveau hält. Rux wird vom Proteasom vor der S phase abgebaut, und dies ist eine Voraussetzung für die Accumulation von CycA abhängiger Kinaseaktivität.

ABBREVIATIONS

APS	Ammoniumperoxidisulfate
ATP	Adenosine Triphosphate
bp	base pairs
BSA	Bovine Serum Albumin
cDNA	complementary DNA
DMSO	Dimethylsulfoxide
DNA	Desoxyribonucleic acid
DTT	Dithiothreitol
EDTA	Ethylene Diamine Tetracetic Acid
Fig.	Figure
g	gram
GST	Glutathione-S-transferase
h	Hour
IPTG	Isopropyl-thio-galactose
k	kilo
kD	kilodalton
l	liter
M	mol per litre
m	milli
μ	micro
mRNA	messenger RNA
n	nano
NGS	Normal goat serum
ORF	Open Reading Frame
PAGE	Polyacrylamide gel electrophoresis
PBS	Phosphate Buffered Saline
PCR	Polymerase chain reaction
RNA	Ribonucleic acid
RT	Room Temperature
SDS	Sodium dodecyl sulfate
TEMED	N,N,N',N'-Tetramethylethylenediamine
U	Unit

Single and three letter code for amino acids

A	Ala	Alanine
C	Cys	Cysteine
D	Asp	Aspartate
E	Glu	Glutamate
F	Phe	Phenylalanine
G	Gly	Glycine
H	His	Histidine
I	Ile	Isoleucine
K	Lys	Lysine
L	Leu	Leucine
M	Met	Methionine
N	Asn	Asparagine
P	Pro	Proline
Q	Gln	Glutamine
R	Arg	Arginine
S	Ser	Serine
T	Thr	Threonine
V	Val	Valine
W	Trp	Tryptophan
Y	Tyr	Tyrosine

Ich versichere, daß ich die von mir vorgelegte Dissertation selbständig angefertigt, die benutzten Quellen und Hilfsmittel vollständig angegeben und die Stellen der Arbeit - einschließlich Tabellen, Karten und Abbildungen -, die anderen Werken im Wortlaut oder dem Sinn nach entnommen sind, in jedem Einzelfall als Entlehnung kenntlich gemacht habe; daß diese Dissertation noch keiner anderen Fakultät oder Universität zur Prüfung vorgelegen hat; daß sie - abgesehen von unten angegebenen Teilpublikationen - noch nicht veröffentlicht worden ist sowie, daß ich eine solche Veröffentlichung vor Abschluß des Promotionsverfahrens nicht vornehmen werde. Die Bestimmungen dieser Promotionsordnung sind mir bekannt. Die von mir vorgelegte Dissertation ist von Prof. Dr. Maria Leptin betreut worden.

Edan Foley

Publications

Foley, E., O'Farrell, P. H. and Sprenger, F. Rux is a cyclin-dependent kinase inhibitor (CKI) specific for mitotic cyclin-Cdk complexes. *Curr Biol* 1999 9(23) 1392-1402

Foley, E and Sprenger, F. Cyclins: Growing pains for *Drosophila*. *Curr Biol* 2000 10(18) R665-R667

Acknowledgements

This work was performed in the lab of Dr. Frank Sprenger. I have benefited from Dr. Sprenger's enthusiasm, support and encouragement during this project and am very grateful to him for his invaluable assistance.

I am also grateful to Prof. Maria Leptin for her interest and comments during my thesis. This work was sponsored by the Boehringer Ingelheim Fonds, who made it possible for me to take part in numerous scientific meetings and courses. I would like to thank all members of the Sprenger, Leptin and Klein labs for creating such a pleasant working atmosphere. In particular, I am grateful to Axel Dienemann, Ruth Grosskortenhau, Markus Kaspar and Thomas Seher for their interest, comments and answers.

I would like to thank my parents, Michael and Brid Foley, for their endless support throughout my time at home and beyond. They always ensured that no obstacle prevented me from furthering my education and reminded me that there was more to life when it counted most.

This work is dedicated with all my heart to my wife Gina and my son Adam who have filled up my years with joyful memories.

LEBENS LAUF

Name:	Edan Foley
Geburtsdatum	4.3.1971, Galway, Ireland Verheiratet mit Gina Norman, ein Sohn Adam, geboren 5.7.99
Staatsangehörigkeit	irisch
1975-1989	Grund und Hauptschule
1989-1993	B.Sc. in Biochemie, University College Galway, Ireland
1994-1997	Biologie-Studium an der universität zu Köln
Sept.1997-Mar.1998	Diplomarbeit am Institut für Genetik der Universität zu Köln unter Betreuung von Prof. Dr. Maria Leptin: “Characterization of Roughex – a novel cell cycle inhibitor”
April 1998-2000	Doktorarbeit am Institut für Genetik der Universität zu Köln unter Betreuung von Prof. Dr. Maria Leptin: “Roughex dependent regulation of the <i>Drosophila</i> cell cycle”

